POPULATION-LEVEL CONSEQUENCES OF ENVIRONMENTAL VARIATION FOR MIGRATORY FISHES

by

GREGORY RUSSELL JACOBS

(Under the Direction of SETH J. WENGER and CRAIG W. OSENBERG)

ABSTRACT

Migratory fishes have evolved to deal with the unique environmental characteristics of their destination and migratory corridor habitats, but these environments are changing, potentially compromising the continued persistence of migratory populations. The most iconic and conspicuous fish migrations traverse narrow riverine corridors between the ocean (or other large bodies of water) and smaller streams. Humans have adversely affected these habitats by constructing migration barriers, changing land cover, and changing the climate. Investigating the relationship between environmental variation and fish migration is a crucial prerequisite for mitigating these effects.

In this dissertation, I quantify the relationship between environmental variation and migration, and evaluate how that relationship affects the population biology of two fishes in two study systems: Chinook salmon (*Oncorhynchus tshawytcha*) that spawn in central Idaho, USA, and lake sturgeon (*Acipenser fulvescens*) that spawn in the Niagara River, USA/Canada. For lake sturgeon, I demonstrate that female lake sturgeon, but not males, are more likely to breed in years with warmer spring water temperatures, suggesting that climate warming leads female lake sturgeon to spawn more frequently. For Chinook salmon, I quantify how spatiotemporal

variation in habitat variables in a pristine watershed influence the distribution of breeding, and how this variation buffers salmon from predicted changes in water temperature arising from climate change. I also develop a life-cycle model to investigate dam removals along the Snake River migration corridor and find, with conservative assumptions, that the regional population growth rate of Chinook salmon increases by ~7% per dam. Dam removal is predicted to increase the proportion of local sites that support positive population growth, from 24% (0 dams removed) to over 60% (4 dams removed). These results are invariant across three spatial scales of inference.

My results add to the disciplines of ecology and conservation biology by developing and applying cutting-edge statistical models that integrate data from multiple sources to assess ecological dynamics. These models can be used to inform future conservation and management actions for Chinook salmon, lake sturgeon, and other imperiled, migratory fishes.

INDEX WORDS: Integrated population models, capture-mark-recapture, lifecycle, population growth, dam removal, climate change

POPULATION-LEVEL CONSEQUENCES OF ENVIRONMENTAL VARIATION FOR MIGRATORY FISHES

by

GREGORY RUSSELL JACOBS

BS, Alma College, 2005

MS, University of Michigan, 2008

A Dissertation Submitted to the Graduate Faculty of The University of Georgia in Partial Fulfillment of the Requirements for the Degree

DOCTOR OF PHILOSOPHY

ATHENS, GEORGIA

2021

© 2021

Gregory Russell Jacobs

All Rights Reserved

POPULATION-LEVEL CONSEQUENCES OF ENVIRONMENTAL VARIATION FOR MIGRATORY FISHES

by

GREGORY RUSSELL JACOBS

Major Professors:	Seth J. Wenger
	Craig W. Osenberg
Committee:	Krista A Capps
	Mary C. Freeman

Electronic Version Approved:

Ron Walcott
Vice Provost for Graduate Education and Dean of the Graduate School
The University of Georgia
May 2021

ACKNOWLEDGEMENTS

First and foremost, I thank my parents Pam and Phil, my brother Doug, my wife Courtney, and my children Logan, Grace, and Charlie. I love you.

Everything about this dissertation is collaborative. None of it gets done without the help of friends and colleagues of all stripes. For the sturgeon work, fieldwork on the Niagara River could not have been accomplished without the help of numerous co-workers, students, and interns including John Sweka, Elizabeth Trometer, Dimitry Gorsky, Zy Beisinger, Michelle Casto-Yerty, and Todd Duval. Molly A. H. Webb, US Fish and Wildlife Service Bozeman Fish Technology Center, and her lab lent invaluable expertise and field assistance to our efforts to assess sex and reproductive status of Niagara River lake sturgeon. David Smith, USGS Leetown Science Center, generously lent us radio telemetry receivers to expand the coverage of our telemetry array. Funding was from the Great Lakes Restoration Initiative. For the salmon work, special thanks goes to Russ Thurow, USFS Rocky Mountain Research Station (RMRS), who lent his amazing Chinook salmon redd dataset. Continuous redd surveys were completed with the assistance of skillful helicopter pilots Will Hogan, James Pope, Sr., Ron Gipe, and John Hubof. US Forest Service helicopter managers assisted, and dispatch personnel on the Boise, Payette, and Salmon-Challis National Forests provided flight monitoring. Idaho Department of Fish and Game (IDFG) biologists participated in aerial surveys since 2013. Collaborators from the RMRS, IDFG, the Shoshone-Bannock Tribes, the Nez Perce Tribe, and the Payette, Boise, and Salmon-Challis National Forests completed ground-based surveys. Aerial surveys were funded by RMRS, the Payette National Forest, and the Bonneville Power Administration. GIS support and

review was provided by Dave Nagel, RMRS. More generally, the Mesolab and Osenberg lab groups at UGA provided constructive feedback, comments, and criticism on chapter manuscripts and presentations. The Limno-lab group at Cornell University provided feedback and constructive comments on manuscripts and presentations of Chapters 3 and 4, and Charlie Petrosky provided helpful feedback on the Chapter 4 manuscript.

TABLE OF CONTENTS

Page

LIST OF TABLES

Page

LIST OF FIGURES

Page

CHAPTER 1

INTRODUCTION

Among the movement modes of animals, migrations comprise some of the most iconic and interesting natural history spectacles: e.g., migrations of caribou across the far north of North America, wildebeest to and from seasonal wetlands in the Serengeti, and salmon from the ocean to mountain streams. Migrations are iconic because they result in conspicuous (sometimes awe-inspiring) aggregations of animals at high densities along migration routes and at their destinations. There are many definitions for the term "migration", comprising a continuum of movement patterns from globe-traversing arctic terns to Allee (1927)'s "bunching" isopods (Dingle and Drake 2007, Lucas and Baras 2008, Dingle 2014, Shaw 2016). Here, I define migrations as en-masse, round-trip, seasonal movements between separate habitats (sensu Lucas and Baras 2008). One of the most common forms of migration occurs between habitats used for breeding, and habitats used for foraging: "breed-and-feed" migrations (Shaw 2016).

Animals are driven to aggregate for a variety of reasons, as noted by Allee (1927):

> *"In many animal species the formation of aggregations … may be controlled by internal developments, such as the maturing of the sex products, or by external factors, as when land isopods are made to bunch by controlling the moisture of the substratum; but more commonly the internal and external factors are closely combined."*

The observation that mobile animals are motivated by both external environmental factors and internal biological state is an essential part of the movement ecology paradigm of Nathan et al. (2008). Under this paradigm, animals are driven to move based on their internal state (breeding,

foraging, etc.), which is affected by external conditions. Internal states that drive foraging, breeding, refuge-seeking can interact with seasonal and spatial variation in environmental conditions to influence migration.

Humans have influenced the planet's environment by altering land cover, accelerating climate change, facilitating species invasions, and hastening species extinctions (Vitousek 1994, Lockwood et al. 2005, Ceballos et al. 2015, Turvey and Crees 2019). Migratory animals (especially long-distance migrants) can be particularly sensitive to human-mediated changes to the environment given their reliance on multiple habitats during different seasons. Environmental changes in the "breeding" habitat can affect reproductive success, environmental changes in the "feeding" habitats can affect somatic growth and survival processes, and environmental changes along migratory corridors can influence or even prevent migrations. Many migratory species are thus imperiled, and exist at small fractions of their former abundances (Wilcove and Wikelski 2008). However, anthropogenic effects, such as those arising from changes in land cover, climate, or connectivity, do not affect all migratory species similarly, due to among-species differences in traits that affect their responses to environmental change (e.g., Hardesty-Moore et al. 2018).

Fish are a particularly interesting group for the study of migration (Lucas and Baras 2008). Migratory fishes often provide significant societal benefits, owing to their economic, nutritional, and cultural importance (Lynch et al. 2016, McIntyre et al. 2016). To maintain these benefits, migratory fishes must persist despite habitat degradation, migration barriers, climate change, and harvest. Modifications to land cover and river network connectivity alter the quality and quantity of habitat for reproduction, growth, and survival; climate change alters the thermal

and hydrodynamic environment of riverine systems; barriers reduce migration survival or outright prevent it; and harvest directly reduces survival.

Lennox et al. (2019) posed several key questions about the role of external stressors on migratory fishes, including: Do external factors influence migration success, or the probability of migrating due to maturation or facultative migration (i.e., skipped spawning)? How might variation in migration behavior influence spatial distribution and temporal dynamics (i.e., what fraction of the population is spawning)? How effective are management actions? To investigate such questions for imperiled migratory fishes in large natural systems, manipulations are often infeasible due to the large spatial scale (e.g., salmon migrating from the Pacific Ocean to central Idaho), small population size, and protected status. Instead, inference on these systems often relies on observational data collected (ideally) over long periods of time.

Since many migratory species breed annually, the consequences of within-year variation in conditions, among seasons or among habitats, are most often meted out annually in terms of the reproduction of young and the recruitment of mature adults. Spatial variation in habitat quality can drive competition among, habitat selection by, and spatial distribution of individuals. Temporal variation within individual habitats can also be very important for migratory species, because within-year variation in environmental conditions can broaden, narrow, or shift the phenology of migrations, altering species interactions and ecosystem processes (e.g., Deacy et al. 2017).

Despite these within-year effects on survival and reproduction, much of the important long-term dynamics of migratory species play out annually. Dingle and Drake (2007) noted as much, pointing out that “seasonal” migrations are often just stages within round-trip “annual” cycles. The aggregation of within-year effects to an overall cumulative annual effect is common

in age- or stage-structured demographic models when one or more life stages last less than a year, such as the egg and larval stages of amphibians or fishes (e.g., Vonesh and De la Cruz 2002). Thus, we can conceptualize the dynamics of migratory species from one year to the next as being determined by the environmental conditions in distinct habitats. Such a conceptualization zooms out from the highly dynamic and fast-paced concept of movement or behavioral ecology (Nathan et al. 2008) and back into a view more similar to classical population dynamics.

In this dissertation, I have integrated multiple observational data sets on each of two imperiled migratory fishes, Chinook salmon (*Oncorhynchus tshawytscha*) and lake sturgeon (*Acipenser fulvescens*), in two very different systems to ask how environmental variation may shape population dynamics via its effects on migration. In Chapter 2, I evaluate how climate and landscape variables drive the distribution of breeding habitat use of Chinook salmon in the Middle Fork Salmon River (MFSR) of central Idaho, using a unique dataset from a high spatial-resolution census of spawning nests (called "redds"), covering 777 km of contiguous habitat accessible by Chinook salmon for spawning, and conducted annually since 1995. Many Chinook salmon stocks across the eastern Pacific coast are in decline (Crozier et al. 2019, Jones et al. 2020, Petrosky et al. 2020, Thurow et al. 2020). Among these declining populations are Snake River Chinook salmon, which includes fishes in the MFSR, that have been protected under the Endangered Species Act since 1992 (NOAA 1992). The MFSR is an important source of wild Chinook salmon production within the larger Snake River watershed (ICTRT 2003, Thurow et al. 2020). Chapter 2 shows how the distribution of wild Chinook salmon spawning habitat responds to variation in biotic and abiotic conditions in a large watershed, and how projected hydroclimatic changes may alter the spatial distribution of spawning habitat. It links a long-term

dataset of Chinook salmon redd locations with several high-quality geospatial datasets that reflect stream habitat conditions to identify important drivers of habitat use. My co-authors and I find spatially heterogeneous changes in the distribution of Chinook salmon habitat with climate change, driven by changes in water temperature and mean summer flow. However, climate change effects are modest and do not change the overall amount of high-quality habitat in the basin.

In Chapter 3, I focus on inter-annual variability of migration behavior in partially migratory lake sturgeon (i.e., individuals do not migrate to breed every year), and ask whether sex or variation in the timing of spring water warming – an important phenological signal – better explains skipped reproductive bouts. There are many indications that lake sturgeon are recovering after decades of protection in the Great Lakes and across their range (Bruch et al. 2016), and there are several populations in the Great Lakes basin that management agencies may consider opening to recreational angling, including one in the Niagara River (the focal population in Chapter 3). Challenges for conservation and management of this species include their long lifespan and late maturation (Bruch 2008, Vélez-Espino and Koops 2009), as well as uncertainties about their life history, including uncertainty in the frequency with which they skip spawn. Spawning frequency of lake sturgeon differs by sex and is likely affected by environmental conditions, but the relationship between skipped spawning and environmental conditions has been untested. With climate change in the Great Lakes likely to alter seasonal variation in water temperature (Collingsworth et al. 2017), a facultative relationship between skipped spawning and early season environmental conditions may lead to changes in reproductive effort. We found that males spawn more frequently than females but do not respond

significantly to variation in spring warming, whereas females are more likely to spawn in warmer years.

In Chapter 4, I return to MFSR Chinook salmon to estimate spatial and temporal variation in reproductive success on the breeding habitat, and temporal variation in survival away from the breeding habitat (which includes migration through the hydrosystem and residency in the marine environment). I use the timeseries data on redds from Chapter 2 coupled with a wealth of supporting data on outside-basin survival processes affecting non-mature stages. I combine redd data with supporting datasets in a Bayesian integrated state-space life-cycle model to explain population growth in the MFSR across space and time, and to predict population growth potential among MFSR spatial units. To investigate the role of spatial scale of inference on the conclusions of such a model, I ran three separate models on redd data aggregated to one of three spatial scales at which Chinook salmon population dynamics are hypothesized to be independent. I then simulate the effect of reductions in migration mortality that might be accomplished with the removal of one or more large hydropower dams on the Snake River. We estimated the fraction of MFSR sub-units that are likely to support positive population growth under a series of Snake River dam removal scenarios. We found significant spatial and temporal variation in per-capita production of young Chinook salmon, which led to high temporal variation in population growth and in the contribution of spatial units to that growth. On average half or more of the spatial units did not support positive population growth at any scale of inference under current conditions. However, we found that significant gains in the number of spatial units that can support population growth in the MFSR may be realized if more than two Snake River dams were removed.

Environmental variation - and anthropogenic environmental change - may affect the population dynamics of migratory fishes by altering aspects of the migration itself. This dissertation investigates three examples of how migratory populations are affected by environmental factors: reproductive habitat quality and the eventual distribution of migratory habitat use, the frequency of "skipped" reproductive migrations, and the interplay between survival probability of migratory animals through non-breeding and corridor habitats and habitat quality variation among breeding habitats. In the three studies included in this dissertation, I show how anthropogenic factors are expected to affect interactions between environmental variation and migration in lake sturgeon and Chinook salmon. General expectations for how migratory animals may be affected by environmental variation are invaluable, but ultimately, more targeted species- and system-specific investigations are most useful for informing management and consertation action. Such targeted, applied ecological investigations are important extensions of general theory, and their results may inform management decisions that aim to enhance recovery, persistence, or production.

CHAPTER 2

CLIMATE, FIRE REGIME, GEOMORPHOLOGY, AND CONSPECIFICS INFLUENCE THE SPATIAL DISTRIBUTION OF CHINOOK SALMON REDDS[1]

[1] This chapter has been published previously (and has been modified slightly for this dissertation): Jacobs, G.R., Thurow, R.F., Buffington, J.M., Isaak, D. and Wenger, S.J., 2021. Climate, Fire Regime, Geomorphology, and Conspecifics Influence the Spatial Distribution of Chinook Salmon Redds. *Transactions of the American Fisheries Society* 150(1):8-23. Reprinted here with permission of publisher.

Introduction

Following European settlement, the distribution and abundance of salmon and steelhead in the Pacific Northwest of North America declined due to habitat degradation, migration barriers, overharvest, and interactions with non-native fishes (NRC 1996; Lee 1997). Subsequent recovery efforts have been manifold and expensive, including protection under the Endangered Species Act of 1973 (ESA) and the investment of mitigation funding from major hydroelectric dam projects (NPCC 2019). However, broad salmon recovery has remained elusive, with many populations persisting at abundances far below historical levels (Thurow et al. 2020). Moving forward, successful conservation will require careful spatial prioritization based on the distribution and abundance of suitable habitat, especially habitat used for spawning (Isaak and Thurow 2006; Peterson et al. 2013).

Mature salmon migrate from the ocean to their natal freshwater streams, where adult females excavate nests (redds) in which adults spawn and the fertilized eggs develop. The quality of salmon spawning and rearing habitat is affected by a variety of physical factors, including channel morphology, stream temperature, flow depth, velocity, hyporheic flow, and substrate size (e.g., Beechie et al. 2008). Egg development and fry survival are sensitive to the degree of fine sediment infiltration (Chapman, 1988; Jensen et al. 2009), scouring flows (Montgomery et al. 1996), water temperature (Richter and Kolmes 2005), and oxygen concentration as influenced by hyporheic exchange (Greig et al. 2007). Where natural fire regimes are intact, wildfire may contribute new and transient high-quality habitat patches resulting from periodic post-fire debris flows that recruit wood and sediment from upstream watersheds (Flitcroft et al. 2016), despite short-term negative effects on stream habitat (Minshall et al. 1990; Minshall 2003). Climate change is altering many of these factors (Luce

et al. 2013; Jolly et al. 2015; Isaak et al. 2018), producing shifts in species distributions (Lynch et al. 2016) that can challenge conservation efforts focused on current habitat distributions. Increasing water temperatures are predicted to cause habitat loss for stream fishes as lower-elevation areas warm (Lynch et al. 2016), although in some cases warming-induced habitat losses can be offset at upstream sites that were previously below thermal optima (Isaak et al. 2016). In addition, climate change can alter stream habitat quality due to changes in stream flow regime (Wenger et al. 2011), and disturbances associated with fire and debris flows (Goode et al. 2012; Flitcroft et al. 2016).

A complicating factor is that salmon habitat use may vary depending on the abundance of annually returning salmon, which is affected by out-of-basin factors, such as ocean productivity and migration mortality (Crozier et al. 2019). Female salmon are territorial, so during years with higher adult returns, breeding expands into previously unoccupied sites (Isaak and Thurow 2006). Thus, variation in conspecific density may shift occupancy–environment relationships (Falcy 2015).

Although the effects of many covariates on salmon are well established in isolation, their relative importance and joint effects in driving variation in spawning distributions across landscapes is less well established. Probabilistic species distribution models are powerful tools for assessing the joint effects of covariates, quantifying the roles of habitat conditions on species, and predictively mapping occurrence probabilities across large domains (Elith and Leathwick 2009). Coupling species distribution models with large datasets from ongoing monitoring programs (e.g., Roper et al. 2019; Thurow et al. 2020) and improved geospatial representations of stream habitat (Hill et al. 2016; Isaak et al. 2017a) creates new opportunities to better quantify salmon habitat relationships and understand or plan for the effects of climate change.

In this study, we examine the distribution of Chinook salmon redds throughout the Middle Fork Salmon River (MFSR) in central Idaho (Figure 2.1). The MFSR populations of Chinook salmon were first listed as "Threatened" under the ESA of 1992 (NOAA 1992) and have been the focus of extensive recovery efforts. Several physical and biological research programs have produced detailed geospatial datasets for the MFSR basin that can be used to evaluate redd occurrence as a function of environmental conditions over space and time. The MFSR is relatively unaltered by humans, and hosts an almost exclusively wild (albeit depleted) Chinook salmon population (Thurow et al. 2020). Hundreds of kilometers of intact Chinook salmon spawning streams flow through the MFSR watershed, the bulk of which lay within the Frank Church River of No Return Wilderness (Thurow et al., 2020). Our goal was to model the relationships between Chinook salmon spawning locations and habitat covariates across a range of inter-annual variation in spawner abundance for all accessible stream reaches in the MFSR. After developing models to describe those relationships, we use the models to predict redd occurrence probabilities and assess the potential effects of changes in summer stream temperature and discharge under two future climate scenarios.

Methods

Redd surveys.– Annually from 1995 through 2015, individual redd locations were georeferenced with a global positioning system at the end of the spawning season. Redd surveys were conducted via low-altitude helicopter flights (Thurow 2000) supplemented by ground-based surveys conducted by a collaborative group of experienced biologists with the Idaho Department of Fish and Game, Shoshone-Bannock Tribes, Nez Perce Tribe, and US Forest Service. Together, these surveys employed a spatially continuous sampling design (Fausch et al. 2002) replicated annually along a 777-km subset of the

MFSR stream network encompassing all potential Chinook salmon spawning habitats within the 7,330-km^2 MFSR watershed (Figure 2.1). Streams deemed inaccessible to Chinook salmon due to small size and steep slopes were omitted from the survey area (Thurow 2000; Isaak and Thurow 2006). The resulting multi-decadal Chinook salmon redd database is unique in its combination of fine spatial detail and large spatial and temporal extent. Georeferenced redd locations were snapped to the stream network depicted on the 1:100,000-scale National Stream Internet (NSI; Nagel et al. 2015), which divides the network at confluences, that are further divided into approximately 1-km reaches (stream reaches in our network averaged 1 km in length with a standard deviation (SD) of 0.7 km). Each reach was classified by the presence or absence of redds each year.

Geomorphic covariates.– Redd occurrence was considered in relation to three geomorphic characteristics: median substrate size, channel slope, and valley confinement. Spatial variation of substrate size within and between stream reaches is a primary control on spawning habitat because the size of sediment that a female salmon can move while excavating a redd is limited by her body size (Kondolf and Wolman 1993); conversely, substrate that is too fine provides poor habitat for egg and fry survival (Chapman 1988; Jensen et al. 2009). Consequently, we hypothesized that Chinook salmon redd occurrence would exhibit a unimodal relationship with substrate size, indicating an optimal value, with avoidance of finer or coarser substrates. Median substrate size (D_{50}) was used as a first-order estimate of bed material in each reach, although it is recognized that the extent of suitable spawning substrate additionally depends on the standard deviation of the size distribution (and thus the amount of unsuitable coarse/fine material) (Riebe et al. 2014) and the degree to which the reach is organized into textural patches (mesoscale substrate heterogeneity) (Buffington and Montgomery 1999). River

slope (*S*) is another primary geomorphic control on salmonid spawning habitat because lower stream slopes (< 3%) are characterized by gravel- and cobble-bed streams that have beneficial fine-scale habitat conditions, while steeper boulder-bed streams are generally avoided (Montgomery et al. 1999). Consequently, we expected a negative relationship between Chinook salmon redd occurrence and *S*. The third geomorphic control on spawning habitat is valley confinement (*V*), which is the lateral extent of the valley floor and floodplain adjacent to the stream. Chinook salmon in the study area commonly spawn in unconfined valleys (Isaak and Thurow 2006; Goode et al. 2013) because of (1) extensive floodplains that allow overbank flooding, which reduces mortality of incubating embryos from streambed scour (Goode et al. 2013; McKean and Tonina 2013); (2) off-channel habitat that provides refuge during rearing; (3) complex hyporheic exchange and associated benefits during incubation (Baxter and Hauer 2000); and (4) lower-gradient channels containing more extensive habitat patches than steeper, confined reaches (Stanford et al. 2005). Thus, we hypothesized that Chinook salmon redds would be more likely to occur in unconfined reaches. We also hypothesized that valley confinement would modify the effects of other covariates; specifically, we expected stronger substrate-size effects on redd occurrence in unconfined valleys because of other beneficial characteristics of such environments, as described above.

Substrate size was predicted from a 10-m digital elevation model (DEM) (USGS 2006) following the methods of Buffington et al. (2004) tailored to field data obtained from 120 sites in the basin. Stream reaches and slopes were defined between 40-ft contour crossings on 1:24,000 scale topographic maps, with digital stream lines obtained from the National Hydrography Dataset (USGS 2010). Substrate size and slope were thus

determined for stream segments of variable length, ranging from less than 100 m to several kilometers, depending on the frequency of contour crossings. Overlap of the 1-km reaches with buffer polygons derived from the above 1:24,000-scale network of variable segment lengths was used to calculate average (weighted by overlapping stream length) slope and substrate size for each 1-km reach. Valley confinement along 1:100,000 NSI stream lines was defined by Nagel et al. (2014), which was used to determine the proportion of each 1-km reach that ran through unconfined valleys. Valley confinement (V) was treated as a binary variable, where 1-km reaches overlapping unconfined valleys by more than 50% of their length were considered "unconfined" ($V = 1$). The three geomorphic covariates (D_{50}, S, and V) were spatially variable, but temporally constant, in our analysis.

Climate covariates.– We considered the effects of stream temperature and summer discharge (a surrogate for wetted stream width) on the occurrence of redds within reaches. Because MFSR streams occur at high elevation and span a wide range of temperatures, Chinook salmon habitat suitability may be limited by cold temperatures at high elevations and warm temperatures at low elevations (range: 4.4 to 17.8˚C; Richter and Kolmes 2005). Similarly, stream size may impose physical limits on spawning habitat availability; small streams (e.g., < 8 m bankful width; Isaak and Thruow 2006) will be inaccessible to large-bodied, adult Chinook salmon, while large streams may have unfavorable hydraulic conditions for spawning (e.g., Moir et al. 2006). Consequently, we hypothesized that redd occurrence would exhibit a unimodal relationship with both stream temperature and summer discharge, indicating an intermediate optimum for spawning.

To represent contemporary spatial variation in stream temperature (T), we used a pre-existing stream temperature scenario quantifying mean August stream temperatures for 1993–

2011 (Isaak et al. 2017a) downloaded from the NorWeST website (*https://www.fs.fed.us/rm/boise/AWAE/projects/NorWeST.html*). To represent interannual variation in stream temperature, we calculated the deviation *(*ΔT) of each year's predicted mean August temperature from the 1993-2011 average, and applied this deviation to all reaches in that year. The annual difference from the study-wide mean August temperature *(*ΔT) ranged from -0.7 to 0.9°C, with a mean of 0°C and a standard deviation of 0.5°C. Since reaches on the cold-edge (or warm-edge) margins would be more (or less) likely to support redds in warmer years, we considered an interaction between T and ΔT in the model.

To represent contemporary spatial variation in discharge (Q), we used a pre-existing stream flow scenario representing mean summer discharge for 1977–1997 (Wenger et al. 2010) downloaded from the Western U.S. Stream Flow Metrics website (*https://www.fs.fed.us/rm/boise/AWAE/projects/modeled_stream_flow_metrics.shtml*). "Summer" was defined as the time period between the first day after 1 June, when flows were lower than the mean annual value for the reach, and 30 September (Wenger et al. 2010). This streamflow variable (used as a surrogate for wetted stream size at the onset of spawning) varied spatially among the 1-km stream reaches, but was a constant during the survey period.

Fire covariates.–We hypothesized that fires in the local area surrounding each reach would initially degrade spawning habitat due to decreased water quality (input of ash and fine sediment) and elevated stream temperatures (loss of vegetative shading), but that habitat would improve in subsequent years due to input of spawning gravels and wood from post-fire debris flows. We focused on local effects (5-km local watershed)

because the effects of post-fire debris flows are most pronounced at subbasin confluences (where debris fans form) and within the first several kilometers downstream of the confluence as the pulse of gravel and wood disperses (Benda et al. 2003; data of M. Lewicki, J. M. Buffington, R. F. Thurow, and D. J. Isaak (paper read at the American Geophysical Union Fall Meeting, 2006)). The perimeters of burned areas within the MFSR from 1990 through 2016 were downloaded from the Monitoring Trends in Burn Severity (MTBS) website (*https://www.mtbs.gov/*), which provides data on burn severity and extent of all large fires in the United States (Eidenshink et al. 2007). We then calculated the proportion of the local watershed area for each reach that had burned within each year (F_0). We defined the local watershed as that within a 5-km upstream radius from the center of the reach, from which we produced local watershed polygons using the Geodata Crawler spatial data processing tool (Leasure 2014). We used within-year local watershed burned area as a short-term fire effects variable (F_0). For longer-term fire effects, we calculated the sum of the local area burned over moving-window 3- and 5-year periods, F_3 and F_5, respectively. These three local watershed fire variables varied spatially by 1-km reach and temporally by year.

Annual redd abundance.– The numbers of adult Chinook salmon returning to the MFSR varied by two orders of magnitude among years during the monitoring period, which we hypothesized would influence reach-level redd occupancy probability. To examine how habitat occupancy probability responded to variation in broader-scale redd abundance (an index of spawning run size), we quantified three scales of annually varying redd abundance: the whole-MFSR-basin (N_{MFSR}), the eight subwatershed-scale populations recognized by the NOAA Salmon Technical Recovery Team that overlap our surveyed network (ICTRT 2003; N_{POP}), and the 23 network segments used by Isaak and Thurow (2006; N_{SEG}) to divide the core network into

roughly equal-sized segments, with divisions placed near major tributary junctions. The N_{MFSR} variable represents the hypothesis that occurrence probability varies with redd abundance across the entire MFSR, the N_{POP} variable represents the hypothesis that occurrence probability varies with "regional" abundance of redds in the local ICTRT population, and the N_{SEG} variable represents the hypothesis that occurrence probability varies with "local" abundance of redds within the network segments of Isaak and Thurow (2006). We also tested interactions between each abundance covariate and physical characteristics of slope and substrate size.

Model fitting and evaluation.- We used logistic regression models to estimate relationships between environmental covariates (Table 2.1) and Chinook salmon redd occurrence within reaches. We identified twenty hypotheses from the variables described above (Appendix A). Plausible combinations of these hypotheses comprised a candidate set of 1,080 models that described occurrence probability as a function of landscape habitat covariates (Appendix B). We evaluated these model hypotheses using a common random effect structure for all candidate models, where reach-specific deviations from landscape habitat–occurrence relationships among 1-km reaches were accounted for by incorporating nested random intercepts for stream reaches within 12-digit hydrologic unit code subbasins (Seaber et al. 1987) (hereafter, "HUC-12") (Figure 2.1). This structure accounted for localized residual spatial autocorrelation within and among HUC-12 subbasins, with each containing between 2 and 24 contiguous surveyed stream reaches (mean = 10.6 reaches, SD = 5.1 reaches).

We fit all candidate mixed-effects logistic regression models in R (R Core Team 2019) using maximum likelihood estimation for comparison by Akaike's information

criterion (AIC) using the R package glmmTMB to leverage its faster speed over other mixed-model-fitting functions (Brooks et al. 2017). Models were ranked by the difference between a given AIC score and that with the lowest score (min(AIC)), $\Delta AIC_i = AIC_i - \min(AIC)$. Models with $\Delta AIC_i < 10$ (our "confidence set") were re-fit using the R package "lme4" (Bates et al. 2015) to leverage that package's internal model-fitting diagnostics and established connections with related R packages. Diagnostic statistics were used to evaluate aspects of model fit that are not described by AIC scores: 1) out-of-sample area under the receiver-operator curve statistic (AUC), which indicates model prediction performance and transferability; 2) conditional and marginal R^2 for mixed-effects generalized linear models (Nakagawa et al. 2017), which indicate goodness of fit; 3) the Kolmogorov-Smirnoff statistic (D) tests for model-misspecification inferred from the distribution of quantile model residuals from the DHARMa package (Hartig 2019); and 4) Moran's I tests residual spatial autocorrelation (in Euclidean space; Hartig 2019). An 8-fold cross validation routine was performed to calculate the out-of-sample AUC score, with folds stratified by population (ICTRT 2003) to maintain the hydrologic-unit-based spatial structure in our random effects (*sensu* Roberts et al. 2017). We evaluated variance inflation factors for parameters in each model in our confidence set, but found no evidence of strong collinearity (Fox and Monette 1992). We used empirical Bayesian model averaging, also called prediction averaging (as opposed to parameter averaging), to combine reach-level predictions from each of the models in our confidence set, weighted by the corresponding AIC weight for that model, using the package MuMIn (Bartón 2019). We used these model-averaged predictions to describe the relationships between redd occurrence probabilities and covariates by constructing response curves of predictions across the observed ranges of covariate values.

Redd Distribution Forecasting In a Changing Climate.- We used the same confidence set of models to evaluate how redd occurrence probabilities across the MFSR network would change under projected future climate scenarios. Although climate is likely to affect a variety of environmental parameters, we focused on changes to stream temperature and summer stream discharge, holding other variables constant. Redd occurrence probabilities were predicted for a baseline scenario using contemporary values of those covariates and compared with expectations for 2040 and 2080 based on the IPCC 2007 A1B emissions trajectory (Isaak et al. 2017a; Wenger et al. 2010). We calculated model-averaged predictions of reach-specific probability of redd occurrence, unconditional on random effects (i.e., ignoring random effects at reach and HUC-12 scales) for 2040 and 2080, assuming other covariates in the final model persisted at the temporal average observed from 1995 – 2015 (e.g., N_{MFSR} = 816 redds; F_5 = 0.82 km^2; and F_0 = 0.18 km^2). Other variables in the final model (i.e., substrate size, slope, and valley confinement) were invariant within a reach, so we used those reach-specific values in our projections. We also evaluated the predictions under the contemporary climate scenario with a +/- 1-standard deviation (SD) in upstream burned area for the 5-year and within-year events to evaluate the sensitivity of model predictions to fire variation.

To represent variation in habitat suitability across the MFSR for current and future conditions, we defined a relative index of total habitat suitability (H_T) following Wenger et al. (2013) as the sum of the products of stream reach lengths ($L_{(i)}$) and unconditional, model-averaged, occurrence probabilities ($\hat{y}_{(i)}$)

$$H_T = \sum_{i=1}^{n} \left(\hat{y}_{(i)} * L_{(i)} \right), \quad (1)$$

where i indexes the n = 772 circa-1-km reaches in our dataset. H_T sums the distribution of predicted spawning habitat across the stream network into a summary metric for the basin, contingent on the limitations of our dataset, such as low observed escapements (Thurow et al. 2020). We emphasize that H_T is a measure of redd occurrence probability as a function of landscape covariates, dependent on observed Chinook salmon densities, which we assume to be a reflection of habitat suitability. Furthermore, H_T is a relative index because it is a function of predicted habitat occupancy, which in our model varies annually with the number of returning Chinook salmon. To visualize how environmental changes may shift the distribution of redds within the basin under a changing climate, we plotted the accumulation of H_T with elevation and distance upstream for contemporary conditions (with and without observed variation in burned area) and for the 2040 and 2080 climate-change projections. Additionally, we calculated and plotted elevations and distances where the 5th, 50th, and 95th percentiles of H_T occurred for each scenario. Elevation was measured in meters from sea level and distance was measured in kilometers upstream from the outlet of the surveyed network.

Results

The final dataset consisted of 15,614 presence/absence records (out of a possible 16,212) across the surveyed network over 21 years. We removed 578 records for reaches that were not sampled in years when adverse conditions, such as high winds or wildfire, prohibited helicopter flights over part of the basin, or when turbid water from storms and debris flows inhibited redd visibility. We removed 20 additional records that were missing hydrological data. Twelve models had AIC scores within 10 units of the best model, comprising our confidence set (Appendix C), from which we derived weighted average predictions of redd occurrence. Additional model diagnostics (Table 2.2) indicated that all models in the confidence set

performed well. AUC scores were all near 0.8, indicating good model fit. Generally high conditional R^2 values near 0.73, indicated that the random effects strongly influenced variation in redd occurrence, but marginal R^2 values near 0.42 showed that main effects also explained a considerable amount of the variation in redd occurrence. P-values for Kolmogorov-Smirnoff *D* and Moran's *I* indicated that models were not mis-specified and only one model showed significant residual spatial autocorrelation (model 5, p(*I*) = 0.045).

Covariate effects

Across our model-averaged predictions, the occurrence of redds was a unimodal function of the mean stream temperature in August, reaching its maximum at 13.4°C and declining at higher and lower temperatures (Figure 2.2a). Inter-annual temperature variation had no appreciable effect on this relationship. Instead, there was a very slight increase in redd occurrence in years when mean temperatures were higher, and a very slight decrease when temperatures were cooler (black vs. light gray curves in Figure 2.2a), which did not conform to our *a priori* expectation (Appendix A). Redd occurrence in confined valleys showed a weak negative response to fire in the short term (within-year effects) and a positive response to fire during the preceding 5 years (Figures 2b and 2c). Redd occurrence in unconfined valleys exhibited a similar short-term response, but showed a stronger positive response to fire during the preceding 5 years (Figures 2b-c). Redd occurrence was also a unimodal function of mean summer discharge (a surrogate for wetted stream size during spawning), as expected, reflecting lower suitability of large and small channels compared to anR optimum channel size (near 2 $m^3 s^{-1}$) (Figure 2.2d).

Reaches were more likely to contain redds if they had median substrate sizes near 25 mm (Figures 2e-f). This pattern was qualitatively similar for both confined and unconfined valleys; however, redd occurence in unconfined valleys was more sensitive to variation in substrate size than in confined valleys, and there was a slightly greater predicted probability of redd occurrence in unconfined valleys for the optimal substrate size ($D_{50} \approx 25$ mm; Figures 2e-f). Confined reaches showed substantial uncertainty in probability of redd occurrence near the optimal substrate size, which attenuated gradually with larger substrate sizes and lower probability of occurrence (Figure 2.2e). In contrast, unconfined reaches showed a more precise relationship (smaller confidence interval) between redd occurrence and substrate size for $D_{50} < 75$ mm (Figure 2.2f). The inclusion of Chinook salmon abundance and its interaction with substrate size in our top models (Table 2.2) indicates that the probability of redd occurrence for a given reach increased with conspecific abundance (main effect of N_{MFSR}) (Figure 2.2g), and that the increase was largest at substrate sizes below 75 mm ($N_{MFSR} \times D_{50}$) (Figures 2h-i). Importantly, all top models contained the whole-MFSR-basin scale conspecific abundance variable, N_{MFSR}, indicating that this variable better explained variation in redd occurrence rates compared to smaller-scale conspecific abundance variables that we considered.

Redd habitat distribution

We predicted the spatial distribution of Chinook salmon spawning habitat from our fitted relationships between landscape variables and observed occurrence, without conditioning on our spatial random effects, for contemporary, 2040, and 2080 scenarios. We calculated the weighted average unconditional model predictions from all models in our confidence set using AIC weights. In the contemporary scenario, these predictions identified many of the high-occurrence areas observed in our data, though some tributaries experienced higher observed occurrence rates

than our model predicted, and many mainstem reaches experienced lower occurrence rates than predicted (Figures 3a and c). Differences between the predicted occurrence probabilities in the contemporary scenario versus those in the 2040 and 2080 scenarios were spatially heterogeneous (Figures 3b and d). Increases in redd occurrence probability were predicted among the furthest upstream reaches of the surveyed area, and progressive declines in occurrence probability were predicted along the lower mainstem and higher-order tributaries compared to current conditions, with effects becoming more pronounced from 2040 to 2080 (Figure 2.3). Interestingly, some of the habitats with the largest observed contemporary redd occurrences (e.g., Bear Valley Creek, the furthest southwest tributary on the maps) were predicted to have lower occurrence probabilities in 2040 and 2080.

The predicted effects of climate change were, overall, fairly small (Figure 2.4), with H_T increasing slightly in 2040 (Figure 2.4) but decreasing by 2080. Decreases in H_T were most pronounced at low- to mid-elevations (and distances), but upstream reach-level occurrence probabilities tended to increase under future climate scenarios, somewhat compensating for downstream losses. The variation in H_T caused by variation in fire effects was small at low elevations (and distance), but increased with elevation (and distance), such that the effect of both of our climate change scenarios on whole-basin H_T fell within the range expected under the contemporary scenario with contemporary inter-annual fire variability. However, it should be emphasized that the fire-related uncertainty in redd occurrence depicted in Figure 2.4 is cumulative, such that the difference between high and low bounds necessarily increases across the x-axis, and that weaker (or stronger) fire effects of individual reaches slow (or speed) that increase.

The close proximity of terminal H_T values for all scenarios in Figure 2.4 (i.e., within the range of cumulative uncertainty in the contemporary scenario due to fire) suggests that the basin-wide effects of climate-driven changes in stream temperature and streamflow could be eclipsed by slight changes in fire regime.

Discussion

Chinook salmon redd occurrence was influenced by hydrogeomorphic features, streamflow, stream temperature, conspecific abundance of spawning Chinook salmon, and fire dynamics across the MFSR, a large watershed of highly connected stream reaches minimally influenced by anthropogenic activities. The effects of stream temperature and stream size were modest compared to effects of substrate size and valley confinement. Further, our analyses indicated that variation in fire extent may be more influential than the moderate changes in stream temperature and flow conditions expected with climate change. Given that the extent and severity of wildfires in the study area will likely continue to increase under a warming climate (Westerling et al. 2006), post-fire increases in sediment yield and wood recruitment may be the dominant effects of future climate change on Chinook salmon spawning habitats in the MFSR, with relatively little effect of changes in stream temperature and streamflow during the spawning period. However, climate-driven changes in streamflow variables that were not considered in our analysis, such as scour regime during embryo incubation, could affect Chinook salmon habitat in the basin (Goode et al. 2013). These possible effects warrant further investigation.

Time-invariant effects

In our top models, substrate size and valley confinement strongly affected Chinook salmon redd occurrence and interacted with other variables to further influence redd occurrence (Table 2.2). We observed a strongly unimodal relationship between redd occurrence and

substrate size, indicating an optimal intermediate substrate size. Notably, the optimal substrate size (25 mm) that we observed was near the bottom of the range of preferred sizes reported in the literature for large-bodied salmonids (Kondolf and Wolman 1993). One might expect that small, marginal, substrate sizes might be tolerated in unconfined valleys due to other ecological benefits (Appendix A), but we found that redd occurrence probability was highest at 25 mm in both unconfined and confined valleys (Figures 2e-f). We are unsure why the fish consistently selected reaches with small substrate sizes, particularly in confined valleys, which magnify flood flows compared to unconfined floodplain rivers (Baxter and Hauer 2000; Goode et al. 2013) and should therefore elevate the scour risk of incubating embryos. However, our use of reach-average median substrate size neglects size variation (Riebe et al. 2014) and the occurrence of textural patches within a reach (Buffington et al. 2004). Consequently, redds in the study area may be within patches with larger substrate size than indicated by the reach-scale prediction of D_{50}.

Temperature

Our results indicate an optimum stream temperature of around 14°C, but little effect of interannual temperature variation (Figure 2.2a), suggesting that average stream temperature is a stronger control on redd occurrence, or that natal homing constrains the response to interannual variability. This may seem unsurprising because the standard deviation of interannual temperature among years was only 0.5°C; however, even small changes in mean temperature can strongly affect the timing of intra-annual temperature variation. Salmon populations are generally thought to respond to temperature variation by changing the timing of spawning (Heggberget 1988; Schindler et al. 2010), rather than

by changing location, which would be consistent with our observations. Isaak et al. (2017a) found no strong negative effect of high stream temperature (up to 22°C) on Chinook salmon occurrence, possibly due to wide *intra*-annual variation in temperatures allowing most streams to experience optimal spawning temperatures, but at different times of year. Our results suggest a decline in occupancy probability in reaches with mean August stream temperatures < 12 or > 16°C in the MFSR; however, the uncertainty in this relationship is high, especially at warmer temperatures (Figure 2.2a). If optimal thermal conditions occur at some point during the spawning season, mean August temperature may be less important than phenology or other physical variables, such as substrate, water depth, and velocity, for determining where females excavate redds (Lisi et al. 2013).

Flow

Average stream discharge in the Pacific Northwest is predicted to decline with climate change, mostly due to changes in precipitation patterns and reduced snowpack (Hamlet et al. 2013). However, predictions for the study area are more nuanced; the magnitude of high flows is expected to increase with climate change, while that of summer low flows is predicted to decline (Goode et al. 2013). Our results suggest that even within the surveyed network where all streams are thought to be accessible by Chinook salmon, the lowest-discharge (smallest) streams are less likely to be occupied by spawning fish (Figure 2.2d). Furthermore, the climate projections used in our analysis predicted declines in mean summer discharge that were too small to reduce occurrence probabilities appreciably among the smaller upstream tributaries in our network (Figures 3-4). However, we did not consider intra-annual variation in discharge, which might differentially affect early-arriving Chinook salmon spawners. Nor did we consider the number and severity of scouring flow events during the winter egg incubation period, which is expected

to increase under climate change scenarios, with negative effects for fall-spawning salmonids (Wenger et al. 2010; Goode et al. 2013).

Fire

Our work supports a growing body of literature showing the benefits of high-quality, highly-connected habitats and natural fire regimes for salmon. Fire is integral to the shifting habitat mosaic concept in large rivers (Kleindl et al. 2015) which drives riverine habitat patch dynamics in space and time (Stanford et al. 2005). Natural fire regimes have an overall positive effect on Pacific salmon, although there is often a mix of positive and negative effects that take time to manifest through ecological and geomorphological processes (Flitcroft et al. 2016). In the short term, effects of fire on stream ecosystems are typically negative (Minshall 2003), and our results support this, though only weakly (Figure 2.2a). The lack of strong negative responses to local fire in the MFSR may be a function of the "Wilderness" designation that covers over 95% of the basin (and a corresponding lack of human-driven landscape alteration), resulting in a more natural fire regime that may moderate burn severity and create diverse habitat (Parks et al. 2014). Positive fire effects are likely the result of post-fire debris flows that input gravel and large wood from the surrounding landscape (Benda et al. 2003; Dunham et al. 2003; Goode et al. 2012; Flitcroft et al. 2016; Lewicki et al. unpublished). We found a stronger positive relationship between fire and Chinook salmon redd occurrence in unconfined valleys than in confined valleys, possibly reflecting the general tendency for lower-gradient, more sinuous reaches to retain inputs of post-fire sediment and wood longer than confined valley reaches that are relatively steeper, narrower, and less sinuous. Others have reported that post-fire sediment inputs can be routed through steep, confined,

valley reaches within 5-10 years (Lewicki et al. unpublished), while sediment pulses in lower-gradient, unconfined rivers may persist for decades (Megahan et al. 1980; Madej and Ozaki 1996). Nevertheless, the periodic creation of transient spawning habitat in steep confined valleys via post-fire debris flows may be particularly important given the overall paucity of spawning habitat in such environments. During 21 years of redd surveys evaluated here, there are documented examples of Chinook salmon spawning in new gravel patches deposited by post-fire debris flows (data of R. F. Thurow and J. M. Buffington (paper read at the Ecological Society of America Annual Meeting, 2018)), demonstrating dynamic response of redd occurrence to wildfire.

Conspecific abundance

We found that Chinook salmon redds tend to occur in a larger number of reaches when run sizes are larger, as has been noted previously in this system (Isaak et al. 2003; Isaak and Thurow 2006). Such colonization of new habitats could be interpreted as habitat selection behavior motivated at the individual level by density-dependent competition for habitat (Fretwell and Lucas 1969). Yet, contemporary Chinook salmon abundance in the MFSR is a small fraction of historical abundances, and habitat has remained abundant, high-quality, and intact (Thurow et al. 2020), so intra-specific competition is not likely to be strong. As noted above, Chinook salmon in the MFSR have also demonstrated the capacity to colonize new post-fire debris-flow deposits, sometimes in locations many kilometers from the nearest prior spawning gravels (Thurow and Buffington, unpublished), an observation that is consistent with our finding of net positive responses to fire. At currently low population densities, the positive occurrence–abundance relationship and new-patch-colonization observations may be the result of density-independent homing and straying behaviors. Natal homing in Pacific salmonids can lead to

differentiation among populations that return to distinct areas (Schindler et al. 2010), while straying allows genetic exchange among sub-populations that can contribute to genetic diversity and metapopulation stability (Neville et al. 2007; Keefer and Caudill 2014). Interestingly, neither homing–straying nor habitat selection, both of which are localized processes, explain why whole-basin abundance of Chinook salmon outperformed finer-scale abundance variables. One possibility is that synchrony in redd counts among subpopulations across the MFSR (Isaak et al. 2003) yields subbasin-scale variation in salmon abundance that, for all subbasins, mirrors that of abundance at the whole-basin scale, such that using local subbasin counts adds no explanatory power over whole-basin counts.

We have shown that interannual variation in Chinook salmon redd occurrence across the MFSR can be explained by spatially or annually varying environmental conditions and conspecific abundance. However, intra-annual processes (e.g., phenology) are also important for salmon population dynamics and their response to environmental variation and change. Chinook salmon life history portfolios (including spawning temperature or spawn-timing preferences) may differ substantially among sub-populations across the MFSR as they do in other systems (Ruff et al. 2011). The annual time-step at which our data were collected do not capture such important intra-annual variation in the MFSR, so further investigation with additional or complimentary datasets is warranted.

Life cycle implications

Salmon need three things: intact natal habitat (spawning and rearing), a suitable migration corridor, and a favorable estuary and ocean environment. In the past c. 70 years, reduced connectivity resulting from hydropower dam construction, along with

changes in the Pacific Ocean ecosystem, have proven more powerful for explaining contemporary Chinook salmon production and escapement than natal habitat quality and abundance in the Snake River basin (Schaller et al. 2014; Crozier et al. 2019). If natal spawning habitat was the limiting factor for Chinook salmon population growth, with its abundance of high-quality, connected spawning and rearing habitats, the MFSR should be highly productive, with abundant salmon returns and most reaches occupied. Instead, 1) occupancy rates vary positively with abundance, suggesting habitats are not saturated; and 2) contemporary run sizes are estimated at less than 3% of those from the 1950s and 1960s, even as contemporary environmental conditions in the watershed remain little changed by human activity (Thurow et al. 2020). Considerable effort historically has been directed toward supplemental stocking and improving hydrosystem passage survival of Chinook salmon and other Pacific salmonids, but salmon and other migratory species rely on all phases of their life cycle to persist, and climate change may impair habitat for all life stages, including salmon spawning habitat. Our results illustrate where favorable spawning habitats are likely to exist under future climate change scenarios, and how future habitat distributions may differ from contemporary conditions, thus identifying habitats that are of high conservation priority: those that are currently high quality and are likely to persist or improve under projected climate change. Importantly, effective out-of-basin management actions to improve adult escapements are needed to take advantage of existing, under-seeded freshwater habitat in areas like the MFSR, where such habitats are likely to remain high quality for the foreseeable future.

Table 2.1. Summary statistics for all environmental covariates included in Chinook salmon redd occurrence models.

Variable	Mean	SD	Median	Min	Max
D_{50} (mm)	51.3	16.2	49.3	13.6	122.1
ln(D_{50})	3.884	0.338	3.897	2.607	4.805
S (percent)	1.8	1.7	1.3	0.1	16.3
V	0.27	0.45	0	0	1
Q (m^3s^{-1})	272.3	442.4	73.9	2.6	2001.6
ln(Q)	4.489	1.516	4.303	0.945	7.602
T (˚C)	12.5	2.2	12.6	6.6	17.5
ΔT (˚C)	0	0.5	-0.2	-0.7	0.9
N_{MFSR} (redds)	816	600	633	20	2271
N_{POP} (redds)	90	125	43	0	690
N_{SEG} (redds)	36	66	10	0	472
F_0 (km^2)	0.177	1.248	0	0	29.39
F_3 (km^2)	0.512	2.093	0	0	29.39
F_5 (km^2)	0.824	2.611	0	0	29.39

Table 2.2. Performance of the twelve best models of Chinook salmon redd occurrence ($\Delta AIC < 10$). The coefficient columns specify fixed effects; the random effects (reach and HUC-12 sub-basin intercepts) are common to all models. All other columns show diagnostic information for each model: AUC is the Area Under the Receiver-Operator Curve statistic calculated from held-out data during an 8-fold cross-validation analysis, ${R^2}_{cond}$ and ${R^2}_{marg}$ are the conditional and marginal R^2 values for mixed-effects generalized linear models (Nakagawa et al. 2017), $p(\mathrm{D})$ is the p-value for the Kolmogorov D-statistic testing the uniformity in quantile model residuals from the DHARMa package (Hartig 2019), $p(I)$ is the p-value for Moran's I statistic testing residual spatial autocorrelation in Euclidean space (Gittleman and Kot 1990, Hartig 2019), ΔAIC is the difference from the lowest AIC in the model set, and w_{AIC} is the AIC weight. Note that squared variables in the table heading (e.g., "$D_{50}{}^2$") always indicate the full polynomial (D_{50} + $D_{50}{}^2$), and interactions with these variables (e.g., "$D_{50}{}^2 * N_{MFSR}$") apply to both terms in the polynomial ($D_{50} * N_{MFSR}$ + $D_{50}{}^2 * N_{MFSR}$).

Rank	$D_{50}{}^2$	V	T^2	ΔT	Q^2	N_{MFSR}	F_5	F_0	$(D_{50}{}^2 * N_{MFSR})$	$(T^2 * \Delta T)$	$(D_{50}{}^2 * V)$	$(Q^2 * V)$	$(F_0 * V)$	$(F_5 * V)$	AUC	${R^2}_{cond}$	${R^2}_{marg}$	$p(\mathrm{D})$	$p(I)$	ΔAIC	w_{AIC}
1	x	x	x	x	x	x	x		x	x	x				0.801	0.726	0.42	0.196	0.458	0	0.373
2	x	x	x	x	x	x	x	x	x	x	x				0.801	0.726	0.421	0.189	0.278	0.555	0.283
3	x	x	x	x	x	x	x	x	x	x	x		x		0.801	0.726	0.421	0.192	0.933	1.972	0.139
4	x	x	x	x	x	x	x		x	x	x			x	0.801	0.727	0.42	0.169	0.536	3.795	0.056
5	x	x	x	x	x	x	x		x	x		x		x	0.798	0.731	0.419	0.204	0.045	4.345	0.042
6	x	x	x	x	x	x	x		x	x	x	x		x	0.801	0.728	0.422	0.263	0.672	4.82	0.033
7	x	x	x	x	x	x	x	x	x	x	x			x	0.801	0.727	0.42	0.19	0.212	5.39	0.025
8	x	x	x	x	x	x	x	x	x	x		x		x	0.798	0.731	0.419	0.168	0.726	5.769	0.02
9	x	x	x	x	x	x	x	x	x	x	x	x		x	0.801	0.728	0.423	0.272	0.587	6.792	0.012

10	x	x	x	x	x	x	x	x	x	x	x		x	x	0.801	0.727	0.42	0.197	0.937	7.955	0.007
11	x	x	x	x	x	x	x	x	x	x		x	x	x	0.798	0.731	0.419	0.168	0.928	8.701	0.005
12	x	x	x	x	x	x	x	x	x	x	x	x	x	x	0.801	0.728	0.423	0.263	0.144	9.713	0.003

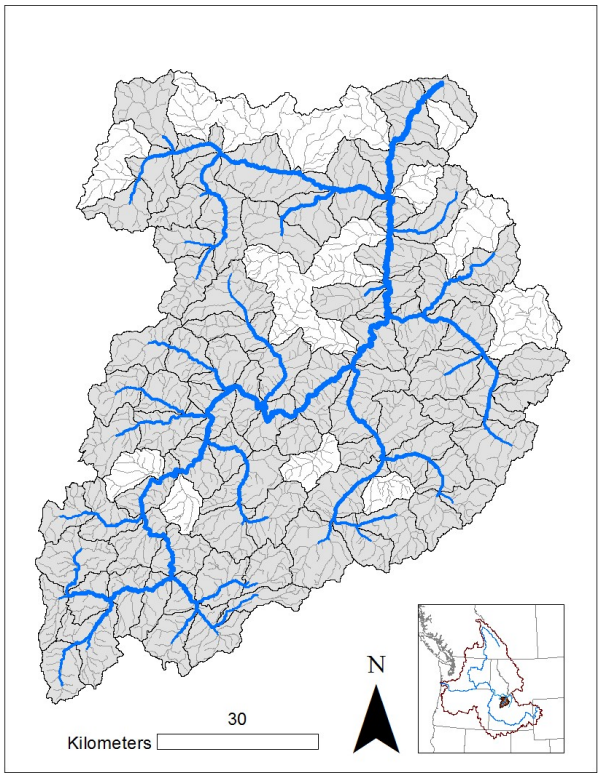

Figure 2.1. Map of the Middle Fork Salmon River (MFSR) in central Idaho. 1:100,000 scale stream reaches are shown in light gray (Nagel et al. 2015), with reaches surveyed annually for Chinook salmon redds overlain in black, where line width scales with the log of upstream drainage area. Gray polygons represent 12-digit Hydrologic Unit Code subbasins that overlap the surveyed portion of the stream network; white polygons are areas that do not overlap. A total of 772 individual reaches comprise the surveyed (black) network. The inset map (39-54°N, 105-126° W) shows the location of the MFSR watershed (dark gray polygon) within the Columbia River basin (light gray polygon) with major tributaries, including the Upper Columbia, Snake River, and Salmon River, drawn in black.

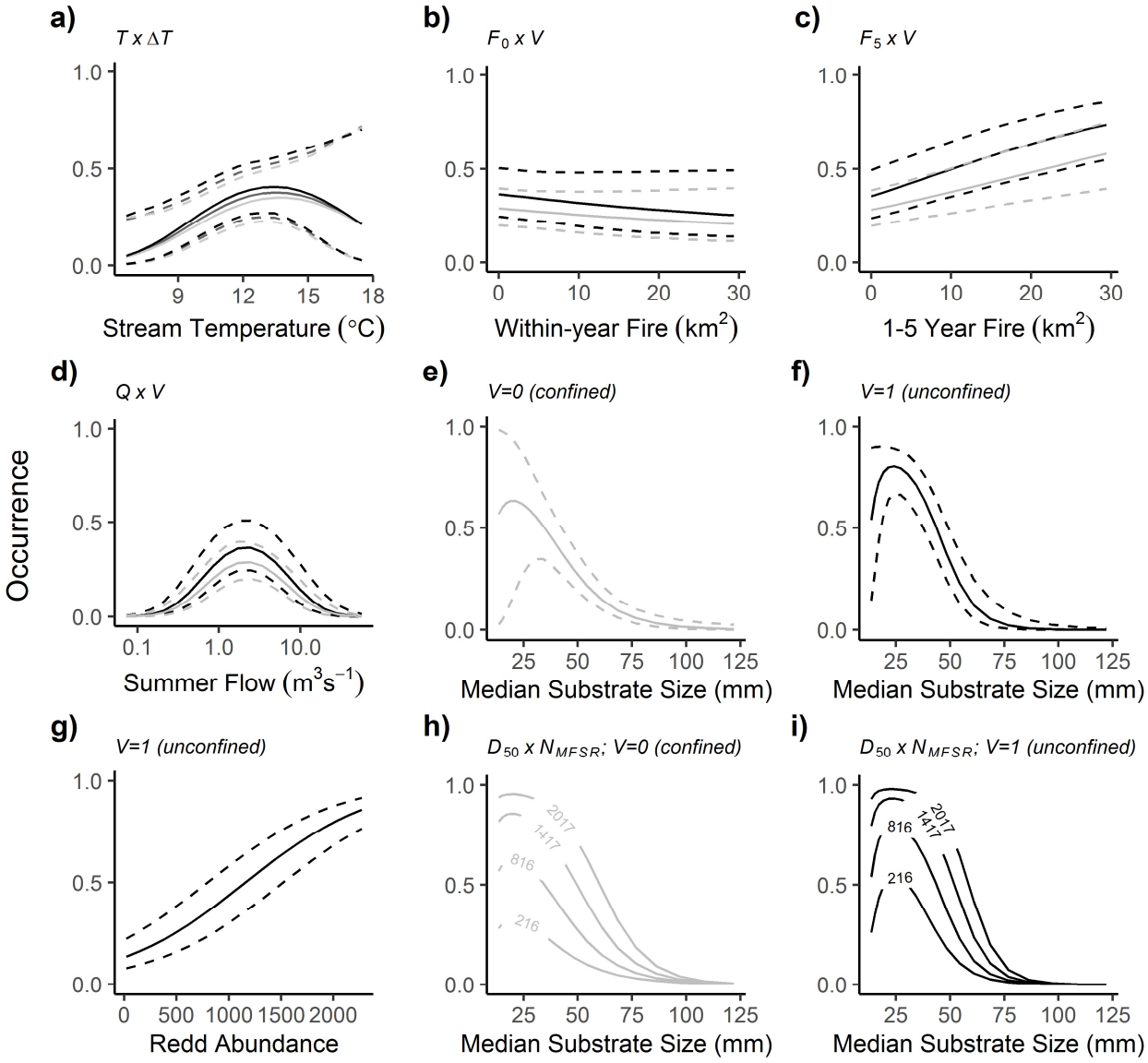

Figure 2.2. Probability of redd occurrence as a function of (a) stream temperature (T), (b) within-year fire extent in the local 5-km watershed (F_0), (c) 5-year fire extent in the local watershed (F_5), (d) mean summer discharge (Q, a surrogate for wetted stream size during spawning), (e) median substrate size (D_{50}) in confined valleys ($V = 0$), (f) median substrate size in unconfined valleys ($V = 1$), (g) the abundance of redds (N_{MFSR}, year-specific basin-wide Chinook salmon redd count), (h) the influence of redd abundance on the substrate-size effect in confined valleys, and (i) the influence of redd abundance on the substrate-size effect in unconfined valleys.

Dashed lines in panels a-g are 95% confidence intervals of the mean (solid lines). Response curves are evaluated at the average of all other covariates, except as indicated by line color or plot labels. Panel (a) shows responses evaluated at one standard deviation below average (light gray), average (dark gray), and one standard deviation above average (black) inter-annual temperature variation. Panels (b-i), show responses evaluated for confined valleys (gray) and unconfined valleys (black). Panels (h) and (i) show responses evaluated at mean redd abundance (816 redds), one standard deviation (SD) below the mean (216 redds), one SD above the mean (1,417 redds), and 2 SD above the mean (2,017 redds). Note that the '816'-redd lines in (h) and (i) are identical to the solid lines in panels (e) and (f), respectively.

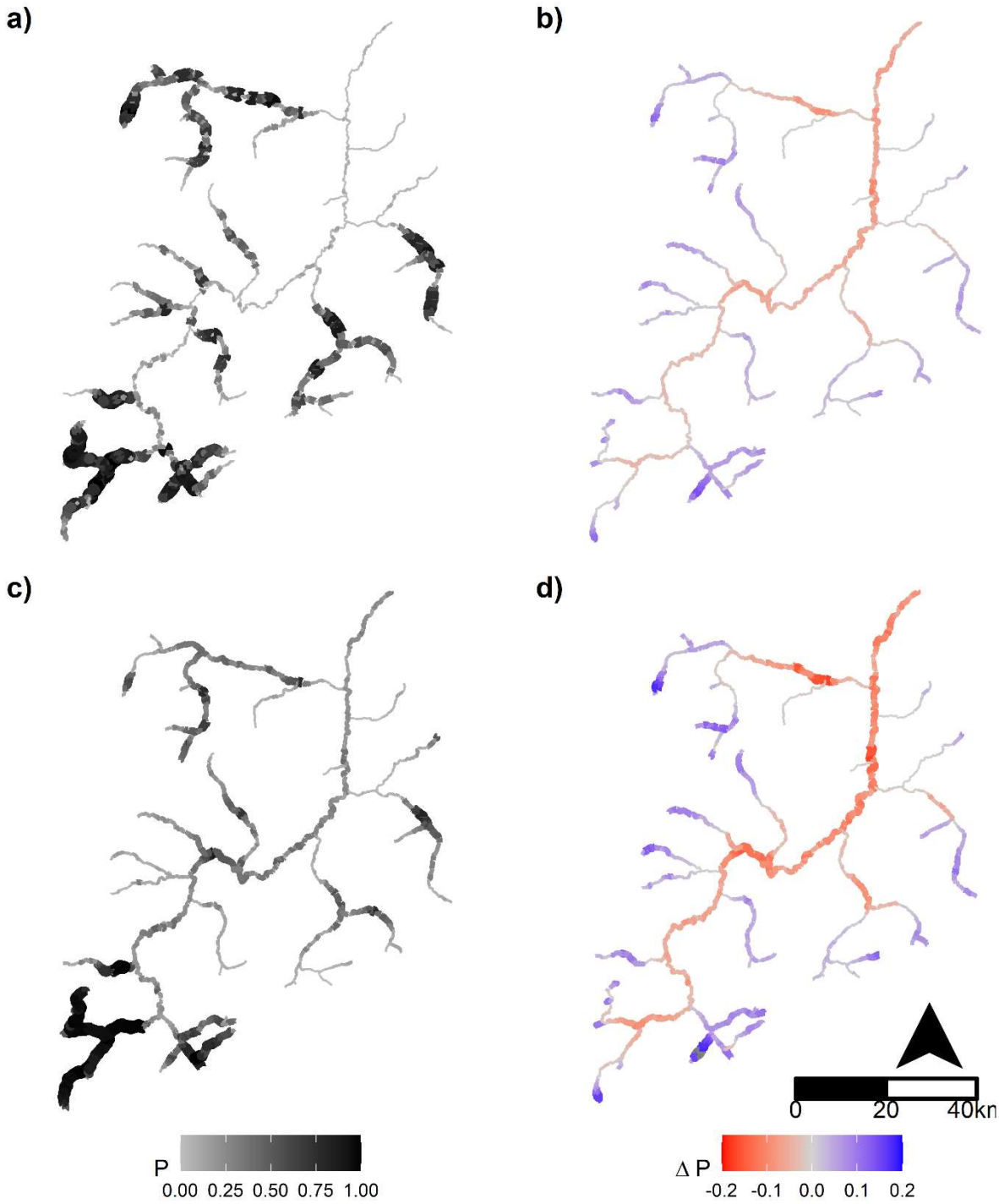

Figure 2.3. Maps describing redd occurrence across potential Chinook salmon spawning habitats in the Middle Fork Salmon River (MFSR), Idaho. Panels (a) and (c) show occurrence probability (P) in terms of: (a) the observed proportion of years each reach was occupied by redds in the dataset, and (c) model-averaged prediction of P derived from the fixed-effect habitat-occurrence

relationships in our top models (ignoring spatial random effects) under contemporary environmental conditions. Panels (b) and (d) predict the change in model-averaged occurrence probability (ΔP) between contemporary conditions and those under climate change projections for 2040 (b) and 2080 (d) downscaled to the MFSR from the IPCC 2007 A1B scenario. Occurrence probability in panels (a) and (c) scales with shading and size where darker, larger line segments denote higher P. Change in occurrence probability (ΔP) with climate change is the difference in occurrence probability between contemporary and projected conditions, such that negative values indicate predicted reductions in occurrence rate and positive values indicate increases. Change in occurrence ΔP in panels b) and d) scale with size and color from red (20% reduction) to gray (no change) to blue (20% increase).

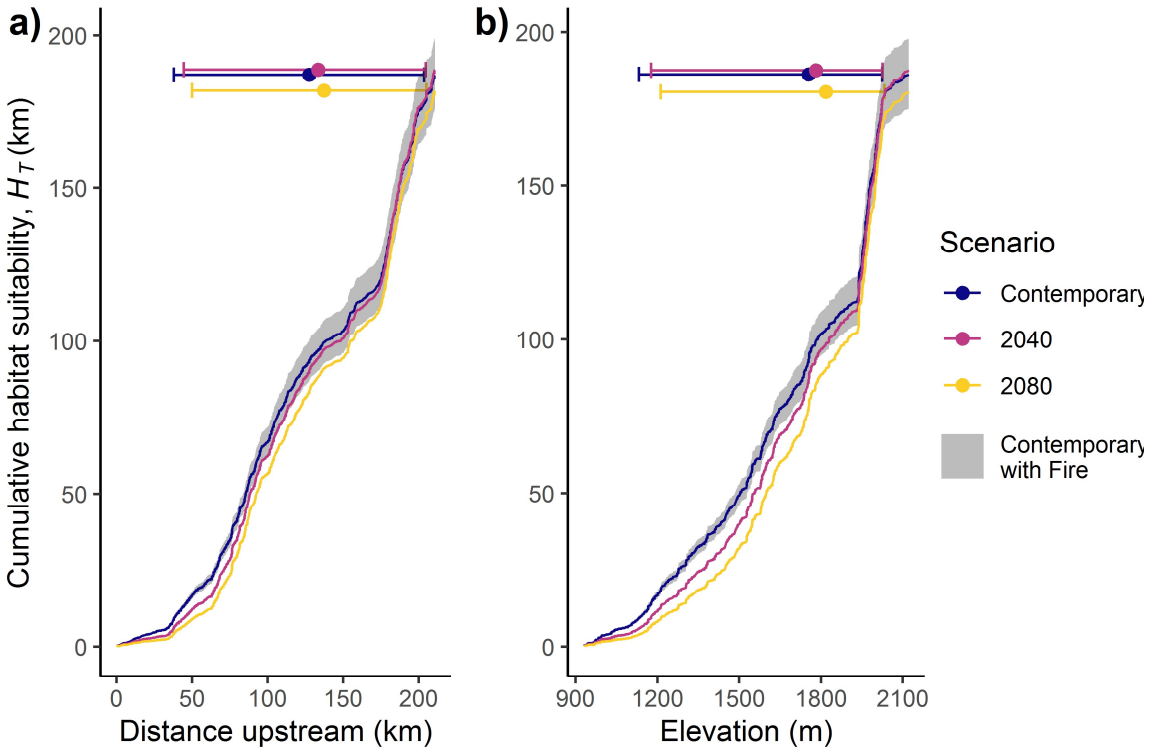

Figure 2.4. Cumulative distributions of H_T (length of stream weighted by the probability of occurrence of Chinook salmon redds) in the Middle Fork Salmon River (MFSR) as a function of (a) distance upstream (km) and (b) elevation above sea level (m) for contemporary stream temperatures and mean summer flows (navy line) compared to those predicted for 2040 (purple line) and 2080 (gold line) using the A1B climate scenario. The gray band around the contemporary curve indicates the prediction space associated with +/- 1 standard deviation (SD) in the with-year and 5-year fire variables (F_0 and F_5) for contemporary conditions; used to assess the relative effects of climate-driven changes in stream temperature and streamflow vs. variation in fire under current climate conditions. Dot-and-whisker plots at the top of each panel show the location on the x-axis variable of the median and 95th percentile range of H_T, plotted on the y-axis at the total cumulative value of H_T for that scenario.

CHAPTER 3

DOES THE TIMING OF SPRING WATER WARMING AFFECT ANNUAL BREEDING DECISIONS IN LAKE STURGEON?[3]

[3] To be submitted to Canadian Journal of Fisheries and Aquatic Sciences with C.W. Osenberg, S.J Wenger, D. Gorsky, and Z. Beisinger as co-authors.

Introduction

Life-history theory explains the evolution of breeding behavior as an optimization of trade-offs. It relates the allocation of time and resources to fitness components, such as maturation or egg production, while avoiding extrinsic mortality risk (Stearns 1989, Roff 2002). The timing and frequency of breeding is often explained by trade-offs between the rewards of current reproduction that are weighed against the risks of waiting to reproduce. These trade-offs are often illustrated using the concept of residual reproductive value (Williams 1966, Pianka and Parker 1975). In increasingly human-dominated landscapes, breeding behaviors that evolved under ancestral conditions may prove detrimental in new environmental conditions (e.g., arising from climate change or harvesting). Predicting how organisms will respond to such changes first requires an understanding of how they respond to contemporary environmental variation.

Skipped breeding, in which a reproductively mature individual does not attempt to reproduce during a breeding event, is common in nature and is typically conceptualized as a response to unfavorable breeding conditions (e.g., Sol and Maspons 2015). For example, animals may choose to breed "later" rather than "now" because they have amassed insufficient resources for egg production (Jørgensen et al. 2006) or parental care (Castro 1996), or because they perceive an elevated mortality risk under given conditions. In other words, the current reproductive potential is lower than the residual reproductive value if breeding is skipped, making it advantageous to wait to breed. In annually breeding species, breeding may be skipped in one or consecutive years, depending on the magnitude of the costs (Bull and Shine 1979, Jouventin and Dobson 2002). Two classes of factors can produce skipped breeding: flexible breeding decisions that respond to extrinsic environmental variation, or fixed breeding schedules that are invariant: e.g., arising from the time or energy requirements tied to gamete production.

Ultimately, it is important to know how the incidence of breeding of individuals may vary across years, and whether that variation is driven by intrinsic or extrinsic factors in order to predict the fraction of a population that breeds in a given year.

Lake sturgeon (*Acipenser fulvescens*) are imperiled across much of their range (Bruch et al. 2016), and managers may be interested in how anthropogenic changes such as climate change, land-cover change, and hydropower development affect their population growth. The relationship between population growth and anthropogenic changes depends in part on how often individuals breed, but lake sturgeon often skip breeding, so we investigate skipped breeding in lake sturgeon and its covariation with the environment. Lake sturgeon migrate from downstream habitats in lakes or large rivers to upstream natal riverine habitats where adult fish aggregate to spawn (Harkness and Dymond 1961, Scott and Crossman 1973). Females breed less frequently than males (Harkness and Dymond 1961, Shaw et al. 2012, Pledger et al. 2013), and have much lower annual mortality rates and longer lifespans (Bruch 2008, Vélez-Espino and Koops 2009). This combination of traits suggests lake sturgeon may make facultative spawning decisions based on environmental conditions in any year, but that trade-offs associated with spawning decisions might differ between males and females. The within-year timing of lake sturgeon spawning appears strongly responsive to water temperature (Bruch and Binkowski 2002, Dammerman et al. 2019), suggesting annual temperature variation may affect fitness. If so, then water temperature might also affect the likelihood that sturgeon will breed in any given year, and thus shorten or lengthen the time interval between spawning events. Alternatively, evidence from lake sturgeon in Black River (Michigan, USA) indicates highly consistent spawning intervals in individual fish, suggesting that breeding behaviors in some populations may be fixed at the individual level (Forsythe et al. 2012).

We focus on a population of lake sturgeon in the lower Niagara River (New York, USA and Ontario, Canada) that was once considered extirpated (Carlson 1995). Niagara River lake sturgeon have experienced a recovery since the 1990s (Withers et al. *in press* 2019, Hughes et al. 2005). Lake sturgeon in the lower Niagara River breed in rocky fast-water habitats positioned amid the outflows of two large hydropower projects, where an active recreational angling community targets sport fishes. Thus, understanding how intrinsic (sex) and extrinsic (temperature) factors contribute to periodic breeding (and migration) could also help predict variation in exposure to hydropower- and angling-associated risks in response to changes in climate or population structure (e.g., sex ratio).

Because sturgeon migrate to breed, their seasonal movement patterns can be used as a proxy of their breeding status. If seasonal movements can be distilled into distinct movement classes or "states", multi-state capture-mark-recapture models quantify transitions between breeding and non-breeding states while accounting for imperfect detection of individuals (Fujiwara and Caswell 2002, Schaub et al. 2004). We used multi-state capture-mark-recapture models to test whether interannual transitions between breeding and non-breeding states varied with sex and water temperature. We extended the multi-state Cormack-Jolly-Seber (CJS) framework of Schaub et al. (2004) and Kéry and Schaub (2012) to infer breeding status from one physical capture dataset and two telemetry datasets, and from these data we estimated annual survival, detection probability, and transition rates between breeding and non-breeding states. We then explored the effects of temperature, sex, and sampling effort on those modeled parameters. Since there is evidence in the literature that both sex and environmental variation may influence lake sturgeon spawning behavior, we tested the hypotheses that (1) males

transition between breeding and non-breeding states more frequently than females, and (2) transition rates vary in response to the timing of warming waters in the spring (March – June).

Materials and Methods

Site description

The Niagara River runs 56 km northward from Lake Erie to Lake Ontario and is divided along its path by the Niagara Falls. The 25 km reach from the Niagara Falls to Lake Ontario is the "lower" Niagara River and contains a 14-km high-gradient section through the Niagara Gorge that is characterized by steep banks, scoured rock and boulder substrate, and rapids ("gorge" habitat) followed by an 11 km section characterized by a broader width, mid-channel depths between 10 and 52 m, lower current velocity, and backwater depositional areas. Historical May 1 flow rates for the Niagara River average 6,088 m^3 s^{-1} (USGS 2016). At the lower Niagara River mouth, Lake Ontario is characterized by depositional sediments and relatively shallow depths (< 20 m). Our study site extends from Lake Ontario, through the lower Niagara River, and into the Niagara Gorge (Figure 3.1). Lake sturgeon breed in the gorge habitat (the 11 km stretch in the upstream portion of our study site), and we therefore used the presence of a sturgeon in the gorge to infer that the individual attempted to breed that year. Importantly, all fish are found in the non-breeding habitat outside of the breeding season, so breeding individuals use both breeding and non-breeding habitats within a single year.

Water temperature

Water temperature data were available from the National Weather Service (https://www.weather.gov/buf/LakeTemp, downloaded: 2/28/2018) for the years of our study, 2011 to 2017. During those years, there was considerable variation in the day of year (i.e., assigning January 1st as day 1) at which temperatures rose from winter lows to 5˚ C, a

temperature just below the range associated with the onset of lake sturgeon breeding behavior (6.6˚ C; Bruch and Binkowski 2002) (Figure 3.2). Thus, we recorded the day of year when water temperatures first exceeded 5˚ C as a measure of the timing of spring water warming conducive to lake sturgeon breeding (Hereafter "DOY5").

Biotic data

Lake sturgeon were monitored during the 10th through 30th weeks of the year (early March to late-July) from 2011 through 2017 in the lower Niagara River as part of a population status assessment. We used data from three types of observations– physical capture, radio telemetry, and acoustic telemetry– in the lower Niagara River to derive and analyze annual multi-state capture histories of individual lake sturgeon for joint estimation of survival, transitions between breeding and non-breeding states, and observation probabilities in the two primary regions of the system (the gorge and elsewhere). Each of these datasets would have inadequate power to estimate parameters of interest if analyzed independently, but the integrated model approach makes the joint estimation of parameters more precise (Powell et al. 2000).

Capture, measure, mark, release -Fish were captured between 2011 and 2017 between the 10^{th} and 30^{th} weeks of each year using 80-m set lines, each with 25 baited hooks, set on the bottom overnight in flow transition zones indicated in Figure 3.1. Two to 8 lines were set per night for 1-4 nights per week. Location at capture was recorded, and all fish were individually marked with PIT tags and external spaghetti or ring tags (or if previously marked, they were identified), assessed for length, weight, spawning status (external), and age (fin spine sample), and then released. Physical capture only occurred in the non-breeding habitats outside of the gorge, to avoid concerns about safety and sampling efficiency due to high flow conditions within the gorge during hydropower peaking operations.

Sex classification -Lake sturgeon cannot reliably be sexed via external traits, so we used multiple methods to confirm or infer the sex of fish in our study (Appendix D). Briefly, (1) we directly observed extruded gametes or reproductive organs (via surgical methods or ultrasound), allowing us to classify known-sex fish; (2) we collected blood samples from known- and unknown-sex fish to quantify the sex steroids, testosterone (T) and 17β-estradiol (E2); and then (3) we used paired known-sex fish and steroid profile information to train a classification algorithm (classification regression tree) to predict the sex of fish for which we only had sex steroid information (Webb et al. 2002, 2019, Allen et al. 2009, Webb and Doroshov 2011). Sample collection methods, analysis methods, and the resulting sex classifications used in the integrated CJS model are detailed in Appendix D.

Telemetry

Radio telemetry - We surgically implanted 63 fish with ATS F1800-series enhanced-signal trailing-whip radio transmitter tags during 2012 (n = 33) and 2013 (n = 30; Advanced Telemetry Systems, Isanti, MN, USA). The location of these fish was monitored from 2012 through 2014 with a fixed-station array of ATS R4500 data logging radio telemetry receivers deployed across the Niagara River in both non-reproductive and reproductive habitats (Figure 3.1). Radio transmitter tag batteries lasted two years: the year of tag implantation, and the year following, so the contribution of these tags to parameter estimation in our model was constrained to only those two years.

Acoustic telemetry - We surgically implanted 90 fish with Vemco V16-6H acoustic transmitters (Vemco Ltd, Halifax, NS, Canada) in 2014 – 2016 (n = 30 per year). Tags were programmed with a randomized transmission routine expected to reduce signal interference between tags, and to result in an approximate 10-year battery life (Bruestle 2017). An array of

Vemco VR2W passive acoustic receivers was maintained in the Niagara River and nearby Lake Ontario from 2014 to 2017 to monitor the location of tagged lake sturgeon in both non-reproductive and reproductive habitats (Figure 3.1).

Capture-mark-recapture model

Data structure - Multi-state capture-recapture models require that observation data represent detection and (if detected) the state in which the animal was observed when detected. In this study, our state variable, $z_{(i,t)}$, could take one of three values: breeding (1), non-breeding (2), and dead (3). We evaluated transitions between breeding and non-breeding, and from non-breeding and breeding to dead by tracking observations of a breeding state of fish i in year t, $y_{k(i,t)}$, to be equal to 1 ("breeding") if the fish was observed in the gorge at any point during that year's sampling period, and equal to 2 ("non-breeding") if the fish was only observed in non-gorge habitats during the year. We used three data sets (physical capture, radio telemetry, and acoustic telemetry), which we assumed resulted from three separate observation processes. Fish may have been unobserved in any of these datasets either because of imperfect detection, or because they were dead and undetectable by our methods.

We specified three covariates for the model. First, sampling effort ($\mathrm{E}_{(t)}$) reflected annual variation in the number of days of sampling effort for the physical capture dataset, $y_{1(i,t)}$, within the 21 week sampling period. Effort was measured in the number of nights set lines were fished during the 21 week sampling period. Second, our temperature variable, $\mathrm{X}_{(t)}$, was the day of the year when rising water temperatures in the Niagara River first exceeded 5˚ C, DOY5. Third, our sex variable, $\mathrm{G}_{(i)}$, indicated whether each individual was male ($\mathrm{G}_{(i)} = 1$), female ($\mathrm{G}_{(i)} = 0$), or unknown ($\mathrm{G}_{(i)} = NA$). Our effort $\mathrm{E}_{(t)}$ and temperature ($\mathrm{X}_{(t)}$) variables were centered and standardized to have a mean of 0 and standard deviation of 1.

Model structure - We conducted a joint analysis of the three multi-state capture-mark-recapture datasets using a Cormack-Jolly-Seber model structure. We estimated variation in state transitions (i.e., breeding to non-breeding, non-breeding to breeding, breeding to dead and non-breeding to dead) while accounting for (a) variation in survival across years and sexes, (b) the probability of observing sturgeon in breeding or non-breeding states, which varied by dataset, effort, and sex, and (c) the probability of mis-assignment of fish to states. Notably, the probability of observing breeding states varied with dataset, effort, and sex, and the probability of incorrectly assigning states was influenced by the dataset. We also evaluated if the state transitions were influenced by sex ($G_{(i)}$) and/or temperature ($X_{(t)}$). The Cormack-Jolly-Seber (CJS) model jointly estimates survival and observation (i.e., recapture) probabilities (Cormack 1964, Jolly 1965, Seber 1965), while assuming that populations are open to births, deaths, immigration, and emigration between survey periods, and that individuals are identified without error.

We constructed a Bayesian state-space MS-CJS model to assess survival and variation in migration behavior in lake sturgeon (Royle 2008, Kéry and Schaub 2012). The model time-step is 1 year, and the data that we used were restricted to the spring and early summer (weeks 10 – 30 of each year). The latent state process of our 3-state MS-CJS model is described by the transition matrix, A, elements of which control stochastic inter-annual transitions among three states: breeding, non-breeding, and dead. We modeled variation in transition rates $\psi_{u(i,t)}$ by origin state (u), and across individuals (i) and time (t), such that the state transition matrix also varied by individual i and time t:

$$A_{(i,t)} = \begin{bmatrix} \phi_{(i)}(1-\psi_{1(i,t)}) & \phi_{(i)}\psi_{2(i,t)} & 0 \\ \phi_{(i)}\psi_{1(i,t)} & \phi_{(i)}(1-\psi_{2(i,t)}) & 0 \\ 1-\phi_{(i)} & 1-\phi_{(i)} & 1 \end{bmatrix} \quad (1)$$

where $\phi_{(i)}$ is the annual survival probability, $\psi_{1(i,t)}$ is the annual transition probability from state 1 (breeding) to state 2 (non-breeding), and $\psi_{2(i,t)}$ is the annual transition probability from state 2 to state 1. The transition matrix $\mathrm{A}_{(i,t)}$ governs transitions among all states in the model, whether the states are observable or not (e.g., the "dead" state, $z_{(k,i,t)} = 3$, is unobservable). In our models, we estimated variation in survival rate ($\phi_{(i)}$) by sex($\mathrm{G}_{(i)}$), and sex- and time-variation in the transition probabilities ($\psi_{1(i,t)}$ and $\psi_{2(i,t)}$) by sex and the timing of warming water ($\mathrm{X}_{(t)}$) by fitting logistic regression sub-models according to equations,

$$\mathrm{logit}\left(\phi_{(i)}\right) = \gamma_0 + \gamma_1 \mathrm{G}_{(i)} \tag{2}$$

and

$$\mathrm{logit}\left(\psi_{u(i,t)}\right) = \beta_{0(u)} + \beta_{1(u)}\mathrm{G}_{(i)} + \beta_{2(u)}\mathrm{X}_{(t)} + \beta_{3(u)}\mathrm{G}_{(i)}\mathrm{X}_{(t)} \tag{3}$$

Observation process - For each individual (i), in time (t), an observation matrix (P_k) described observed data in dataset k (1 for physical capture, 2 for radio telemetry, and 3 for acoustic telemetry) as a function of the latent state variable $z_{(i,t)}$, imperfect detection, and imperfect state assignment:

$$\mathrm{P}_{k(i,t)} = \begin{bmatrix} p_{k(1,i,t)}\left(1 - \varepsilon_{k(t)}\right) & 0 & 0 \\ p_{k(1,i,t)}\varepsilon_{k(t)} & p_{k(2,i,t)} & 0 \\ 1 - p_{k(1,i,t)} & 1 - p_{k(2,i,t)} & 1 \end{bmatrix} \tag{4}$$

where $p_{k(u,i,t)}$ is the probability of observing a fish in the breeding state $z = u$ in dataset k, and $\varepsilon_{k(t)}$ is the probability that when a breeding-state fish was observed, it was incorrectly assigned the non-breeding state in dataset k. We assumed that a fish observed in breeding habitats were in the breeding state. However, we assumed that some breeders may not have been observed in the gorge, and some individuals that were breeding were misclassified. The $\varepsilon_{k(t)}$ parameter represents this misclassification. We estimated state assignment error for both telemetry datasets.

However, the physical capture method only occurred in the non-breeding habitat; thus the state assignment error for breeding individuals in the physical capture dataset was 100%, so we set $\varepsilon_1 = 1$.

The estimation of observation probability was most complex for the physical capture dataset. We modeled variation in observation probabilities for the physical capture dataset as a state-specific (u) logistic regression model with parameters accounting for the effects of sampling effort $\mathrm{E}_{(t)}$, and sex $\mathrm{G}_{(i)}$,

$$\mathrm{logit}\left(p_{1(u,i,t)}\right) = \alpha_{0(u)} + \alpha_{1(u)}\mathrm{E}_{(t)} + \alpha_{2(u)}\mathrm{G}_{(i,t)} + \alpha_{3(u)}\mathrm{E}_{(t)}\mathrm{G}_{(i,t)}. \quad (5)$$

The estimation of observation probability for the telemetry datasets ($k = 2$ and $k = 3$) was somewhat simpler, since telemetry effort was consistent across years, and distributed across both breeding and non-breeding habitats. We estimated telemetry observation probabilities, $p_{2(u,c)}$ and p_3, directly on the probability scale (see "Bayesian priors and constraints" section). For the radio telemetry observation process we assumed that trailing whip antennas and expected tag life of less than 2 years would increase the risk of tag failure and decrease detectability for the second year tags were deployed. We constrained the model to assume that radio tags were undetectable after 2 years, and indeed none were observed after that period of time in the field. Thus, we modeled radio telemetry observation probability that varied with the duration tagged, $p_{2(u,c)}$, where u is the latent migration state, and c is either 1 for the first year radio tagged ($f_{2(i)}$) or 2 for the year after ($f_{2(i)} + 1$). For acoustic telemetry, we assumed constant observation probability for fish in each state, $p_{3(u)}$, because no tag in this study was deployed for longer than its expected 10-year tag life.

First capture contingency - We estimated state transition and observation parameters contingent on the assumption that the observed state at first capture equaled the true state,

$y_{k(i,f_{(i)})} = z_{(i,f_{(i)})}$, where $f_{(i)}$ is defined as the year t that fish i was first observed. This model specification has two consequences. First, contingency on first capture means that only recaptures of animals inform parameter estimates, and any information that may be derived from the first capture year (also called an "occasion") is ignored. Second, the state at first capture is deterministic and defined by the first observation in the data. In our system, all individuals were physically captured in non-breeding habitats ($y_{1(i,t)} = 2$). But after release, some of these individuals could have migrated to breed, if they were in the breeding state ($z = 1$). This means that states were imperfectly classified in our datasets, and first observations from multiple datasets $y_{k(i,f_{(i)})}$ could have differed during the first capture occasion $f_{(i)}$. For example, if a fish was captured for the first time using physical capture, it would have been assigned the non-breeding state in the physical capture data even if it was actually in the breeding state. However, if that same fish was also radio tagged during the first year it was tagged, and then observed in the breeding habitat using radio telemetry methods, it would have been classified as a breeding individual in the radio telemetry dataset. Given a situation where the physical capture dataset classified a fish as "non-breeding" during the first year it was observed, $f_{(i)}$, but a telemetry dataset classified the same fish during the same sampling year as "breeding", we defaulted to the "breeding" classification. All subsequent state classifications were then informed by a stochastic imperfect state assignment process. We defined our model contingent on the furthest upstream state observed across all observation datasets during the first capture occasion, which simplified to the minimum of our state variable $z_{(i,t)}$ across datasets during $f_{(i)}$,

$$z_{(i,f_{(i)})} = \min\left(y_{1(i,f_{(i)})},\ y_{2(i,f_{(i)})},\ y_{3(i,f_{(i)})}\right). \quad (6)$$

Bayesian priors and constraints - We used Bayesian methods for estimation, requiring that we specify prior distributions for each parameter. Since we had information on the sex of

only a subset of marked individuals in our dataset, we treated the sex of unknown-sex individuals as stochastic variables where sex ($G_{(i)}$) was drawn from a Bernoulli distribution with probability θ, representing the proportion of unknown sex fish that were male, $G_{(i)} \sim \text{Bernoulli}(\theta)$, where i indexes individuals for whom $G_{(i)} = NA$, and where we provided an informative prior on θ reflecting an expected population sex ratio near 0.5, $\theta \sim \text{Beta}(3,3)$. We use this stochastic assignment procedure for all individuals with unknown sex so that we could use information about individuals whose sex was known to improve our estimation of the sex ratio and the effect of sex on other parameters. Additionally, this allowed us to apply the uncertainty associated with the subsequent sex assignments to the parameters we estimated with our models.

We used an informative prior on the logit-intercept for survival, $\gamma \sim \text{Normal}(2.2,2)$, corresponding to an an average annual survival probability of near 0.9 (SD from 0.54 to 0.98), given evidence from this and other lake sturgeon populations (Vélez-Espino and Koops 2009, Pledger et al. 2013, Withers et al. 2019). Remaining coefficients of the logistic regression equations, γ_1, $\beta_{0(u)}$, $\beta_{1(u)}$, $\beta_{2(u)}$, $\beta_{3(u)}$, $\alpha_{0(u)}$, $\alpha_{1(u)}$, $\alpha_{2(u)}$, and $\alpha_{3(u)}$, were given Gaussian priors with a mean of 0 and a standard deviation of 2, which are weakly informative on probability scale (Hobbs and Hooten 2015, Northrup and Gerber 2018). Radio and acoustic telemetry parameters were estimated on the probability scale and were given flat uniform priors from 0 to 1. We also used flat uniform prior distributions between 0 and 1 for the telemetry state assignment error parameters, ε_2 and ε_3.

Derived parameters - We allowed survival to vary by sex, such that the survival rate of females was defined by γ_0 (i.e., $\text{logit}(\phi_F) = \gamma_0$), and that of males was defined by γ_0 and γ_1 (i.e., $\text{logit}(\phi_M) = \gamma_0 + \gamma_1$). After stochastic assignment of sex to unknown-sex fish in $G_{(i)}$ each

iteration, we calculated an estimated population sex ratio (number of males per female), $PSR = \frac{n(G=1)}{n(G=0)}$).

Transition probabilities were also allowed to vary by sex, such that sex-specific average transition rates were a function of the equations, $\text{logit}(\overline{\psi}_{F(u)}) = \beta_{0(u)}$ and $\text{logit}(\overline{\psi}_{M(u)}) = \beta_{0(u)} + \beta_{1(u)}$. We subsequently used these average rates to estimate breeding frequency (the average breeding interval length, T) for each sex. We defined T as the number of years between two sequential breeding bouts, such that a periodicity of $T = 1$ indicates that a fish breeds each year, and $T = 2$ indicates breeding every other year. The probability of returning to breed in two consecutive years in our system is $1 - \overline{\psi}_{(1)}$, the probability that a fish does not transition out of the breeding state. However, the probability of not returning to breed for 2 years is the product of the probability of migrating from breeding to non-breeding $\overline{\psi}_{(1)}$, the probability of remaining in the non-breeding state for $t - 2$ years ($(1 - \overline{\psi}_{(2)})^{t-2}$), and the probabilty of transitioning from non-breeding to breeding $\overline{\psi}_{(2)}$. Hence, the average breeding interval T was calculated as the sum of the probabilities of transitioning from state 1 back into state 1 in t time-steps, multiplied by t. We calculated the interval T across return intervals from $t = 1$ to $t = 100$ years,

$$T_F = \left(1 - \overline{\psi}_{F(1)}\right) + \sum_{t=2}^{100} \left(t \times \overline{\psi}_{F(1)} \times \left(1 - \overline{\psi}_{F(2)}\right)^{t-1} \times \overline{\psi}_{F(2)}\right) \quad (7)$$

where the equation for T_M is identical except for using the parameters $\overline{\psi}_{M(u)}$ instead of $\overline{\psi}_{F(u)}$.

Model estimation - We analyzed our model using Markov-Chain Monte Carlo (MCMC) estimation in JAGS 4.3.0 (Plummer 2017), implemented in the program R version 4.0.2 (R Core Team 2020) using the R package runJAGS (Denwood 2016). Posterior parameter estimates were drawn from 50,000 posterior sampling iterations in each of three MCMC chains that followed

1,000 iterations of adaptation and 50,000 iterations of burn-in. Convergence was assessed using the $\hat{R}$ statistic (Gelman and Rubin 1992) and by visually inspecting and comparing the MCMC sample traces and posterior sampling distributions for each chain. We summarize parameter estimates by their median and 90% highest density interval (HDI) which is a credible interval that contains the 90 % most probable parameter values from the posterior distribution, and is not constrained to be equal-tailed (i.e., the interval will skew to match that of the posterior distribution) (Kruschke and Liddell 2018).

Results

Fish summary

Our analysis included a total of 797 sturgeon captured and marked in 2011 through 2016, and 122 recaptured in 2012 through 2017. These fish averaged 138 cm total length (SD = 13 cm), and the size distribution of captured fish appeared to shift to larger sizes through time suggesting a consistent cohort structure with little recruitment during the study (Figure 3.4). One hundred and sixteen fish were of known sex (59 female, 57 male), and we were able to infer the sex of another 44 fish (28 male and 16 female) based on their sex steroids (leave-one-out cross validation error rate: 86.2%, Appendix D). Among the 122 fish recaptured, 19 were female, 20 were male, and 83 were unclassified. Of these recaptured fish, 11% of recaptured females (2/19), 20% of recaptured males (4/20), and 13% of unclassified recaptured fish (11/83) were observed visiting the spawning grounds more than one year consecutively.

Covariate summary

Long term average low temperature occurred on DOY 44 at the Buffalo water intakes (USGS 2016) (Figure 3.2). During our study, water temperatures rose from annual lows to 5˚ C by DOY 115, on average, and varied among years with a standard deviation of 11.8 (Figure 3.3

b). The range in DOY5 we observed during our study (DOY5 = 97 – 132) was within the range of DOY5 values observed across all years prior to this study (DOY5 = 96 – 146) (Figure 3.2). Physical capture sampling effort averaged 23.7 nights (SD = 7.8) during weeks 10-30 of each year (Figure 3.3 ab). Fishing nights occurred during 5 to 14 weeks within the 21-week sampling period each year (mean = 9.75 weeks, SD = 3.7).

Model results

Our model indicated no strong effect of either sex or DOY5 on the transition of sturgeon from a breeding state to a non-breeding state (ψ_1), as the 90% HDI overlapped zero for the coefficients $\beta_{1(1)}$, $\beta_{2(1)}$, and $\beta_{3(1)}$ (Table 3.1). In contrast, we found the transition from non-breeding to breeding (ψ_2) was weakly influenced by a sex-by-DOY5 interaction ($\beta_{3(2)}$ = 1.47, HDI = -0.81 – 1.68); females transitioned from non-breeding to breeding less often as DOY5 increased (i.e., later warming), whereas male transition probabilities were not responsive to DOY5 variation (Table 3.1, Figure 3.5). Under average conditions, transition probabilities were roughly 50% in both directions for males ($\overline{\psi}_{M(1)}$ = 0.45, HDI = 0.24 – 0.64; $\overline{\psi}_{M(2)}$ = 0.51, HDI = 0.33 – 0.68). In contrast, the probability of transition from the non-breeding to the breeding state for females was more disparate ($\overline{\psi}_{F(1)}$ = 0.59, HDI = 0.37 – 0.83; $\overline{\psi}_{F(2)}$ = 0.26, HDI = 0.11 – 0.41) although uncertainty in these parameters was considerable. We observed a male-biased population sex ratio of 1.86 (HDI: 0.20 – 3.72) males per female. We estimated an annual survival rate of 0.99 (HDI = 0.97 – 1.00) for males and 0.96 (HDI = 0.92 – 0.99) for females.

Resulting estimates of breeding interval T under average spring warming conditions (DOY5 = 115) indicated 2.94 years (HDI = 2.40 - 3.48) for males and 4.64 years (HDI = 2.71 - 6.56) for females. To the extent that our model supports an interaction between DOY5 and sex, increases in DOY5 (e.g., resulting from climate cooling) would increase the difference in

breeding frequency between males and females ($T_F \gg T_M$), whereas decreases in DOY5 (e.g., due to climate warming) would make male and female intervals more similar ($T_F \approx T_M$).

The average probability of recapturing a fish was on the order of 3-4 %: logistic regression intercepts were $\alpha_{0(1)}$ = -3.24 (HDI = -4.21 – -2.26) for breeding individuals and $\alpha_{0(2)}$ = -3.60 (HDI = -4.33 – -2.85) for non-breeding individuals. There was some support for an effect of effort (E) on observation probability in the physical capture dataset, but less for sex (G), and very little for an E × G interaction (Table 3.2; Figure 3.6). Observation probabilities were much higher in the telemetry datasets, approaching 100% for radio telemetry observation during the first year a tag was deployed (for breeding fish: $p_{2(1,1)}$ = 0.97, HDI = 0.93 – 1.00; and for non-breeding fish: $p_{2(2,1)}$ = 0.97, HDI = 0.93 – >0.99), and declining the second year to approximately 20% ($p_{2(1,2)}$ = 0.21 (HDI = 0.07 – 0.35); $p_{2(2,2)}$ = 0.14 (HDI = 0.03 – 0.25)). The acoustic telemetry dataset also yielded very high observation probabilities, which we assumed were invariant across years due to the long battery life ($p_{3(1)}$ = 0.99, HDI = 0.97 – >0.99; $p_{3(2)}$ = 0.99, HDI = 0.98 – >0.99). State assignment error was very small for telemetry datasets: ε_2 = 0.03 (HDI = <0.01 – 0.08) and ε_3 = 0.08 (HDI = <0.01 – 0.18), suggesting that most observed fish were correctly assigned to breeding vs. non-breeding.

Discussion

We present evidence that warmer temperatures occurring earlier in the spring may increase the reproductive frequency of female lake sturgeon, but not of males. Our results indicate that warmer springs are associated with increased likelihood that sexually mature females engage in breeding migrations. The Laurentian Great Lakes have been increasing in temperature and decreasing in winter ice cover for at least the past half-century (Mason et al. 2016, White et al. 2018), resulting in earlier warmer water temperatures in the spring across

much of the Great Lakes. Research has suggested that increased temperature may influence tradeoffs associated with mortality risk, time investment, or energy availability (sensu Shaw and Levin 2013). Therefore, temperature-induced changes to breeding behavior may be detrimental to population growth and management.

The covariation of breeding frequency with spring warming may have important implications for population dynamics. For example, if spawning were to increase in frequency, then individuals could bear higher mortality risk and lower per-capita reproductive success in order to maintain the same lifetime reproductive rate. Conversely, to maintain the same reproductive rate under decreased breeding frequency, there must be a commensurate increase in the breeding success of females during periods when they do spawn. However, the ability to respond to changing environmental conditions may be limited by biotic and environmental constraints such as limited resource availability or development time; hence, changes in breeding frequency may come with substantial tradeoffs. Sturgeons are either polyandrous or polygynandrous (Jarić et al. 2018), so if warming yields more frequent breeding by females (but not males), then the higher proportion of breeding females could increase population growth rate (all else being equal). However, fecundity may be constrained by the rate of energy acquisition for egg production, producing a trade-off between spawning frequency and fecundity. Under such a trade-off, females that breed more often, but at lower fecundities, may not increase population growth rate.

What affects breeding frequency?

There is tremendous variation in spawning intervals that have been reported for lake sturgeon. Some sources report spawning intervals as short as one year (i.e., returning every year) to three years (Forsythe et al. 2012, Shaw et al. 2012, Pledger et al. 2013), while others report

intervals as long as five to 10 years (Scott and Crossman 1973). Conducting additional years of capture-mark-recapture methods, especially for high-detection-probability methods like acoustic telemetry (Krueger et al. 2018), could provide data for a more precise comparison among populations, and between sexes within the lower Niagara River. Prior research, as well as our own, demonstrates that breeding intervals vary between sexes, but more could be done to explain differences in spawning intervals – or their estimates – among populations.

To our knowledge, our study is the first to demonstrate that inter-annual breeding frequency is affected by water temperature. Dammerman et al. (2019), also working with lake sturgeon, observed that reproductive success increased with temperature within a breeding season, which may suggest an incentive for female sturgeon to decide to spawn during warmer years. However, they also found that stream discharge and the number of males on the breeding site may have just as strong an influence on reproductive success as temperature (Dammerman et al. 2019).

Age has also been shown to drive variation in breeding frequency in other species of fish (e.g., Dolly Varden charr, *Salvelinus malma*; Gallagher et al. 2019, Bond et al. 2015), with older fish breeding more frequently than larger fish. Though we did not investigate an age effect on breeding frequency in our lake sturgeon, we hypothesize that they may increase their spawning frequency as they age and residual reproductive value declines.

Sex ratio and survival

Population sex ratio can be affected by sex-specific survival. For example, Arendt et al. (2014) found female-biased sex ratios in Trinidadian guppy (*Poecilia reticulate*) that were attributable to differences in survival rate and lifespan, both of which are greater in females. Operational sex ratio, the sex ratio of breeding individuals, is male-skewed in lake sturgeon due

to a more frequent spawning in males than in females (Harkness and Dymond 1961, Auer 1999, Forsythe et al. 2012, this study), but we expected population sex ratios, the sex ratio of all breeding and non-breeding individuals in the population, to be female-biased as in other lake sturgeon populations (Shaw et al. 2012), due to higher mortality and shorter lifespan in males (Bruch 2008). However, we observed a male-biased population sex ratio of 1.86 males per female, though the credible interval was very wide indicating high uncertainty. Annual survival probability of our study population was very high for both males (0.99, HDI: 0.97 - >0.99) and females (0.96, HDI: 0.93 – >0.99). These findings are comparable to survival rates of lake sturgeon in the Black River system as estimated by Pledger et al. (2013) for males (0.98, 95% Confidence Interval (CI): 0.96 – 0.99) and for females (0.98, 95% CI: 0.87 – 1.0)). However, other research has produced lower estimates of survival (e.g., Withers et al. 2019). Furthermore, estimates of male survival in lake sturgeon are generally lower than those of females (e.g., Bruch 2008, Vélez-Espino and Koops 2009). Our study suggests that survival rate may not differ substantially between sexes, at least for the animals in our population. Notably, the age structure of the study population was comprised of younger adult cohorts (Withers et al. *in press*); thus, young juveniles or individuals in senescent stages, which are expected to have much lower survival, were not commonly found during the period of study.

Integrated analysis

Our physical capture rates were quite low, and the relatively short duration of our study yielded few occasions during which breeding state transitions could be observed. However, by tracking individual fish with multiple capture-mark-recapture datasets, we were able to more accurately estimate observation probability using integrated model analysis (Powell et al. 2000,

Lee et al. 2015, Zipkin and Saunders 2018). Our model estimates borrowed strength across multiple datasets that partially overlapped in time, locations, and individual fish.

Caveats

We made several important assumptions to conduct our analyses. Initially, we assumed that lake sturgeon in the gorge were breeding even though it was located close to the area we classified as "non-breeding". The occurrence of individual lake sturgeon in their breeding grounds may not result in breeding if (a) individuals refrained from spawning and reabsorbed their gametes, (b) the fish was not in spawning condition, or (c) the fish died after migration, but prior to reproducing. Mortality in the gorge seems the least likely of these possibilities, given our high survival estimates. The failure of mature organisms to breed is not uncommon. In semelparous sockeye salmon (*Oncorhynchus nerka*), pre-spawning mortality of mature individuals can result from poor environmental conditions, especially at high conspecific density (Tillotson and Quinn 2017). Similarly, iteroparous animals may encounter conditions that evoke a skipped breeding response, as has been observed in cod in response to low resource availability (Jørgensen et al. 2006), or higher body burdens of contaminants (Tartu et al. 2013). Even within-season delays of reproduction may result in reduced reproductive success of female lake sturgeon (Dammerman et al. 2019), though unspent eggs are reabsorbed after the breeding season, so recovery of some of that energetic investment may shorten the time to the next breeding season. Nevertheless we expect that the energy cost of a failed breeding season is substantial.

The possibility that immature fish migrate to spawning grounds may also confound our results. Migration in some taxa is a learned behavior (e.g., in birds, Able and Able 1998), and there is evidence that the same is true of many fish species (Dodson 1988, Rose 1993, Petitgas et

al. 2006). Such learned migration behavior, where juveniles "go with the older fish", may increase the degree of spatial aggregation during the breeding season and increase the population's vulnerability to harvest (MacCall et al. 2018). Sequential breeding bouts are not unexpected for males, but should be unlikely in female lake sturgeon, given our results and under the assumption that only breeding animals migrate. We observed sequential-year visits to the breeding habitat in four male-classified individuals (20% of the males observed in multiple years), reasonable behavior for organisms that can breed annually. However, the observation of sequential-year visits in two female-classified individuals (~10% of the females observed in multiple years) is high when compared to observations from other comparable studies (e.g., 0 sequential-year visits of 69 females observed during multiple years across an 8-year period; Forsythe et al. 2012). If migration of immature lake sturgeon occurs, then our estimates of the intervals T_M and T_F may be biased low when interpreted as a breeding interval (as we have here), though still unbiased if interpreted as a migration interval. In shortnose sturgeon (*Acipenser brevirostrum*), telemetry methods failed to document immature fish migration to breeding habitats over many years and across several populations (Kieffer and Kynard 2012), so the assumption that migration of immature fish is rare may be credible. However, this would be an important assumption to test with future work.

In migratory species, the distance between migratory habitats may influence the costs of migration, and thus the frequency of engaging in breeding migrations. For some organisms, breeding mostly occurs annually, and skipped breeding may only occur in response to poor environmental conditions or poor physiological state (e.g., Rideout and Tomkiewicz 2011, Johnston and Post 2009, Dammerman et al. 2019). For other organisms, the frequency of skipped reproduction may be invariant due to individual-level constraints (e.g., Jouventin and Dobson

2002). Kieffer and Kynard (1996) suggested that in areas where shortnose sturgeon foraging habitats are more productive and the close proximity of breeding and overwintering habitats require shorter migrations, males migrate more frequently (annually) than those of other shortnose sturgeon populations. Lake sturgeon are longer-lived and later-maturing. They also have longer inter-spawning periods than shortnose and other sturgeons. Yet, the breeding and non-breeding habitats in the lower Niagara River are in relatively close proximity, so more frequent breeding migrations as documented by Kieffer and Kynard (1996) may be expected. Neither the lower Niagara River population nor the well-studied Black River population have terribly long-distance migrations between breeding and foraging grounds, so similar frequencies would be expected.

We assumed that breeding decisions made by sturgeon were dependent only on whether individuals bred the previous year, but the probability of an individual returning may vary with the number of sequential years in which breeding was skipped. Pledger et al. (2013) structured a multi-state model with a breeding state, and a series of time-sequential non-breeding states for each year an individual refrained from spawning up to a maximum considered that (in their analysis) did not exceed 4 years. Shaw and Levin (2013) used an almost identical stage-structure in their evolutionarily stable strategy-analysis of time, energy, and mortality trade-offs that may have led to the evolution of breeding periodicity. The expanded multi-state structure of Pledger et al. (2013) and Shaw and Levin (2013) is well suited for evaluating the return interval as a fixed, repeated-timing trait of individual animals (also called “periodicity”; Pledger et al. 2013) or of the population or phenotype (Shaw and Levin 2013). In both studies, only one periodicity was “right” or “most likely”. The simpler two-state model (breeding, non-breeding) in our analyses allowed us to evaluate how breeding behavior varied with temperature, DOY5. Since

our results suggest the covariation between water temperature and breeding behavior may be sex-dependent, it would be interesting to expand our analysis and incorporate variation in breeding response to larger and more explicit models that incorporate stage-structured breeding periodicity to evaluate whether breeding behavior changes with the time since last breeding migration. However, such models would be much more data-hungry, requiring many additional years of observations that our dataset cannot accommodate.

Management implications

Lake sturgeon are a sport fish species in North America, and recreational angling is an explicit goal of US state and Canadian provincial government conservation efforts (e.g., Briggs et al. 2020). Harvest regulation is often place-based, and overlaying spatial variation in the mortality risk associated with harvest with the spatial distribution of target fishes is essential for determining sustainable harvest policy (Post and Parkinson 2012). Lake sturgeon populations are spatially heterogeneous through time due to their breed-and-feed style migratory behavior (sensu Shaw 2016). Importantly, harvest mortality rates may vary between the sexes because of differences in interannnual breeding frequency. Moreover, temperature-dependent interannual variation in female breeding frequency may cause the abundance and sex ratio of males and females to vary among years, which may complicate the development of effective management policy. Sex differences in breeding behavior can lead to differential harvest of one sex, but this bias should be unlikely to affect population growth if the non-limiting sex is at increased risk of capture (e.g., male Walleye, *Sander vitreus*; Bade et al. 2019). However, females are most likely the limiting sex in lake sturgeon, so the effects of environmental variables such as temperature on their breeding frequency are likely more consequential for population growth under harvest or other migration-associated mortality risks. Our results suggest that in a warmer world, female

lake sturgeon in the Niagara River may migrate to breed more often and could be exposed to higher angler mortality.

Table 3.1: Table of posterior median and 90% highest density intervals (HDI) for sex assignment, survival, and state transition variables.

	Median	HDI		$\hat{R}$
θ	0.60	0.29	0.93	1.03
PSR	1.86	0.19	3.72	1.02
γ_0	3.33	2.30	4.37	1.00
γ_1	1.31	-0.24	2.79	1.00
ϕ_F	0.96	0.92	0.99	1.01
ϕ_M	0.99	0.97	1.00	1.00
ϕ_{diff}	-0.03	-0.07	0.01	1.00
$\beta_{0(1)}$	0.39	-0.65	1.48	1.00
$\beta_{0(2)}$	-1.10	-1.95	-0.27	1.01
$\beta_{1(1)}$	-0.61	-1.95	0.67	1.00
$\beta_{1(2)}$	1.13	0.02	2.23	1.00
$\beta_{2(1)}$	0.02	-0.92	1.01	1.01
$\beta_{2(2)}$	-0.40	-1.24	0.46	1.01
$\beta_{3(1)}$	0.24	-0.97	1.44	1.00
$\beta_{3(2)}$	0.47	-0.81	1.68	1.01
$\overline{\psi}_{M(1)}$	0.45	0.24	0.64	1.00
$\overline{\psi}_{M(2)}$	0.51	0.33	0.68	1.00
$\overline{\psi}_{F(1)}$	0.59	0.36	0.83	1.00
$\overline{\psi}_{F(2)}$	0.26	0.11	0.41	1.00
T_M	2.94	2.40	3.48	1.00
T_F	4.64	2.71	6.56	1.01

Table 3.2: Table of posterior median and 90% highest density intervals (HDI) for parameters describing the physical capture and telemetry observation process.

	Median	HDI		$\hat{R}$
$\alpha_{0(1)}$	-3.242	-4.207	-2.262	1.00
$\alpha_{0(2)}$	-3.601	-4.325	-2.852	1.01
$\alpha_{1(1)}$	0.722	-0.359	1.809	1.00
$\alpha_{1(2)}$	0.646	-0.206	1.507	1.00
$\alpha_{2(1)}$	-0.623	-1.910	0.653	1.01
$\alpha_{2(2)}$	-0.451	-1.616	0.754	1.00
$\alpha_{3(1)}$	-0.122	-1.453	1.199	1.00
$\alpha_{3(2)}$	-0.402	-1.835	1.009	1.00
$p2_{1(1)}$	0.971	0.934	1.000	1.00
$p2_{2(1)}$	0.969	0.929	1.000	1.00
$p2_{1(2)}$	0.211	0.070	0.349	1.00
$p2_{2(2)}$	0.144	0.033	0.249	1.00
$p3_{(1)}$	0.988	0.973	1.000	1.00
$p3_{(2)}$	0.993	0.984	1.000	1.00
ε_2	0.034	0.000	0.078	1.00
ε_3	0.082	0.000	0.183	1.00

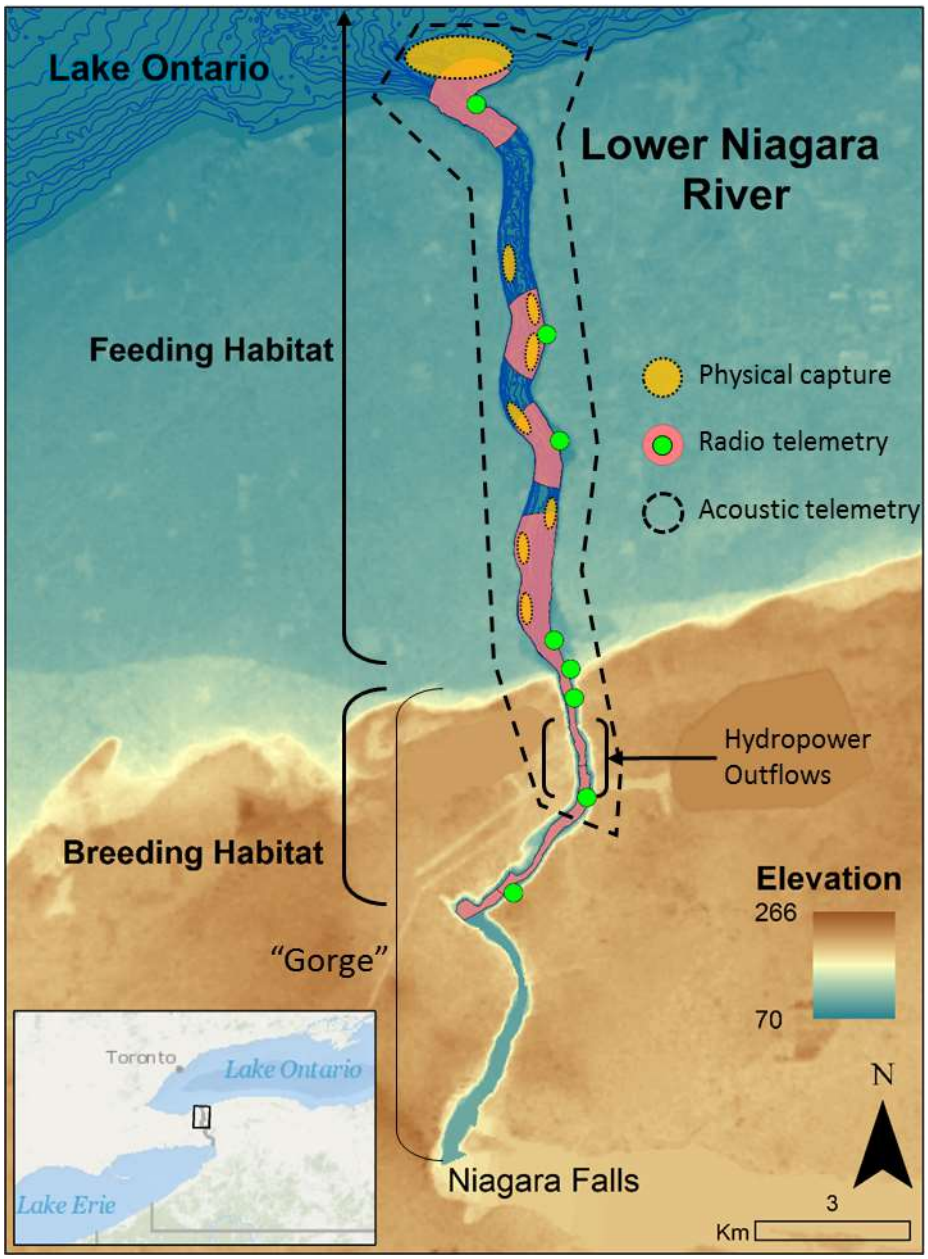

Figure 3.1: Map of the lower Niagara River and approximate spatial extent of area sampled for each capture-mark-recapture dataset.

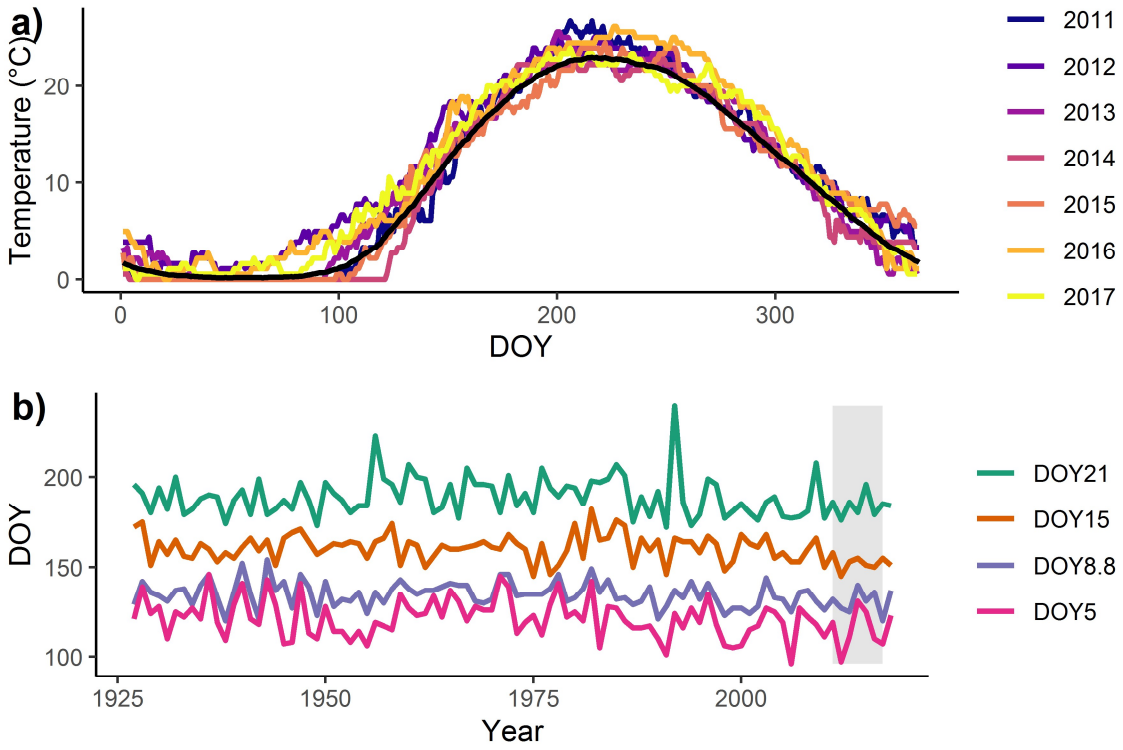

Figure 3.2: Water temperature variation in the Niagara River at the upper river NYPA water intake. Panel a shows variation in daily mean water temperature across the day of the year (DOY) for the years within the study period (colored lines) and the long-term average from 1927-2018 (black line). The DOY with the lowest average water temperature is DOY 44. Panel b shows the first DOY after 44 that temperatures increased to 5, 8.8, 15, and 21 ºC: DOY5, DOY8.8, DOY15, and DOY21, respectively. The grey box indicates our study window from 2011 through 2017.

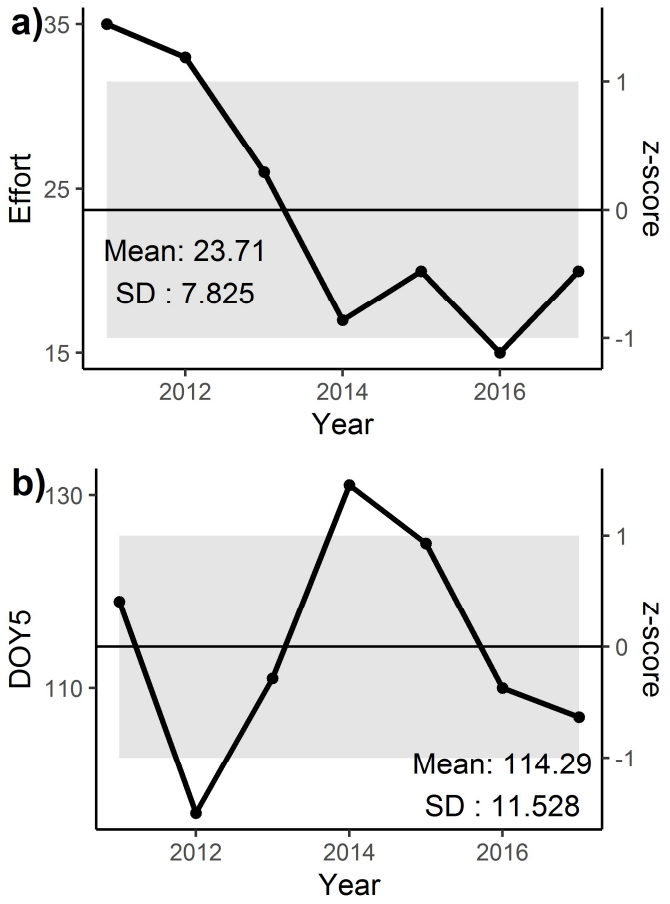

Figure 3.3: Time-varying covariates used in the model: a) DOY5 is the first day of year (DOY) that water temperature rises to 5° C following annual lows, and b) Effort is the number of nights set lines were set within one occasion (sampling year between weeks 10 and 30). The right-had y-axis and greyed area show the mean and standard deviation of DOY5 (a) and Effort (b).

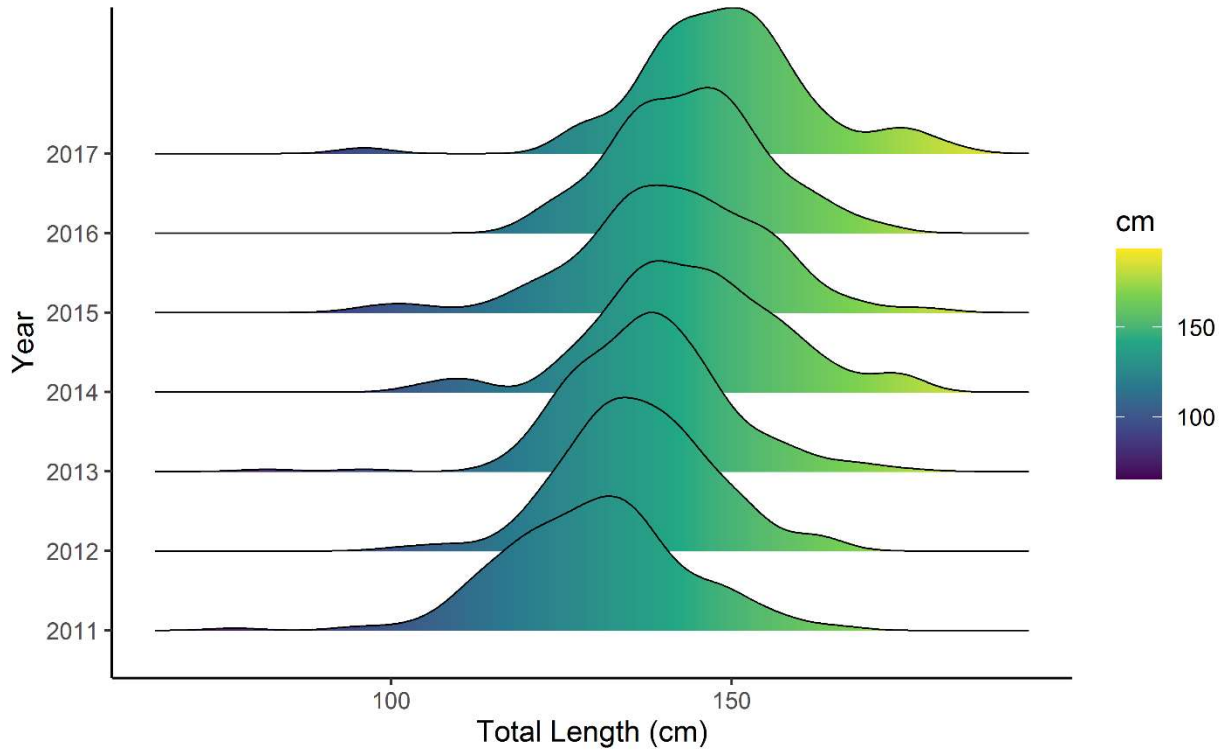

Figure 3.4: Empirical density distributions of lake sturgeon total length (cm) observed in 2011 through 2017. Density plots differ across rows as designated by the y-axis, and total length is depicted on a color ramp for easier comparison of annual density plots.

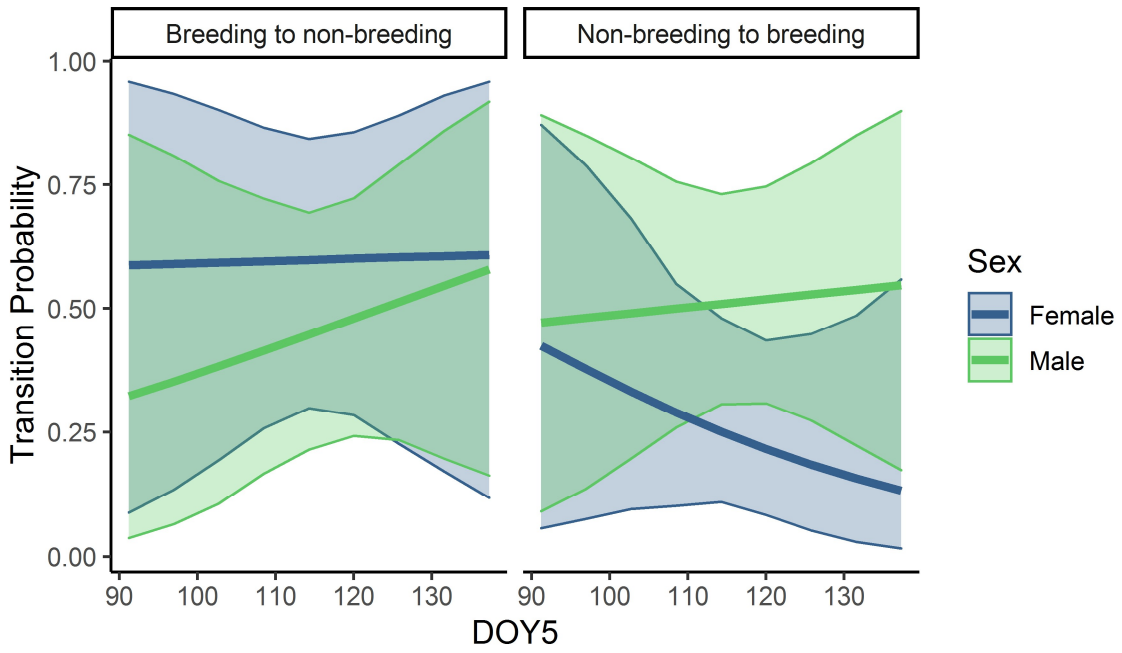

Figure 3.5: The mean probablilty of transitioning between breeding and non-breeding states (Breeding to non-breeding: ψ_1; Non-breeding to breeding: ψ_2) as predicted by the interaction between DOY5 and sex. Uncertainty bands around regression lines for each sex reflect the 90% highest density interval of the posterior predictions for ψ_1 and ψ_2 across DOY5.

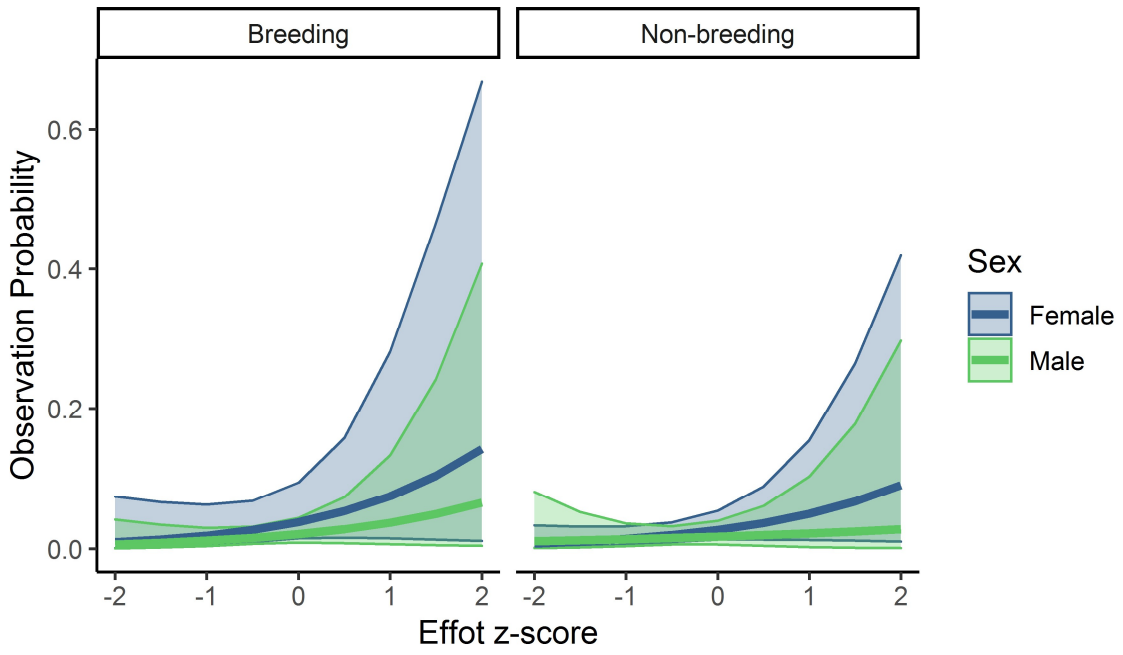

Figure 3.6: The mean observation probability by physical capture methods of fish in breeding and non-breeding states (Breeding to non-breeding: $p_{1(1)}$; Non-breeding to breeding: $p_{1(2)}$) as predicted by the interaction between sampling effort and sex. Uncertainty bands around regression lines for each sex reflect the 90% highest density interval of the posterior predictions for $p_{1(1)}$ and $p_{1(2)}$ across DOY5.

CHAPTER 4

A CHINOOK SALMON LIFE CYCLE MODEL REVEALS SPATIAL PATTERNS OF RECRUITMENT AND THE EFFECTS OF DAMS ON RECOVERY[4]

[4] To be submitted to Proceedings of the National Academy of Sciences with, R.F. Thurow, C.W. Osenberg, S.J. Wenger as co-authors

Introduction

Salmon are commercially, culturally, ecologically, and recreationally important fishes that are the focus of intensive and extensive management efforts across the northern hemisphere. After European settlement of North America, Pacific salmon stocks declined due to overharvest, habitat degradation, hatchery production, and the construction of hydropower dams that blocked or degraded migratory corridors (NMFS 2000). These declines brought many salmon populations close to extinction, prompting intense conservation effort and, in several cases, federal listing under the US Endangered Species Act (NOAA 1992). The Columbia River in the Pacific northwest of North America is a focal system for conservation efforts the United States. In the Columbia River, efforts to increase stock abundance and productivity must overcome the many deleterious effects of barriers, habitat alterations, and climate changes that have degraded migratory corridor conditions (Budy et al. 2002, Faulkner et al. 2019, Petrosky et al. 2020, Crozier et al. 2019, 2020).

A major challenge for the conservation of Pacific salmon is accounting for processes that affect population growth at widely varying temporal and spatial scales. Habitat selection, juvenile growth, and dispersal influence Pacific salmon at the patch scale (Hendry et al. 2001, Pess et al. 2011, Carmichael et al. 2020); trait diversity and hatchery introgression influence Pacific salmon at the population scale (Hilborn et al. 2003, Schindler et al. 2010, Pearsons and O'Connor 2020); fragmentation by dams and predation by pinnipeds, orcas, and humans influence Pacific salmon at the scale of large river basins (Schaller et al. 2014, Chasco et al. 2017a, 2017b); and climate change in ocean and migratory corridor conditions influence Pacific salmon at a global scale (Crozier et al. 2019, 2020). Although climate changes and migration barriers strongly affect Pacific salmon (Schaller et al. 2014, Crozier et al. 2019, 2020), local

influences such as habitat quantity and quality are also important. Heterogeneity in habitat quality among stream reaches may be masked by spatial averaging, possibly obscuring information needed to understand population's potential given conservation actions such as dam removal.

The Middle Fork Salmon River (MFSR) in central Idaho hosts hundreds of kilometers of far-inland, high-elevation, high quality natal (spawning and rearing) habitat for salmon. Population dynamics of Chinook salmon (*Oncorhynchus tshawytscha*) in the MFSR are well studied (Schaller et al. 1999, 2014, Isaak and Thurow 2006, Copeland et al. 2014, Thurow et al. 2020). This watershed is notable for its wild and diverse spring/summer Chinook salmon stocks (Neville et al. 2006). The basin also retains natural landscape processes that have not been greatly altered by humans (e.g., fire regime, hydrogeological processes, and patch connectivity; Jacobs et al. 2021). Chinook salmon natal habitat in the basin remains vast, highly connected, and persistently high quality. Because of its high elevation, predicted effects of global climate change on average annual temperatures and precipitation are unlikely to substantially reduce habitat quality for the next ~50 years (Isaak et al. 2017b, Jacobs et al. 2021), so habitat will likely remain high quality in the near future. Despite abundant habitat, contemporary Chinook salmon abundances in the MFSR remain at 1-3% of the basin's mid-20th century numbers, and likely <1% of late 19th century abundances (Thurow et al. 2020), because downstream dams and harvest have reduced salmon survival. As such, dam removal is advocated by some conservationists to restore this and other populations in Snake River tributaries.

Habitat selection by spawning Chinook salmon females is highly variable and correlated with a suite of habitat variables across the MFSR (Isaak and Thurow 2006, Isaak et al. 2007, Jacobs et al. 2021); however, we do not know if this variation in female occurrence reflects

variation in the production of young. Birth rates of MFSR Chinook salmon have been estimated before (e.g., Petrosky et al. 2001, Wilson 2003) but at relatively coarse spatial scales. With increasing availability of high-quality, long-term MFSR datasets with high spatial resolution, it is now possible to estimate Chinook salmon population dynamics with higher accuracy at finer spatial scales, facilitating spatial analysis of population dynamics, habitat heterogeneity, and the influence of outside-basin factors controlling survival and recruitment.

Here we build on decades of prior research on MFSR and Snake River Chinook salmon, to estimate per-capita reproduction rates of wild Chinook salmon within the MFSR, the spatial variation in these rates, and the corresponding sensitivity of recruitment to outside-basin mortality. We constructed a stochastic age-structured life-cycle model of Chinook salmon and estimated its parameters using a Bayesian integrated state-space model framework. We coupled long-term Chinook salmon redd (nest) count data from the MFSR with Columbia River smolt-to-adult return passage data (Data Access in Real Time, http://www.cbr.washington.edu/dart/overview (DART)), annual in-river passage survival and barge transport estimates (Widener et al. 2018), and female Chinook salmon carcass age survey data (Davison, Idaho Department of Fish and Game, personal communication). We applied our model to examine spatial variation in reproductive rate and recruitment at three spatial scales ("coarse-scale" (n=2 subdivisions of the MFSR), "intermediate -scale" (n=8 subdivisions), and "fine-scale" (n=23 subdivisions)) using an integrated population modeling approach to simultaneously estimate temporal variation in survival and recruitment processes from multiple supporting datasets. Our goals were to 1) estimate spatial variation in smolt production rates across MFSR spawning tributaries, 2) test the sensitivity of recruitment potential to migration

corridor restoration by dam removal, and 3) evaluate the spatial scale-dependence of model results.

Methods

Site description

The 7,330-km^2 MFSR watershed in central Idaho, USA, contains an estimated 777 km of contiguous intact Chinook salmon spawning streams that flow through a mountainous landscape largely unaltered by humans, much of it protected within the Frank Church River of No Return Wilderness. The MFSR flows into the Salmon River, a major tributary of the Snake River, which in turn is part of the larger Columbia River system in the Pacific Northwest of North America. The migratory corridor for these fish, between the MFSR and the Pacific Ocean, has been altered by eight large dams in the Federal Columbia River Power System (FCRPS) impounding the Columbia and Snake Rivers (hereafter, the "hydrosystem"). Each dam includes systems to monitor and facilitate fish passage. Downstream of the Bonneville Dam, the first dam upstream from the ocean, the migratory corridor extends through the lower Columbia River Estuary (LRE) before entering the Pacific Ocean. MFSR spring/summer Chinook salmon were first listed as "Threatened" under the Endangered Species Act in 1992 (NOAA 1992) which has precipitated extensive recovery efforts. MFSR Chinook salmon have been the subject of long-term broad-scale spawning redd monitoring effort since 1957, and of an annual, spatially continuous, and georeferenced redd survey conducted once annually since 1995 (Thurow et al. 2020).

Throughout, we use the term "watershed" to refer to the entire MFSR basin, which is shown in Figure 4.1 along with spatial subdivisions at the three scales of analysis we use herein: (1) "coarse-scale", (2) "intermediate -scale", and (3) "fine-scale". Our coarse scale of analysis refers to the upper vs. lower MFSR sub-basins (n=2), our intermediate scale of analysis refers to

the Interior Columbia River Technical Recovery Team (ICTRT 2003) population management areas within the MFSR (n=8), and our fine scale of analysis refers to distinct river segments identified by Isaak and Thurow (2006) (n=23) (Figure 4.1).

Life cycle

Here, we focus explicitly on the female Chinook salmon life cycle (Figure 4.2). Chinook salmon in the Snake River spawn from late summer (July) to early fall (September), when females excavate redds in gravel substrates, spawn, and bury fertilized eggs. Female Chinook salmon defend redds from predators and conspecific competitors until death; all salmon are semelparous and die after spawning. Eggs incubate over winter and hatch the next spring as larvae and emerge as fry. Fry grow into parr that remain in freshwater habitats until migration. After surviving the age 0 parr stage, a majority of MFSR Chinook salmon migrate to the ocean at age 1, during which time parr transform into smolts. Some male salmon exhibit precocial or early maturation life histories and do not migrate (Gebhards 1960), but most female MFSR Chinook salmon spend between 2 and 4 years in the ocean, returning to spawn as mature age 4, 5, or 6 fish. Adults returning from the ocean arrive at Bonneville dam, navigate eight hydroelectric dams to pass Lower Granite dam (the uppermost and eighth dam) and return to spawn in the MFSR.

In our model, we defined six age classes and one multi-age spawning class as state variables: N_0 (age 0 parr), N_1 (age 1 smolts), N_2 (marine phase juveniles), M_3–M_5 (age 3-5 marine phase fish), and S (spawning fish of ages 4, 5, or 6) (Figure 4.2). To account for three age classes and their survival between two locations along the adult migration corridor, we introduce one additional set of state variables: B_4, B_5, B_6 (the number of fish at age 4, 5, and 6 that return to Bonneville dam), which after surviving passage through the hydrosystem together comprise S

(the number of fish at age 4, 5, and 6 that passed the most upstream dam, the Lower Granite dam). State transitions governing the variation in state variables over time included survival rates, maturation probabilities, and reproductive rates. Our data were derived from redd counts, carcass-derived mature female ages on the spawning grounds, and PIT tagged Chinook salmon passage observations through the hydrosystem.

Data

We defined multiple data objects as response variables in our integrated model. We use a lower case "y" to designate each response variable, then we use subscripts outside of parentheses to indicate the data type, and subscripts inside parentheses to index the data matrix: redd count data varying spatially (i) and annually (t) ($y_{(i,t)}$), carcass counts varying spatially, annually, and by age (a) ($y_{age(i,t,a)}$), and FCRPS passage datasets varying annually, (counts of downstream passing smolts at LGR and upstream passing adults at BON by cohort, $y_{SAR(t)}$; returning adult passage counts at BON and then at LGR by year, $y_{ret(t)}$; in-river smolt survival rate by year, $y_{H(t)}$; and the proportion of smolts transported by year, $y_{T(t)}$).

Redd counts - Annual, spatially-continuous redd surveys were conducted from 1995 through 2016 via low-altitude helicopter flights supplemented by ground-based surveys conducted by the Idaho Department of Fish and Game, Shoshone-Bannock Tribes, Nez Perce Tribe, and US Forest Service as per methods described by Thurow (2000). Individual redd locations were georeferenced with a global positioning system at the end of the spawning season, employing a spatially continuous sampling design (Fausch et al. 2002). Streams deemed too small and steep to be accessible to Chinook salmon were omitted from the survey area (Thurow 2000, Isaak and Thurow 2006). Georeferenced redd locations were snapped to the stream network and aggregated at the coarse, intermediate, and fine scales. Aggregated count data

comprised three datasets, one for each scale of inference with n (number of spatial units) rows, and Y (number of years) columns.

Carcass fin age - From 1998 – 2016, post-spawning MFSR carcass surveys monitored the age and sex of adult Chinook salmon (Davison, IDFG, personal communication). We used female-only age estimates, derived from annual growth ring formation in fin ray cross-sections (y_{age}). Three age classes were observed among females in the MFSR: age 4, 5, and 6. We counted the number of returning fish at age a for each spatial unit i in each time period t to populate our age data matrix, $y_{age(i,t,a)}$. Age data were aggregated to coarse and intermediate scales for analysis at those scales of inference, but age data were too sparse to aggregate at the fine scale. When we modeled fine-scale counts as a function of carcass age variation at the intermediate scale, thus relating fine-scale "segment" redd counts to the intermediate-scale ICTRT populations they overlapped with spatially (Figure 4.1).

Hydrosystem passage - We downloaded passage data for MFSR spring/summer Chinook salmon from the Columbia River Data Access in Real Time database (www.cbr.washington.edu/dart/query/pit_sar_esu, Accessed: 6 October 2020), which comprised two datasets: (1) counts of tagged age-1 smolts passing Lower Granite dam (LGR) and returning as adults to Bonneville Dam (BON), (organized by downstream passage year cohort) ($y_{SAR(t)}$), and (2) counts of tagged adult fish passing BON and again at LGR within the return year (also organized by passage year cohort), reflecting adult survival through the hydrosystem ($y_{ret(t)}$). In one case, a fish was not recorded passing LGR but was recorded at BON. In that case, we edited the data file to record that the fish passed both BON and LGR. We assume that all Chinook salmon pass downstream as age-1 smolts, so we assigned a brood year (the year the eggs they hatched from were deposited) to each cohort in $y_{SAR(t)}$ and $y_{ret(t)}$ as the passage year minus 2.

There are two pathways by which smolts migrate from LGR to BON: 1) via barge; and 2) in-river, passing through (or over) the 8 dams and intervening river corridors. To isolate the effects of early ocean and marine phase survival from survival processes in the hydrosystem, we also included annual estimates of in-river survival and the proportion transported through the hydrosystem by barge (Widener et al. 2018). We estimated annual variation in in-river smolt mortality and the proportion transported from Snake River spring/summer Chinook salmon smolt survival and transport estimates for the years 1998 – 2016 presented by Widener et al. (2018), fed to our model as data: $y_{H(t)}$ and $y_{T(t)}$, respectively.

Marine survival - Marine survival of Chinook salmon is affected by a combination of ocean conditions and carryover effects from freshwater passage conditions – especially barging (Budy et al. 2002, Schaller et al. 2014). We used three ocean variables and one in-river variable known to affect marine survival in MFSR Chinook salmon during their out-migration year and ocean residency (Schaller et al. 2014): (1) Pacific Decadal Oscillation index (PDO) in September following out-migration as smolts, (2) 4-year average PDO from May-July, (3) Western North America coastal upwelling index (UWI) in April during the year of smolt migration, and (4) the proportion transported by barge, δ. The proportion transported by barge affects marine survival through carryover (i.e., delayed) mortality related to stress, crowding, and injury while on the barge. The PDO index reflects differential sea surface temperature variation between the western and eastern Pacific Ocean, where positive phase index values indicate warmer ocean conditions along North America's Pacific Coast (Mantua and Hare 2002). The UWI (cubic meters/second/100 meters of coastline) reflects the degree of coastal upwelling in the spring (e.g., April) and downwelling in the fall. We related marine survival to September PDO, April UWI, and October UWI during the migration year (brood year + 2), and to 4-year average May-

July PDO during each cohort's ocean residency two years after migration (brood year +4). We downloaded monthly PDO index data from http://research.jisao.washington.edu/pdo/PDO.latest.txt (Accessed: 6 October 2020) and monthly UWI data from https://www.cpc.ncep.noaa.gov/products/GODAS/coastal_upwelling.shtml (Accessed: 3 November 2020).

Integrated population model

We specified our model as an age-structured state-space model where redd counts were predicted from counts of redds in previous years (Figure 4.2), a model structure similar to those used in other studies (Su and Peterman 2012, Fleischman et al. 2013, Winship et al. 2014, Scheuerell et al. 2019). State-space models explain time-series data as arising from an unobserved latent state process (i.e., population dynamics via births and deaths), reflecting the true system state, and a data-generating observation process that is conditional on the latent state, and which is an estimate of the underlying latent state. In our case, a stochastic count process explains how count data arose from the true (latent) abundance. We modeled the dynamics of Chinook salmon females on a 1-year time step (t), and across spatial units (i), treating each of the i units as isolated populations closed to immigration and emigration. Since Chinook salmon are semelparous, adults contribute to the next generation via reproduction, not survival. Since MFSR Chinook salmon are at historically low density in the MFSR (Thurow et al. 2020), we assume that population growth is density independent. Our model is built around a simple geometric population growth function, where spawning females (S) produce a cohort of juvenile females that return to spawn as adults (R, for "recruits"): $R = Sb\phi$, where the birth rate (b) denotes the per-capita production of smolts, and survival to maturity (ϕ) denotes the proportion of smolts that survive to reproduce, which includes juvenile survival during hydrosystem passage

(from LGR to BON), juvenile survival during the ocean phase (from BON to BON), and adult survival during migration back to their spawning grounds (at ages 4, 5, or 6; from BON to LGR). In our model, we allow per-capita smolt production to vary spatially within the MFSR but not temporally, and we allowed survival processes to vary temporally, but not across spatial units in the MFSR.

Life cycle process - The number of age 1 smolt class, $N_{1(t)}$, was estimated by multiplying the number of redds $S_{(i,t)}$ by a spatially varying reproductive rate, $b_{(i)}$. We lack data on variation in the population density of Chinook eggs, larvae, and parr over time in our study area, so data-driven estimates of smolt production (at $t+2$) per redd (at t) are possible, but those of parr (at $t+1$) per redd are not, since parr and smolt survival terms would be confounded. Instead, $b_{(i)}$ is the product of per-capita fecundity, egg survival rate, and parr survival rate, none of which we directly estimate.

$$N_{1(i,t+2)} = S_{(i,t)} b_{(i)} \quad (1)$$

Since we have little information on the survival dynamics of marine phase Chinook salmon, we estimate the fraction of outmigrating smolts counted at LGR that will return as adults to BON at any age, (the smolt-to-adult return (SAR) rate, $\phi_{SAR(t)}$), which includes outmigrating smolt survival through the hydrosystem and ocean survival. Because multiple ages return to breed, we applied this rate to the transition between N_1 and N_2 (Figure 4.2), rather than trying to distribute it between multiple age classes:

$$N_{2(i,t+1)} = N_{1(i,t)} \phi_{SAR(t)} \quad (2)$$

The parameter $\phi_{SAR(t)}$ has two components: (1) the survival through the hydrosystem, and (2) marine survival after passing Bonneville dam ($\phi_{M(t)}$). Survival through the hydrosystem is further differentiated depending on whether the smolts are transported by barge or not, which

requires estimates of: (1) the proportion of age 1 smolts transported downstream through the FCRPS dams by barge ($\delta_{(t)}$), (2) transport survival (ϕ_T), and (3) in-river migration survival for fish not transported ($\phi_{H(t)}$). These assumptions yield:

$$\phi_{SAR(t)} = \left(\delta_{(t)}\phi_T + \left(1 - \delta_{(t)}\right)\phi_{H(t)}\right)\phi_{M(t)} \quad (3)$$

We treat ϕ_{SAR} as a cohort-specific survival probability applicable to all individuals in that cohort, regardless of sex or return age.

We assumed that the youngest females return to spawn at age 4, and the oldest at age 6. Thus, these age-classes are split between fish that return to spawn (B) and those that remain in the ocean (M; N=$B + M$) according to a maturation probability, ρ. Age-specific abundances and maturation probabilities define the distribution of ages among the breeding stock:

$$\begin{aligned} B_{4(i,t+1)} &= N_{3(i,t)}\rho_{4(t)} \\ B_{5(i,t+1)} &= M_{4(i,t)}\rho_{5(t)} \\ B_{6(i,t+1)} &= M_{5(i,t)} \end{aligned} \quad (4)$$

where $\rho_{4(t)}$ is the proportion of adults that return to spawn at age 4 and ρ_5 is the proportion of adults that return at age 5, conditional on not returning at age 4. We assume that all fish that did not return at age 4 or 5 retuned at age 6.

Adults that return to Bonneville Dam must survive passage upstream through the hydrosystem to successfully spawn in their natal habitat in the MFSR. Thus, the number of spawning females is:

$$S_{(i,t)} = \phi_R\left(B_{4(i,t)} + B_{5(i,t)} + B_{6(i,t)}\right) \quad (5)$$

Where ϕ_R is the survival of fish during their upstream migration from BON to the spawning grounds (which we estimate using observations of fish entiering BON and exiting LGR: i.e., we assume all fish survive from LGR to the spawning grounds).

Stochastic parameter estimation - We allow $b_{(i)}$ to vary according to an MFSR-wide mean natural logarithm-transformed production rate, $log.b$, and a random effect for variation among spatial units,, $\alpha_{b(i)}$,

$$b_{(i)} = \exp\left(log.b + \alpha_{b(i)}\right) \quad (6)$$

We estimated cohort-specific survival, ϕ_{SAR}, using our y_{SAR} dataset, which is comprised of the number of tagged fish released at LGR ($y_{SAR(t,1)}$), and the number returning to BON ($y_{SAR(t,2)}$),

$$y_{SAR(t,2)} \sim \text{Binomial}\left(\phi_{SAR(t)}, y_{SAR(t,1)}\right) \quad (7)$$

We estimated variation in the proportion transported, δ, using a beta regression, and we allow estimates to vary randomly by year and according to barge schedule, which differed between two time periods, 1993-2006 and 2007-2017, coded as a categorical variable, $\text{Z}_{(t)}$ (Widener et al. 2018),

$$\begin{aligned} y_{T(t)} &\sim \text{Beta}\left(r_T\ \delta_{(t)},\ r_T\left(1-\delta_{(t)}\right)\right) \\ \text{logit}\left(\delta_{(t)}\right) &= \beta_{0T} + \beta_{1T}\text{Z}_{(t)} + \alpha_{T(t)} \end{aligned} \quad (8)$$

Here, $\delta_{(t)}$ is the proportion of Chinook salmon smolts transported from LGR to BON per year, r_T is the scale coefficient for the beta distribution (which controls variance), β_{0T} and β_{1T} are logit-scale regression coefficients, and α_T is the random effect of time (year). Barge-transported smolts survive at very high rates (McMichael et al. 2011), but carryover effects may significantly reduce the survival rate of barge-transported smolts passing through the lower river estuary on their way to the ocean (Gosselin et al. 2018). We assumed a barge transport survival rate of ϕ_T = 0.98, and we accounted for delayed mortality in our regression sub-model for marine survival, which uses the proportion transported, $\delta_{(t)}$, as a covariate. We allow survival of smolts through the hydrosystem to vary annually according to a beta regression, similar to our approach for estimating barge transport.

$$\begin{aligned} y_{H(t)} &\sim \text{Beta}\left(r_H\,\phi_{H(t)},\, r_H\left(1-\phi_{H(t)}\right)\right) \\ \text{logit}\left(\phi_{H(t)}\right) &= \mu_H + \alpha_{H(t)} \end{aligned} \tag{9}$$

In-river passage survival, $\phi_{H(t)}$, is thus a function of the mean survival probability on the logit scale, μ_H, and its annual variation, $\alpha_{H(t)}$. Survival through the hydrosystem according to $\delta_{(t)}$, ϕ_t, and $\phi_{H(t)}$ explains the proportions of Snake River spring/summer Chinook salmon (including those from the MFSR) that survive migration to pass downstream of Bonneville dam and into the lower river estuary and the Pacific Ocean.

We allow marine survival rate to vary in time on the logit scale in response to covariates related to marine conditions during the smolt year and beyond (Schaller et al. 2014).

$$\text{logit}\left(\phi_{M(t)}\right) = \beta_{0M} + \beta_{1M}X_{1(t)} + \beta_{2M}X_{2(t)} + \beta_{3M}X_{3(t)} + \beta_{4M}X_{4(t+2)} + \alpha_{M(t)} \tag{10}$$

We assume the probability of return at age 4, $\rho_{4(t)}$, is time varying. However, an overall rarity of age 6 spawning females in the MFSR suggested that the probability of return at age 5, ρ_5, is high and its inter-annual variation is low, so we assume that ρ_5, is invariant. We allow $\rho_{4(t)}$ to vary across years as a random walk, where we estimate $\rho_{4(t)}$ at time $t = 1$, and then estimate each subsequent time step's return probability as the sum of the return probability and an annual deviation, $\Delta_{\rho_4(t-1)}$, evaluated on the logit scale,

$$\text{logit}\left(\rho_{4(t)}\right) = \text{logit}\left(\rho_{4(t-1)}\right) + \Delta_{\rho_4(t-1)} \tag{11}$$

Adult return survival is estimated from counts of PIT-tagged adult Chinook salmon passing through the FCRPS. We estimate ϕ_R according to the likelihood,

$$y_{ret(t,2)} \sim \text{Binomial}\left(\phi_R, y_{ret(t,1)}\right) \tag{12}$$

We exclude years with no PIT tagged adult Chinook salmon from the MFSR observed migrating upstream at BON or LGR.

The resulting age distribution of reproductive females returning to the MFSR in any given year is then the relative proportion of $B_{4(i,t)}$, $B_{5(i,t)}$, and $B_{6(i,t)}$: $\hat{p}_{age(i,t,a)}$, where a is the age index {1, 2, 3} representing ages {4, 5, 6}. We model variation in the distribution of age 4, 5, and 6 spawning females in each spatial unit i during each year t as

$$y_{age(i,t,1:3)} \sim \text{Multinomial}\left(\hat{p}_{age(i,t,1:3)}, n_{age(i,t)}\right) \tag{13}$$

where $n_{age(i,t)}$ is the number of carcasses aged per spatial unit per year, given as data along with y_{age}.

Our focal dataset is the spatially-explicit redd count dataset from the MFSR, ($y_{(i,t)}$). We model the number of redds observed in spatial unit i at time t as

$$\begin{aligned} y_{(i,t)} &\sim \text{Poisson}\left(\mu_{(i,t)}\right) \\ \mu_{(i,t)} &= S_{(i,t)} e^{\varepsilon_{(i,t)}} \\ \varepsilon_{(i,t)} &\sim \text{Normal}(0, \tau_{Pois}) \end{aligned} \tag{14}$$

where $\mu_{(i,t)}$ is the expected number of observations, $S_{(i,t)}$ is the latent number of spawning females, and $\varepsilon_{(i,t)}$ is a natural logarithm-scale normally distributed random effect with a mean of 0 and a precision of τ_{Pois}, which adds a free parameter to account for overdispersion in the Poisson count process.

Priors and constraints - To explain initial redd counts in the time series, we hindcast the adult female spawning stock, $S_{(i,t)}$ (i.e., the number of redds), in each spatial unit i in each of the 7 years prior to our redd survey. For each spatial unit i, and for each year t,

$$\log\left(S_{(i,t)}\right) \sim \text{Normal}(\mu_0, \sigma_0) \tag{15}$$

We provided informative priors μ_0 and σ_0 on $S_{(i,t)}$ based on the number of redds observed per spatial unit early in the time series. We set μ_0 equal to the the natural logarithm-scale mean of redd counts (plus a small constant) from the first 7 years of data collection. We set σ_0 equal to

double the standard deviation of the log-transformed redd counts from the first 7 years. Similarly, we provided an informative Gamma prior for $log.b$, with $\alpha = 64$ and $\beta = 14$. We chose the informative prior on $log.b$ to mimic the mean and distribution of likely numeric-scale smolt production rates for Chinook salmon in the MFSR basin from the literature (e.g., Petrosky et al. 2001), while still constraining the parameter to non-zero values.

Random variance terms, $\alpha_{b(i)}$, $\alpha_{T(t)}$, $\alpha_{H(t)}$, $\alpha_{M(t)}$, $\Delta_{\rho_4(t-1)}$, and $\varepsilon_{(i,t)}$, were drawn from a Gaussian distribution with a mean of 0 and a precision parameter: τ_b, τ_T, τ_H, τ_M, τ_{ρ_4}, and τ_{Pois}, respectively (note that the standard deviation, σ, is equal to $1/\sqrt{\tau}$). These precision parameters, along with the Beta distribution-scale coefficients r_T and r_H, were given weakly informative half-Cauchy priors with a mean of 0 and a standard deviation of 2.25 (Gelman 2006). Logit-scale regression coefficients, β_{0T}, β_{1T}, μ_H, β_{0M}, β_{1M}, β_{2M}, β_{3M}, and β_{4M}, along with the initial logit-scale return probability of age 4 marine phase female Chinook salmon ($\rho_{4(1))}$), were given Gaussian priors with a mean of 0 and a standard deviation of 2, that were weakly informative when back-transformed to the probability scale (Hobbs and Hooten 2015, Northrup and Gerber 2018). We provided an informative Gaussian prior for ρ_5 with a mean of 2 and a standard deviation of 2 on the logit scale (with a mean of 0.88 on the probability scale), reflecting our belief that very few Chinook salmon from our study population remain in the ocean at age 5. Return survival, ϕ_{ret}, was given a flat uniform prior between 0 and 1.

Model fitting and assessment - We fit our model using MCMC sampling in JAGS 4.3.0 (Plummer 2017) via the R package 'runjags' (Denwood 2016) in R version 4.0.2 (R Core Team 2020). We ran our model for a 1000 iteration adaptation period and 1,000,000 iterations of burn-in, followed by 250,000 iterations of posterior sampling thinned to every 100 iterations across 5 chains. We used the function extend.jags() to extend the posterior sampling period by 250,000-

iteration increments until the convergence diagnostic, $\hat{R}$ (Gelman and Rubin 1992), was below 1.1 for all parameters. We also assessed convergence by visually inspecting and comparing each chain's MCMC sample traces and posterior sampling distributions. For regression coefficients that represent deviations from a null hypothesis of no effect, we report the proportion of samples from the posterior distribution that overlapped with a region of practical equivalence (ROPE) between -0.18 and 0.18 on the logit scale, where the proportion of the posterior estimate that overlaps with the ROPE interval indicates the degree of support for the null hypothesis of no effect (Kruschke 2014). We also calculated the Freeman-Tukey discrepancy statistic for our data versus model expectations, $T(y, \boldsymbol{\theta})$, and for a dataset simulated from model parameters, $T(y^{Sim}, \boldsymbol{\theta})$,

$$\begin{aligned} T(y, \boldsymbol{\theta}) &= \sum_{i=1}^{n} \sum_{t=a_{max}+1}^{Y} \left(\sqrt{y_{(i,t)}} - \sqrt{E[\theta]} \right)^2 \\ T\left(y^{Sim}, \boldsymbol{\theta}\right) &= \sum_{i=1}^{n} \sum_{t=a_{max}+1}^{Y} \left(\sqrt{y_{(i,t)}^{Sim}} - \sqrt{E[\theta]} \right)^2 \end{aligned} \tag{16}$$

where n is the number of spatial units, Y is the total number of years, and $E[\theta]$ is the expected redd count. We evaluated goodness by plotting the Freeman-Tukey discrepancy statistic for real data versus that from simulated data, and calculated a Bayesian P-value indicating the probability that the simulated discrepancy would be more extreme than that of our real data (Conn et al. 2018).

Sensitivity of growth rate to river restoration - We conducted simulations of salmon growth rate (per-capita population growth; λ) across the MFSR under four river restoration scenarios corresponding to the removal of one, two, three or four of the four dams on the Snake River, using the fitted model as a reference condition (no dam removal). These simulations represent predictions of future growth rates that may be attained under conditions similar to those

experienced during the study period. We conducted these simulations at each of our three scales of inference. To carry through uncertainty in birth and survival parameter estimates, simulations were conducted by using posterior samples of parameter estimates to calculate the posterior distribution of λ under dam removal scenarios. We defined λ as the number of breeding females produced per breeding female for each spatial unit i from each brood year cohort t.

To simulate the sensitivity of growth rate to dam removal, we assumed that (1) mortality from habitat degradation associated with each dam is equivalent and (2) that 100% of migration mortality is due to dams. Thus, survival through the hydrosystem (ϕ) is equal to the product of survival rates across all eight dams, whereas survival after the removal of one dam is the product of 1/8 fewer dams, $\phi^{-7/8}$. We introduced a variable, π, representing the number of dams removed under our simplifying assumptions, and thus we expressed recruitment potential as a function of our life cycle birth and survival rates with reductions in ϕ_H and ϕ_R as a function of π.

$$\lambda = b\Big((1-\delta)\phi_H^{1-(\pi/8)} + \delta\phi_T\Big)\,\phi_M\,\phi_R^{1-(\pi/8)} \tag{17}$$

where λ was indexed by spatial unit and brood year such that $\lambda_{(i,t)}$ was a function of $b_{(i)}$, $\phi_{H_{(t+2)}}$, $\delta_{H_{(t+2)}}$, $\phi_{M_{(t+3)}}$, ϕ_R, ϕ_T, and π. For the purposes of this study, we limited our inference on λ to year classes observed during MFSR redd surveys starting in 1995, and by the last year for which we estimated ϕ_M, 2014 (brood year 2014 fish experienced our estimated ϕ_M in 2016, the last year of our analysis).

We simulated growth rates for π=0 (i.e., our fitted model) to π=4 (the total number of dams on the Snake River). To illustrate the sensitivity of growth rate to dam removal, we estimated the percentage change in λ as a function of π. To predict the efficacy of dam removals for improving population growth conditions in the MFSR, we estimated the number of spatial

units that could support positive population growth ($\lambda > 1$) as a function of π across all simulation iterations at each scale of inference.

Results

Data summary

Redd counts - A total of 17,829 individual redds were counted across the 777 km of surveyed stream in Middle Fork Salmon River watershed between 1995 and 2016. The fewest redds were counted in the first survey year 1995 (20 redds), and the most redds were counted in 2003 (2271 redds), with an average annual total of 811 redds (SD 603). Loon Creek downstream from Warm Springs Creek and all of Warm Springs Creek could not be surveyed in 2013 due to turbid conditions. Thus, we interpolated the number of unobserved redds in these reaches using generalized least squares regression analysis predicting lower Loon Creek and Warm Springs Creek redd abundances from upper Loon creek redd abundance in other years. Interpolated redd abundance was 17 in lower Loon Creek (segment "n"), 7 in Mayfield Creek (segment "m"), and totaled 47 (observed + interpolated) for the MFLOO population in 2013, and brought the total number of individual redds in our dataset up to 17,852 (Figure 4.1). There was considerable spatial heterogeneity in redd counts, and time-series of counts often (but not always) strongly covaried across spatial units (Figure 4.3). Pairwise Pearson's correlation coefficients were 0.80 among units at the sub-basin scale (one pairwise comparison only), 0.80 (SD 0.14) among units at the population scale, and 0.63 (SD 0.23) among units at the segment scale.

Carcass age - We used fin ray age estimates from a total of 2,241 female Chinook salmon carcasses collected from 1998 – 2016. Of these, 1,125 were age 4, 1,089 were age 5, and 27 were age 6. Most female age estimates came from carcasses in the upper sub-basin (1,908), but 333 age estimates were from carcasses in the lower sub-basin (Figure 4.1, Table 4.1). Due to

low number of carcasses from some segments at the fine spatial scale (e.g., Big Creek and Loon Creek), we assumed that fine-scale age-structure was a function of intermediate-scale age structure.

Hydrosystem passage - In-river passage survival estimates for yearling Chinook salmon migrating from their trapping location in the Snake River watershed to BON averaged 49.5% (SD 8.4; range: 26.6-61.2) from 1999-2016 (Widener et al. 2018), but did not show an obvious trend through time. We also extracted the estimated proportion of yearling wild Chinook salmon that were transported through the hydrosystem, and were thus not subject to in-river mortality (Widener et al. 2018). The proportion transported by barge declined precipitously between 2006 and 2007 from an average of 0.81 (SD 0.12) prior to 2007 to an average of 0.30 (SD 0.12) in 2007 through 2017, corresponding to a change in barge schedule (Widener et al. 2018).

The smolt-to-adult return data (y_{SAR}) were comprised of the tagged yearling MFSR Chinook salmon observed passing downstream at LGR, and the number returning to BON as adults, organized by brood year. An average of 1,346 fish (SD 785) were observed passing downstream at LGR each year, and an average of 17 (SD 27) were observed returning to BON as adults. For 2 brood years, 1999 and 2001, no adult MFSR fish were observed returning to BON. Fish returning to BON and passing further upstream at LGR comprised our adult passage survival dataset, y_{ret}. Of those that returned to BON, an average of 14 out of 17 adult fish (SD 22) were observed passing LGR.

Covariate data - The upwelling and PDO index covariates we chose varied substantially across the study period (Figure 4.4). Inter-annual variation in smolt year September PDO and April upwelling was high, and very low values were observed early in the April upwelling time-

series. The 4-year average May-July PDO index variable displayed an approximately decadal cycle with troughs near the years 2000 and 2010 during our study.

Model results

Reproduction - The MFSR-wide average smolt production rate had a median of 125 smolts per redd (90% HDI 67 – 186) at the coarse scale, 116 smolts per redd (90% HDI 89 – 146) at the intermediate scale, and 99 smolts per redd (90% HDI 78 – 121) at the fine scale (Figure 4.5). Reproductive rates and their spatial variation were fairly consistent across scales, as median estimates sometimes differed but had overlapping 90% HDIs (Figure 4.5b), suggesting no scale-dependence in parameter estimates. The only aspect of the results that appeared sensitive to scale was whether the 90% HDI of average population growth rate overlapped 1 (Figure 4.5c), though this affects the interpretation of the results little, as the most likely result at all scales is that the average spatial unit within the MFSR does not support positive population growth. Hereafter, we focus on the fine-scale model results, unless otherwise noted.

Survival - In-river survival through the hydrosystem, $\phi_{H(t)}$, was fairly consistent throughout the time period we evaluated, with a median on 0.49 (logit-scale median: -0.03; 90% HDI: -0.23 – 0.17). However, it varied annually with a logit-scale standard deviation of 0.27 (90% HDI: 0.03 – 0.46). The proportion transported through the hydrosystem, $\delta_{(t)}$, averaged 0.75 prior to 2007 (logit scale median: 1.10, 90% HDI 0.63 – 1.54) and 0.32 during 2007 and beyond (logit scale coefficient: -1.85, 90% HDI: -2.63 – -1.10), varying annually with a logit-scale standard deviation of 0.47 (90% HDI 0.06 – 0.92). Assuming a probability of survival during transportation of ϕ_T = 0.98, overall FCRPS passage survival varied annually according to the sum of in-river and transport survival, $(1-\delta)\phi_{H(t)} + \delta\phi_{T(t)}$.

Interannual variation in marine survival was explained most strongly by 4-year average PDO, proportion transported, and random interannual variation (Table 4.2). The effect of September PDO was slight, and that of April UWI was negligible, as coefficients were near zero and large portions of posterior sample distributions lay inside the region of practical equivalence (ROPE; Kruschke 2014). Resulting median annual marine survival rates varied between 0.001 and 0.08, except for estimates in 1997 (0.22, HDI 0.09 – 0.41) and 1998 (0.40, HDI 0.24 – 0.61). High interannual random variation in marine survival (σ_M=1.50, HDI 1.11 – 2.06) indicated substantial unexplained variation in ϕ_M. The median marine survival across all years of study was 0.01 (HDI <0.01 – 0.22). We estimated a median survival probability of 0.81 (HDI 0.76 – 0.85) for returning adult Chinook salmon passing through the FCRPS and returning to the MFSR.

Model fit - All parameters had $\hat{R}$ below 1.1, after 750,000 iterations for the coarse scale (37,500 samples), 1,000,000 iterations for the intermediate scale (50,000 samples), and 1,250,000 iterations for the fine scale (62,500 samples). Posterior chains for all parameters appeared adequately mixed, though the parameters in the marine survival sub-model were the slowest to mix. Particularly, the intercept parameter β_{0M} was slow to converge and produced one of the higher $\hat{R}$ statistics. Model results were reasonably consistent with the data for all spatial scales of inference as indicated by Bayesian P-values based on the Freeman-Tukey discrepancy statistic for redd counts. However, this consistency declined with increasing spatial resolution, from P = 0.513 at the coarse scale, to P = 0.216 at the intermediate scale, to P= 0.100 at the fine scale. As spatial scales became finer, the discrepancy between the expectation and the data increased for the real data relative to that for the simulated data, indicating poorer model fit at finer scale driven by an increase in outliers in the real data (Appendix G).

Sensitivity of growth rate to river restoration - Estimates of MFSR-wide average population growth rate varied somewhat by scale of inference between 1995 and 2014: median λ was 0.86 (90% HDI: 0.43 – 1.33) at the coarse scale, 0.86 (90% HDI: 0.62 – 1.13) at the intermediate scale, and 0.72 (90% HDI: 0.52 – 0.92) at the fine scale. The lower growth rate estimates at finer spatial scales reflected variation in estimates of smolt production rate b, though these differences were much smaller than the uncertainty around each estimate (Figure 4.5). Temporal variation in MFSR-wide growth rate was consistent among spatial scales of inference (Figure 4.7).

At each spatial scale, the median λ fell below replacement ($\lambda = 1$) for at least half of spatial units (Figure 4.6). The highest growth rates occurred where redd counts were the highest, typically in higher elevation habitats at or near the upstream extent of the MFSR network accessible by Chinook salmon. This indicates that MFSR Chinook salmon were sustained by high productivity in a small minority of the MFSR basin's reproductive habitats in upstream tributary streams during the study period.

Our simulation of river restoration efforts to increase migrant survival via dam removal showed an increase in population growth rate of 7.32% (HDI: 5.81 – 10.04) if one dam was removed ($\pi = 1$), and an increase in population growth rate of between 20% and 50% if all four Snake River dams were removed ($\pi = 4$). The number of segments with $\lambda > 1$ increased with π, as was expected, although the pattern of increase was somewhat different using different descriptions of the distribution (e.g., there was a step-change in the modal number of segments with $\lambda > 1$ beween $\pi = 2$ and $\pi = 3$, but the mean (and median) showed a linear change as π increased). At the fine scale, removing more than 2 dams shifted the expected number of populations with positive growth from 8 of 23 (35%) to 14 of 23 (61%) (Figure 4.8). Similarly,

at the intermediate scale, removing 3 dams instead of 2 dams resulted an expectation of 7 of 8 instead of 3 of 8 populations with $\lambda > 1$.

Discussion

Variation in Chinook salmon redd counts in the MFSR is attributable to spatial heterogeneity in productivity. High redd-density areas within the Middle Fork Salmon that have the largest and most contiguous patches of natal habitats like Bear Valley, Marsh, and Big creeks (Thurow et al. 2020, Jacobs et al. 2021) supported the highest reproductive rates, which approached an estimated 200 smolts per spawning female. In contrast, the lowest-productivity areas supported smolt production rates near or below an estimated 50 smolts per female. This range of reproductive rates, however, is comparable or higher than published estimates of low-density smolt production rates for Snake River spring/summer Chinook salmon (e.g., Petrosky et al. 2001, Wilson 2003).

The spatially continuous sampling with which these data were collected (sensu Fausch et al. 2002) allowed us to aggregate our data at different scales in order to evaluate the role of spatial scale on our smolt production estimates. Without such a comparison, this study and others like it risk ignoring important scale dependence leading to erroneous results at any given spatial scale. The estimated variance among sub-populations did not differ across spatial scales of inference (Figure 4.5). However, we did observe higher variation among spatial units in reproductive rate at smaller scales of inference. This was not surprising because heterogeneity at small scales is always masked by larger-scale aggregation. A slight decrease in our estimates of whole-basin average reproductive rates with decreasing spatial scale is notable because estimated whole-basin average growth rates ranged from estimates with HDIs that overlapped $\lambda = 1$ (coarse and intermediate scales), and estimates with HDIs that were completely below $\lambda = 1$ (fine scale).

In our case, the differences among estimated average reproductive rate across scales were well within the highest density intervals of those estimates within spatial scales, indicating no scale dependence. Variation in whole-basin average growth rate thus appeared to be driven by a small number of highly localized areas with high reproductive rates distributed across the basin.

We incorporated long term monitoring of (1) the spatial distribution of spawning Chinook salmon females across a large river basin and (2) individual-level migrant survival data (and data analysis products) into a single data-driven statistical model. This novel approach allowed us to test the relative importance of spatial heterogeneity in reproduction in spawning habitat and variation in migration and marine-phase survival processes in a way not previously possible. Inference on the spatial distribution of spawning Chinook salmon has proven informative in the MFSR (e.g., Jacobs et al. 2021) and elsewhere (e.g., Falcy 2015), but inference on population dynamics and how they vary in space is often confounded by variation in the number and age of returning fish driven by outside-basin processes. We leveraged a wealth of existing data that allowed us to account for outside basin survival and maturation patterns, including passage survival and barge transport estimates (Widener et al. 2018) and data on dam passage by smolts and adults throughout the hydrosystem (CBR 2020). We estimated marine survival as a function of marine covariates and the proportion of the run transported, adding the estimated probability of barge transport (δ) as a covariate to account for differential survival of barge transported versus in-river smolts (Budy et al. 2002). Admittedly, our estimation of marine and freshwater smolt survival was coarse relative to the high variability and interacting large scale freshwater, marine, and climate covariates that may explain smolt and post-smolt survival (Budy et al. 2002, Schaller et al. 2014, Faulkner et al. 2019, Petrosky et al. 2020, Gosselin et al. 2021). However, by fitting our model to observed PIT tag SARs we were able to reproduce

observed patterns in MFSR smolt recruitment rates with reasonable parameter estimates for the effects of PDO and δ on marine survival, and for time variation in freshwater survival and transport probability variation, ultimately allowing us to estimate population growth within the MFSR and partition variation in that growth spatially.

Our results confirm the findings of others that MFSR Chinook salmon remain in decline and are at risk of extirpation, as demonstrated by low average growth rates (Figure 4.5c). Furthermore, our results suggest a worsening decline over the course of our study, as depicted by the negative trend in population growth rate through time (Figure 4.7). Despite the abundance of highly connected, high-quality habitat for Chinook salmon in the MFSR basin (Isaak and Thurow 2006), these and other Chinook salmon stocks have progressively declined since the 1970s. It is reasonable to infer that this decline is at least partly attributable to large dams, which previously have been shown to reduce the survival and recruitment of salmon populations (e.g., Petrosky et al. 2020). For example, Schaller et al. (1999) documented abrupt declines in salmon production coincident with the construction of dams in the Columbia and Snake Rivers. In the 1960s, Raymond (1988) measured spring/summer Chinook salmon SARs to the Snake River that ranged from 3-5 to 6% with four dams in place along the migratory corridor. In 1970s, four additional large hydropower dams were constructed along the migratory corridor, leading to reductions in Chinook salmon survival. From 1994 to 2017, Snake River Chinook salmon SARs averaged 0.76 % (McCann et al. 2019), which is consistent with our estimates. When SARs decline below 1%, salmon populations exhibit steep declines (ISAB 2018; McCann et al. 2020). Correspondingly, our MFSR-wide estimated average population growth rates were slightly below replacement for all spatial scales (Figure 4.5).

Despite poor population growth rates for the MFSR as a whole, we show that Chinook salmon in the MFSR basin have been sustained by a minority of subpopulations with particularly high growth rates during our study period. Several spatial units, such as Marsh Creek (MAR, intermediate scale) and segment "w" (fine scale) within the Big Creek population (BIG, intermediate scale) (Figure 4.1), experienced population growth during our study. These are exceptions, however, since our model suggests that half or more of the MFSR (depending on scale of inference) cannot currently support positive population growth.

Linking migrant survival to variation in productivity

Our model results show that increasing migrant survival by removing dams would substantially increase population growth rates in the basin. In our simulations, removing 3 or 4 dams increases the number of MFSR stream segments that can support population growth, leading to a transition from a condition where a minority of segments are capable of supporting growing populations to one in which a strong majority of segments are capable of supporting population growth (Figure 4.8). If four dams were removed, growth rates would increase by 20-50%, after which 69% of stream segments in the MFSR would support viable population growth, compared to only 26% with no dams removed. These substantial gains result in part from an increase in juvenile survival of roughly 40% ($\overline{\phi_H}^{1-(\pi/8)} = 0.5^{(4/8)}$), which is higher than that predicted by the Comparative Survival Study (CSS), where dam breaching was predicted to increase in-river survival by as much as 25% for Snake River Chinook salmon (see figure 2.8 in McCann et al. 2019). However, our scenarios assumed no benefit of dam breaching for marine survival, in contrast to the substantial benefits predicted by the CSS (figure 2.12 in McCann et al. 2019) due to carryover effects of increased flow rates and fewer powerhouse passages after dam removals (Haeseker et al. 2012, McCann et al. 2019). In this sense, our dam removal scenarios

are more conservative than McCann et al. (2019). It is striking then, that significant improvements in MFSR recruitment may be expected even with conservative estimates of dam removal benefits.

Overall benefits of improving migrant survival will also depend on marine conditions. Climate change appears to have degraded marine survival and growth conditions and may have negative consequences as ocean productivity and predation regimes continue to change with ocean temperatures and currents (Ohlberger et al. 2018, Crozier et al. 2019, 2020). If SARs continue trending downward due to climate change, harvest, predation, or other factors (Chasco et al. 2017a, Crozier et al. 2019), it becomes even more imperative to improve conditions in the migration corridor in order to boost SARs and population growth (NPCC 2014).

Dam removals benefit Chinook salmon by releasing them from mortality associated with the novel environments that dams and impoundments create. Dam removals not only eliminate acute and delayed mortality when passing dams, removal also eliminates the severe and deleterious effects of reservoirs and other habitat alterations on the timing and success rate of migrating salmon (Keefer et al. 2012, Caudill et al. 2013) as well as increased predation from birds and other fishes (Wiese et al. 2008). McCann et al. (2019) found that breaching 4 dams could have a strongly positive effect on Chinook salmon SARs. McCann et al. (2019) suggested that in-river survival without dams may be as low as 80% after reducing powerhouse passages and transit times to "natural" levels, but ignoring the influence of reservoirs and other novel riverine conditions produced by dams. Available estimates of survival through an unregulated Snake River are few, but Widener et al. (2018) reported survival rates in excess of 90% from the trap site to LGR in recent years and Raymond (1979) reported survival rates of 90% (range:

85%-95%) along the undammed section of Snake river above Ice Harbor dam in 1966-1968 (prior to the construction of 3 additional upstream dams, including LGR).

Our observation that the MFSR Chinook salmon population is supported by only a few sub-populations, combined with the estimation that many or most MFSR sub-populations are in decline, suggests that dispersal may explain the continued observation of redds in low-productivity areas during annual surveys. At increasingly fine spatial scale, the assumption of isolation of sub-populations is increasingly unsupportable, which motivates the need to account for the roles of connectivity and dispersal in driving (re-)colonization among habitats in this large wilderness watershed. Most Chinook salmon home to their natal reaches, but some stray, allowing meta-population connectivity (Isaak et al. 2006, Neville et al. 2006). Recent work in the upper Columbia River indicates that straying rates of individuals to neighboring habitats (at scales equivalent to our "intermediate" scale) was near 15%. In the MFSR, juvenile dispersal appears highly localized, where an estimated 87% of juvenile fish dispersed less than 10 km from their natal site (Hamann and Kennedy 2012). Spatial autocorrelation in population genetics of Chinook salmon in the MFSR suggests females tend to be closely related at a spatial scale of 10-40 km between spawning locations (Neville et al. 2006), which is roughly comparable in size to the segments at our fine spatial scale. At our "fine" scale, dispersal may play a role in explaining the distribution of redds through the MFSR. Dispersal may occur with the formation of new habitat patches, such as by debris flows of wood and sediment from the landscape into the river. New redds have been observed in places with new debris flows, despite a long history of redds never being observed near those locations (Thurow 2015). However, the extent to which dispersal repopulates low-productivity areas within the MFSR is unknown and warrants further investigation.

Limitations

There are a number of factors we did not include in our model that are important for salmon ecology, survival, and conservation. Marine survival is difficult to estimate, and we have done so coarsely here (though others have treated it more coarsely, or assumed a survival rate: e.g., Ricker 1976, Zabel et al. 2006). Estimation of survival during each full ocean year, rather than one integrated estimate for the entire ocean residency period, would allow more refined use of covariates (such as annual or monthly PDO measures) and also be useful for estimating annual variation in maturation probabilities, though there is very little information with which to estimate these parameters. Estimation of marine survival could also be improved by incorporating harvest of adults by fisheries or by predation by orcas and seals (Chasco et al. 2017a, 2017b). However, human harvest rates for Snake River wild Chinook salmon are low. Ocean harvest rates averaged <1 % (Schaller et al. 2014) and the Columbia River treaty and non-treaty fishery harvested an average of 9% of returns from 1980 to 2018 (Joint Columbia River Management Staff 2019).

When estimating parameters from our supporting datasets, we have included temporally-varying random effects terms to account for variation not explained by the covariates we did include. These random effects terms allow variation due to harvest, predation, or river flow without explicitly estimating their individual effects. Since we are interested primarily in accounting for variation in outside-basin conditions on MFSR Chinook salmon rather than explaining them, our approach was appropriate. However, our model could be expanded to accommodate additional data in regression sub-models such as those for marine survival or in-river hydrosystem survival.

Recent spawner abundances in the MFSR are less than 3% of abundances during the mid-1900s, based on redd surveys conducted as early as the 1950s (Thurow et al. 2020). Furthermore, the MFSR has avoided much of the anthropogenic land alterations that have reduced Chinook salmon habitat in other basins and may intensify competition among juveniles or among nesting females. Thus, we assume no density dependence in smolt production. However, density dependence has been documented in Columbia/Snake River Chinook salmon, where high densities of smolt and parr may reduce growth and survival. A model of density-independent recruitment consistently performed worse than several models of density-dependent recruitment (Zabel et al. 2006). Petrosky et al. (2001) found evidence of density-dependent mortality in the juvenile stage for Snake River Chinook salmon between 1962 and 1997 using a regression analysis based on the Ricker recruitment model. Even in the areas of the MFSR with the lowest quality habitat, habitat quality remains quite high (Thurow et al. 2020), suggesting that displacement of fish to these habitats might not result in poor performance. It is possible that density dependence may affect some of the higher-density spawner areas of the MFSR such as in Bear Valley Creek, Marsh Creek, or Big Creek (Figure 4.1). Extensions of our model could accommodate density dependence, as Achord et al. (2003) argued should be done specifically for Snake River spring/summer Chinook salmon. However, apparent density dependence in productivity among these ICTRT "populations" (ICTRT 2003), equivalent to our intermediate scale, may be strongly influenced by clustering at very low adult densities (Isaak and Thurow 2006). Variation in clustering with density may indicate density-dependent dispersal, which might lead to the observed positive relationship between the number of stream reaches occupied by spawning Chinook salmon and the size of the spawning run, as noted previously in the MFSR (e.g., Jacobs et al. 2021). Clustering behavior may limit productivity at highly local scales, which

can lead to the false appearance of habitat limitation at large scales of inference, underscoring the importance of selecting the right spatial scale for analysis.

Summary

The results of our analysis are immediately useful for discussions of management actions and cost-benefit analyses that consider Snake River restoration, and they illuminate future directions for research and management application. Any consideration of river restoration requires information on the predicted responses to those actions. Our data provide a high resolution assessment of freshwater habitat productivity for Chinook salmon, demonstrating the heterogeneity in productivity that may exist even within the current scale of management defined by the ICTRT (2003), and the consequences of that heterogeneity under management scenarios that mitigate outside basin mortality. Lastly, our model highlights the value of high-resolution time-series data for ecological research and management in general, and of the value of this unique spatially continuous, long term dataset of Chinook salmon in the MFSR.

Table 4.1. The total number of carcasses of females and their age distribution for the eight intermediate-sclae spatial units (ICTRT "Population", Figure 1) in the Middle Fork Salmon River from 1998 through 2016.

Sub-basin	Population	Age 4	Age 5	Age 6	Total
Lower	BIG	0	0	0	0
Lower	CAM	81	51	0	132
Lower	LMA	139	57	0	196
Lower	LOO	2	3	0	5
Upper	BEA	158	99	5	262
Upper	MAR	41	31	0	72
Upper	SUL	341	461	14	816
Upper	UMA	363	387	8	758
Total		1125	1089	27	2241

Table 4.2 Model parameters, their 90% highest density intervals (HDI), and the probability that the parameter lies in the area of practical equivalence (ROPE) to a null (equal to zero) effect (logit-scale parameters only) from the model evaluated at the population scale of inference.

Parameter	Description	Median	HDI		pROPE (logit)
$\overline{\delta_{t<2007}}$	Median proportion of wild fish transported prior to 2007	0.7	0.6	0.8	
$\overline{\delta_{t>2006}}$	Median proportion of wild fish transported after 2006	0.3	0.2	0.4	
$\beta_{0\delta}$	logit-scale average transport probability prior to 2007	1.09	0.60	1.52	0.00
$\beta_{1\delta}$	logit-scale difference between $\beta_{0\delta}$ and average transport probability after 2006	-1.85	-2.59	-1.04	0.00
σ_{δ}	logit-scale random temporal variation in the proportion transported	0.47	0.05	0.91	0.08
r_{δ}	Beta distribution scale parameter	7.54	2.31	26.18	
$\overline{\phi_H}$	Study-wide median in-river smolt survival	0.50	0.35	0.63	
μ_H	logit-scale mean survival probability	-0.03	-0.22	0.18	0.92
σ_H	logit-scale random temporal variation in survival probability	0.27	0.05	0.47	0.24
r_H	Beta distribution scale parameter	47.81	7.13	396.10	
$\overline{\phi_M}$	Study-wide marine survival probability (across cohorts)	0.02	0.00	0.25	
β_{0M}	logit-scale intercept of survival probability	-3.37	-4.50	-2.24	0.00
β_{1M}	logit-scale effect of smolt year September PDO	0.15	-0.54	0.71	0.40
β_{2M}	logit-scale effect of smolt year April UWI	0.01	-0.03	0.05	1.00
β_{3M}	logit-scale effect of the proportion of smolts transported, δ	-1.10	-2.85	0.46	0.07
β_{4M}	logit-scale effect of 4-year average May-July PDO from smolt year-1 through smolt year+2	-0.83	-1.93	0.28	0.08
σ_M	logit-scale random temporal variation in survival probabilit	1.50	1.06	2.11	0.00
ϕ_R	Adult migratory survival probability	0.81	0.76	0.85	

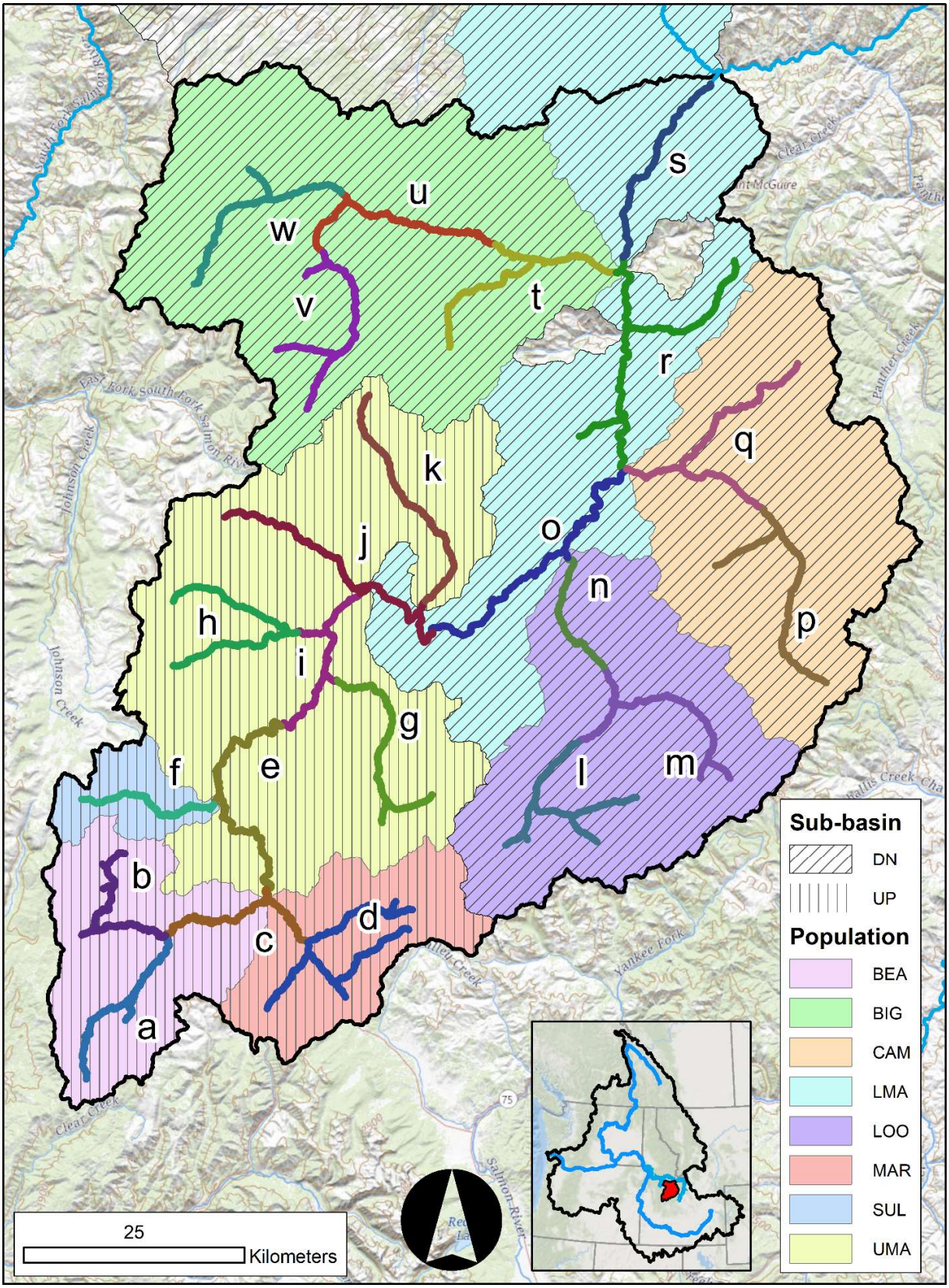
a
b
c
d
e
f
g
h
i
j
k
l
m
n
o
p
q
r
s
t
u
v
w
Sub-basin
DN
UP
Population
BEA
BIG
CAM
LMA
LOO
MAR
SUL
UMA
25
Kilometers

Figure 4.1. Map of the lower Middle Fork Salmon River watershed (black outline), and the Sub-basins, ICTRT populations, and segments that comprise it. “Sub-basins” represent our coarse scale of inference and are indicated by hatch marks (vertical hatch marks for the “Upper” MFSR sub-basin, diagonal hatch marks for the “Lower”). “Populations” represent our intermediate scale of inference and are indicated by color polygons, referring to the ICTRT-defined (2003) populations, Bear Creek (BEA), Big Creek (BIG), Camas Creek (CAM), the lower MFSR management area (LMA), Loon Creek (LOO), Marsh Creek (MAR), Sulphur Creek (SUL), and the upper MFSR management area (UMA). Stream segments representing our fine scale of inference are indicated by colored stream lines labeled with letters of the alphabet. Part of the LMA population lies outside of the watershed outline and outside our sample area. The inset map shows the Columbia River basin outlined in black, the Columbia River and its major tributaries in blue, and the MFSR watershed outlined in black with red fill.

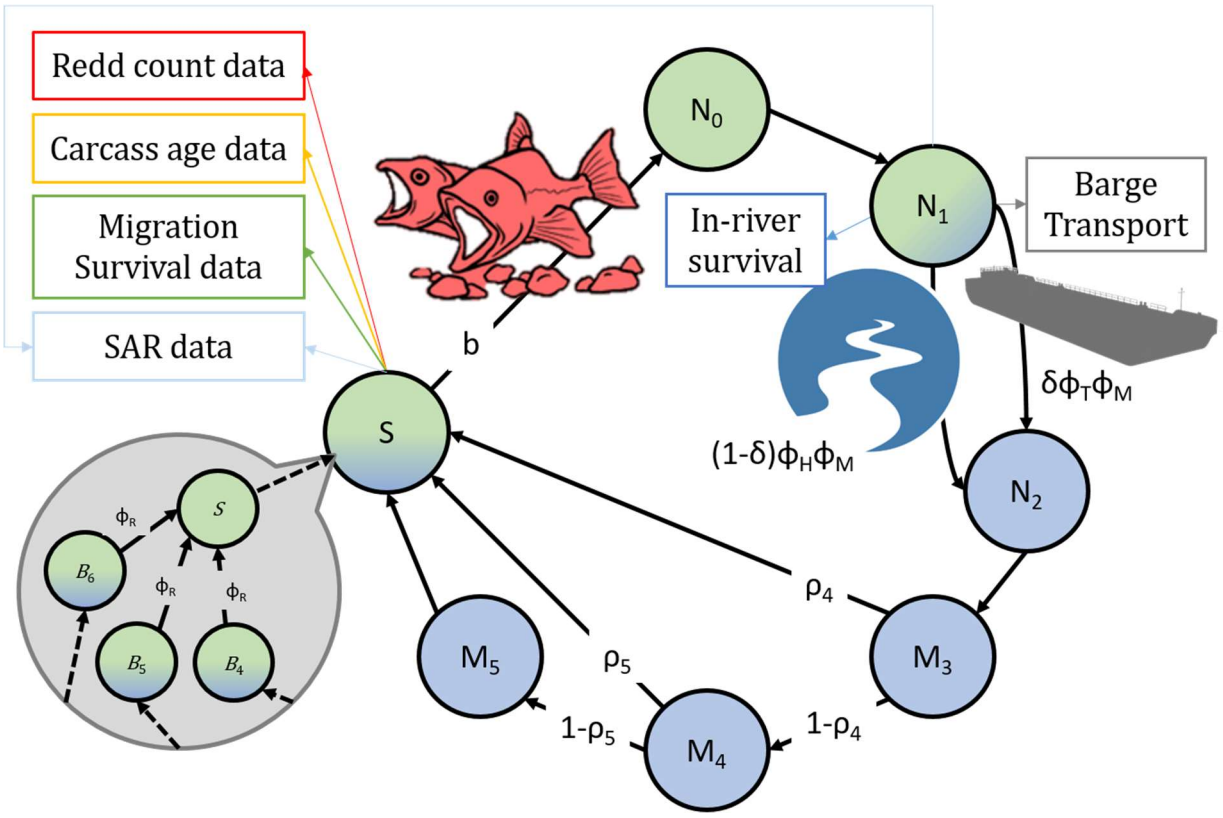

Figure 4.2. Chinook salmon life cycle diagram of used to structure our integrated Bayesian state-space model. Subscripts on stages (e.g., N_0) indicate the age of fish that comprise those stages. The *S* stage is the spawning fish stage comprised of multiple ages, the *N* stages are juveniles, the *M* stages are non-migratory adults, and the *B* stages are migratory adults. Green color indicates a freshwater stage, blue indicates a marine stage, and color gradients indicate a migratory stage. Arrows between stages represent stage transitions controlled by survival and birth processes, as described in the manuscript. Boxes indicate datasets, and arrows leading to boxes indicate which stages contributed data.

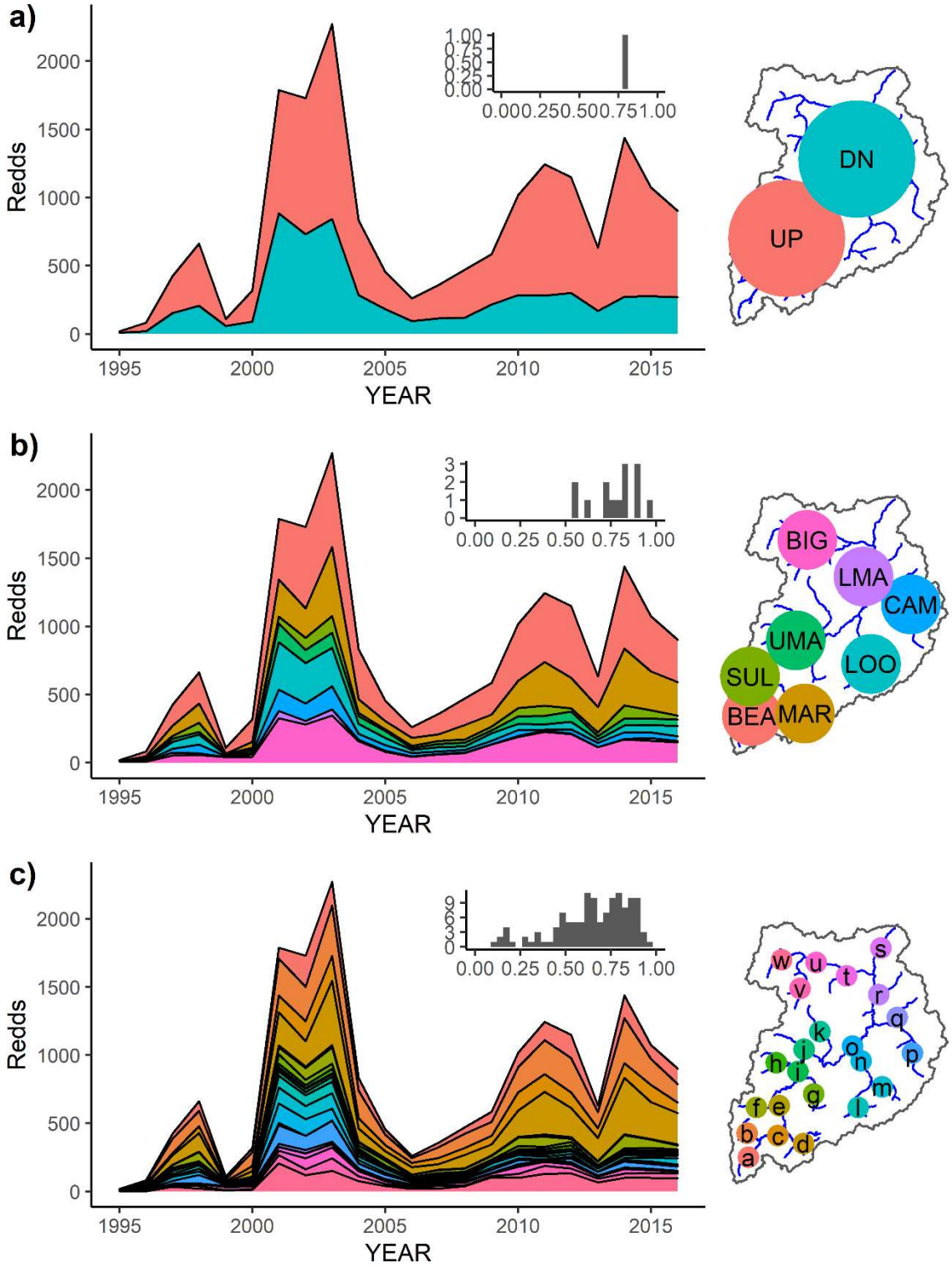
a)
Redds
YEAR
DN
UP
b)
Redds
YEAR
BIG
LMA
CAM
UMA
LOO
SUL
BEA
MAR
c)
Redds
YEAR

Figure 4.3. A stacked time-series plot for continuous MFSR redd counts aggregated at (a) coarse scale (Sub-basins) , (b) intermediate scale ("populations" (ICTRT 2003)), and (c) fine scale (segments (Isaak and Thurow 2006)). Sub-panels in the upper right corner of each time series plot show the distribution of pairwise Pearson's correlation coefficients among spatial units at that panel's spatial scale (i.e., coarse, intermediate, and fine). Map legends indicate the location of each spatial unit in the basin by color.

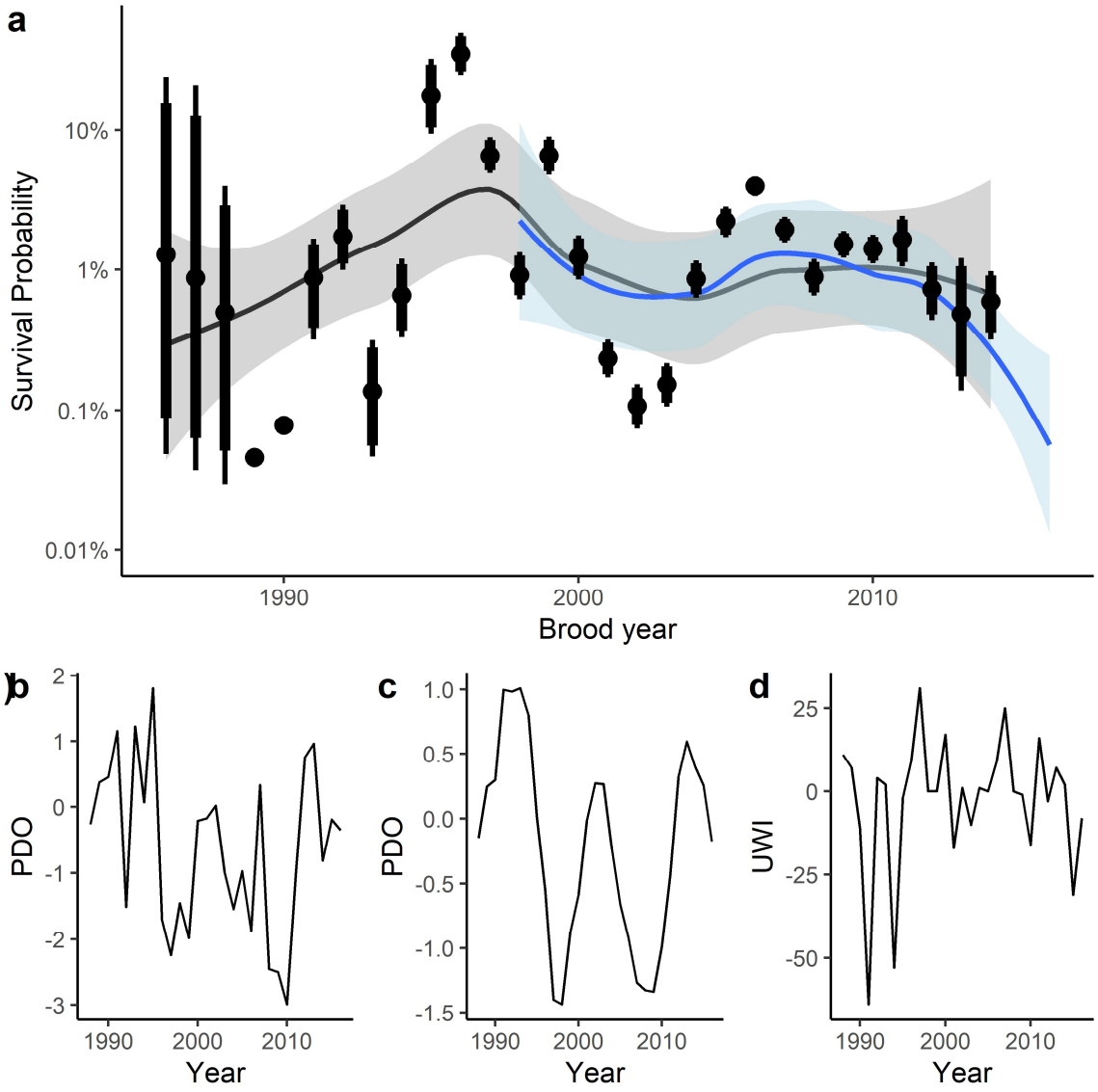

Figure 4.4. Observed smolt-to-adult return (SAR) rate in panel (a), with black circles, thick vertical lines, and thin vertical lines representing (respectively) the median, 90% highest density interval, and 95% highest density interval of SAR estimates during each year. A dark grey curve (with grey error bounds) follows the smoothed annual variation in estimated SARs, and the blue curve (with light blue error bounds) follows the smoothed annual variation in observed PIT tag-based SAR data for MFSR stocks. Panel (b) shows annual variation in September Pacific Decadal Oscillation (PDO) during our study. Panel (c) shows annual variation in 4-year average

PDO during the months of May, June, and July. Panel (d) shows annual variation in the upwelling index during April for 125W and 45N.

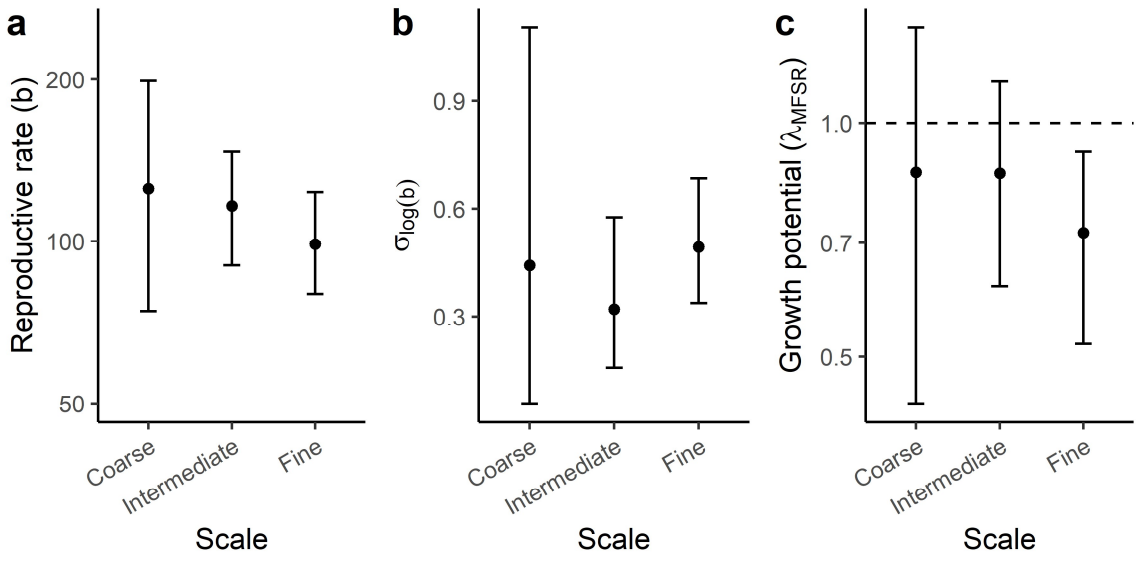

Figure 4.5. Variation in the median and 95% highest density interval estimates of average reproductive rate b (panel a), its standard deviation σ_b (panel b), and the basin-wide growth rate λ_{MFSR} in the MFSR across spatial scales of inference: coarse (sub-basin), intermediate (population), and fine (segment) (panel c).

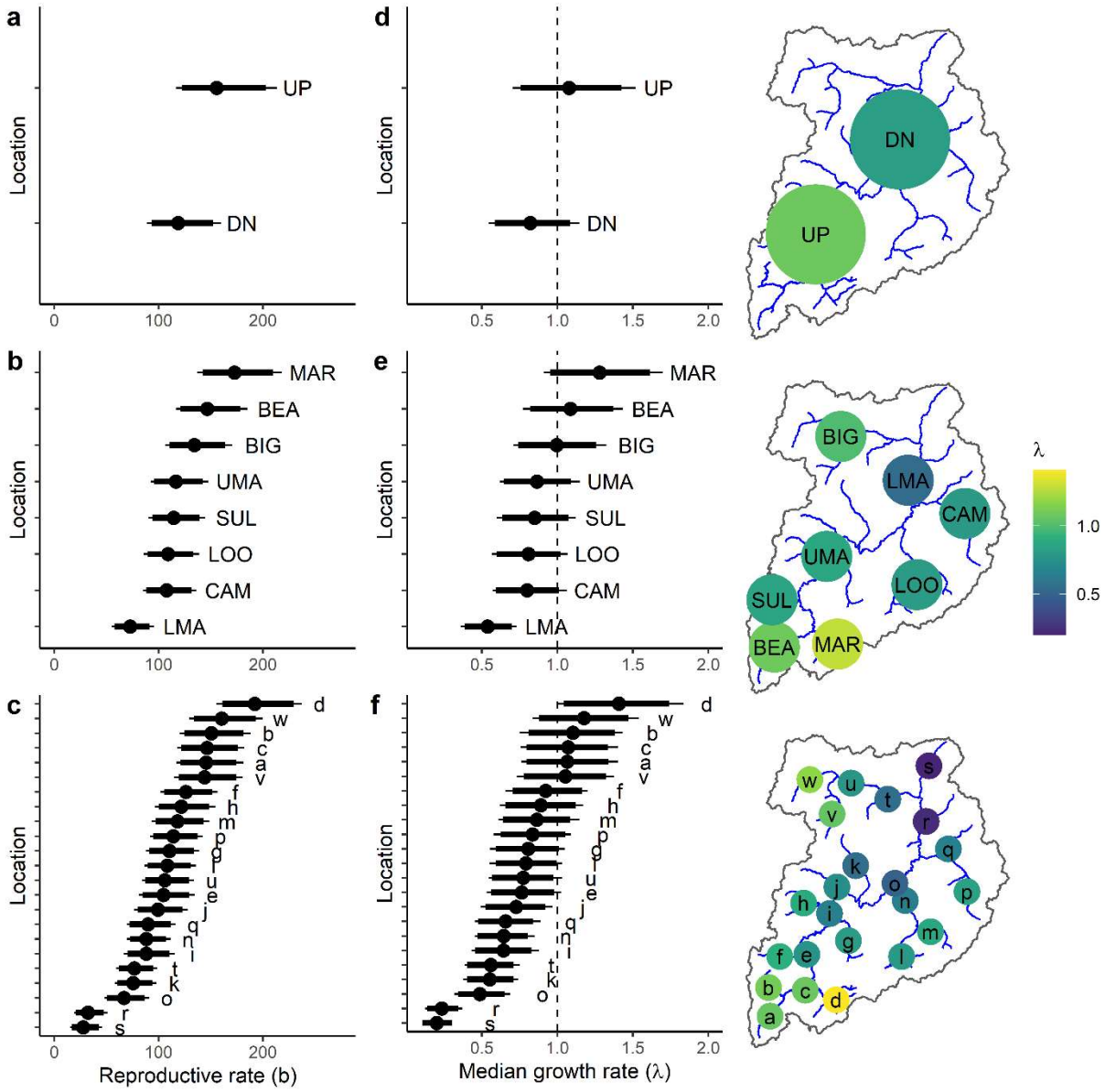

Figure 4.6. Spatial distribution and variation in reproductive rate, b (smolts per redd), and growth rate, λ (redds per redd). Panel rows correspond to spatial scales, and columns to reproductive rate b (first column), and growth potential λ (second and third columns). Panels (a), (b), and (c) show the median reproductive rates (dot), 90% highest density interval (thick line) and 95% highest density interval (thin line) for each spatial unit in caterpillar plot format with b plotted on the x axis, and the location plotted on the y axis. Panels (d), (e), and (f) show the median growth rate (dot), 90% highest density interval (thick line) and 95% highest density

interval (thin line) for each spatial unit in caterpillar plot format with λ plotted on the x axis, and the location plotted on the y axis. The right hand column of panels (d), (e), and (f) show the approximate spatial distribution of median growth rate estimates across a map of the MFSR (blue line) and its watershed (black outline), where points are scaled by color (lighter is higher) and labeled to match median and highest density interval plots.

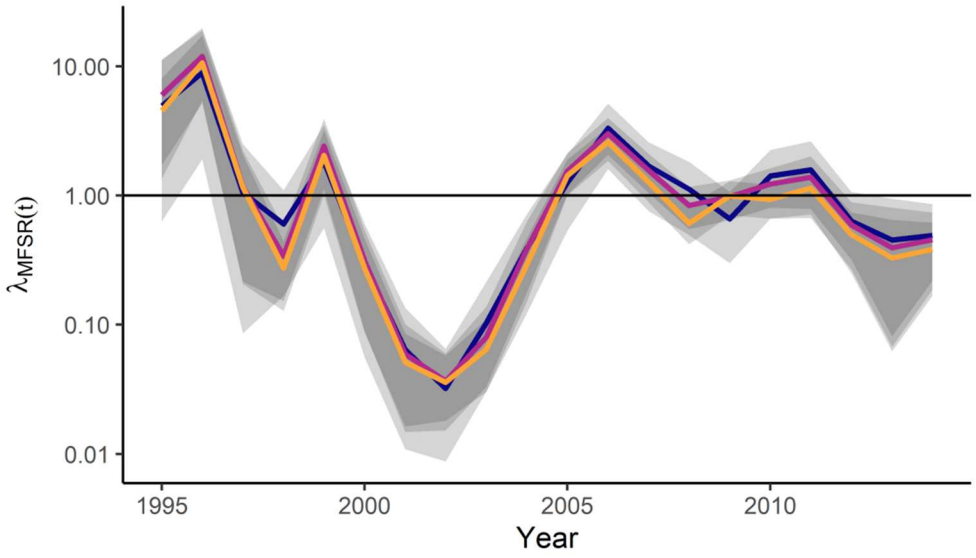

Figure 4.7. Estimated MFSR basin average population growth potential (λ) over time from 1996 through 2014. Colors denote the scale of inference used for the estimate: blue for coarse scale, purple for intermediate scale, and yellow for fine scale.

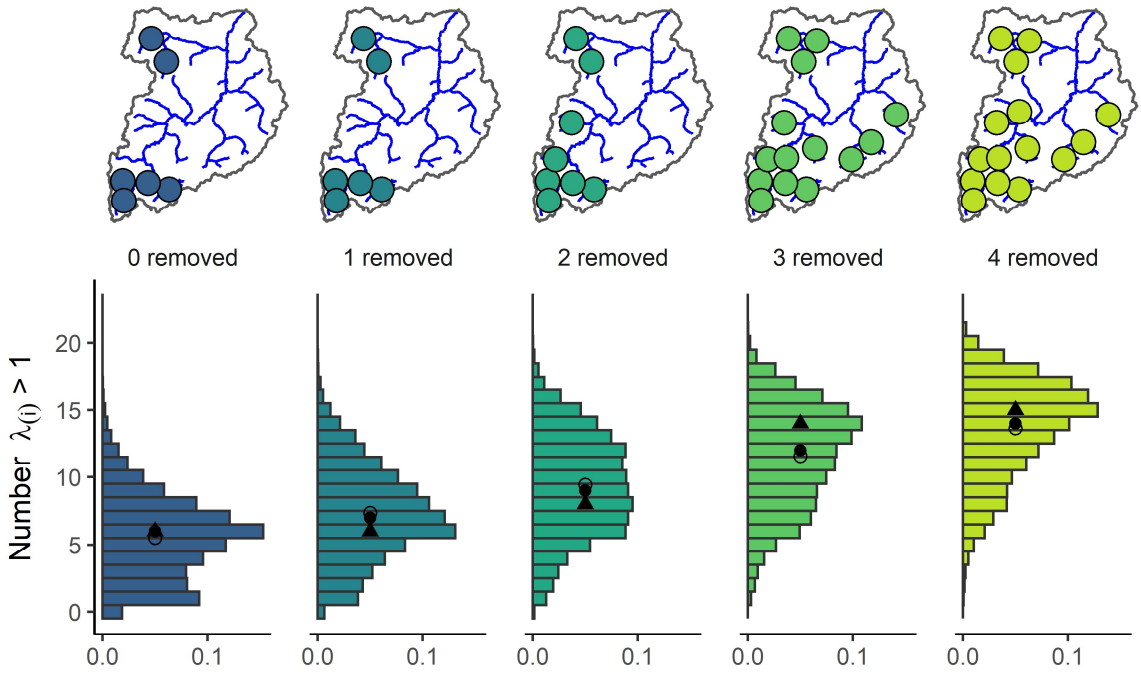

Figure 4.8. The predicted number and location of suitable river segments for Chinook salmon production in the MFSR under dam removal scenarios. The horizontal bar plots indicate the posterior distributions of the number of fine-scale segments (out of 23 total) with a median population growth rate above replacement ($\lambda > 1$), under scenarios varying the number of Snake River dams removed from 0 (left-most panel) to 4 removed (right-most panel). The mean of each distribution is indicated by an unfilled circle, the median by a black filled circle, and the mode by a black filled triangle. The mode is the most likely number of spatial units with growth rates above replacement. Map panels above bar plots indicate the locations of the segments most likely to have growth rates above replacement in each dam removal scenario.

CHAPTER 5

CONCLUSION

In this dissertation, I have investigated the relationship between environmental variation and migration probability, migratory destination, and population growth of migratory fishes. I have used empirical case studies to show how environmental variation affects population dynamics in time (via covariation of environment and reproductive frequency) and in space (via spatial heterogeneity in habitat use and population growth) for two migratory fishes. The results of the three studies in Chapters 2 through 4 add to the disciplines of ecology and conservation biology by (1) reinforcing the utility of statistical state-space models to answer salient ecological questions of populations and their dynamics by simultaneously incorporating information from multiple explanatory and response datasets, (2) documenting and quantifying a previously unobserved association between water temperatures and lake sturgeon breeding frequency, and (3) demonstrating that spatial heterogeneity in the productivity of Chinook salmon breeding habitats determines the population response to dam removals (and associated survival benefits) via a positive but non-linear relationship between the number of dams removed and the amount of viable habitat upstream.

Integrated state-space models

State space models can be used to explain ecological timeseries data as arising from two concurrent and independent processes: a latent (unobserved) population dynamic process and an observation process that imperfectly observes the latent state. Examples include mark-recapture models, integrated population models, and lifecycle population dynamics models fit for a variety

of species and in a variety of circumstances (Kéry and Schaub 2012, Su and Peterman 2012, Fleishman et al. 2013, Lee et al. 2015, Aeberhard et al. 2018). Statistical state-space models are often implemented using Bayesian analysis software such as JAGS (Plummer 2017) because model construction in such software is highly flexible and customizable (Kéry and Schaub 2012). A useful feature of both Bayesian statistical models (generally) and state-space models (specifically) is that multiple response variable datasets can be integrated into a single model's structure, allowing parameter estimation to draw consensus from multiple observational data sources. In this dissertation, I have built two Bayesian state-space models, each integrating several responses and explanatory variables, and purpose-built for the questions at hand: An integrated capture-mark-recapture model of lake sturgeon breeding decisions (Chapter 3), and an integrated lifecycle model of Chinook salmon survival and reproduction (Chapter 4). In both of these implementations, I have demonstrated how Bayesian state-space models can be tailored to specific questions, and can incorporate multiple information sources to infer ecological dynamics. With continuing increases in computational power and the amount and availability of data in fisheries, ecology, and conservation research (e.g., Hampton et al. 2013, Dauwalter et al. 2017), multiple complementary datasets are increasingly available, and thus integrated state-space models are increasingly useful for answering important ecological questions.

In a warming world, female lake sturgeon may spawn more frequently

Individuals may not breed at every opportunity due to constraints imposed through physiology, resource availability, and time. For example, Atlantic cod (*Gadus morhua*) will skip spawning opportunities due to lack of energetic resources, which may lead to partial migration in which only a subset of mature animals migrate (Jørgensen et al. 2006). Alternatively, an animal's breeding schedule may be unresponsive to environmental variation. A fixed periodic

reproductive schedule could still give rise to partial migration if individuals do not have synchronized schedules. Such a pattern is expected based on theory developed to understand the evolution of skipped breeding (Shaw and Levin 2013), and has been observed empirically in other taxa (e.g., Albatrosses, Family: Diomedeidae; Jouventin and Dobson 2002). Forsythe et al. (2012) argued that individual lake sturgeon tend to express inflexible spawning intervals, and that intervals differ most strongly by sex, with females spawning less frequently. My results in Chapter 3 reinforce the result that female sturgeons spawn less frequently than males.

However, my work in Chapter 3 also demonstrated that patterns of reproduction and migration responded to interannual environmental variation, an effect not previously documented in this species. Specifically, adult female lake sturgeon were more likely to attempt breeding migrations when spring water temperatures were warmer, and as a result, the ratio of males to females in the breeding habitat decreased as water temperature warmed. Such changes suggest that this population may be sensitive to climate change through increased exposure of valuable (for population growth) female lake sturgeon to novel anthropogenic stressors found in or near breeding habitats in the lower Niagara River, such as hydropower and recreational angling. The prospect of climate-induced increases in female reproductive frequency raises other more general questions for lake sturgeon conservation. For example, what are the fitness costs of females spawning more frequently in a warming world? Spawning more frequently may increase the demand for food resources if female reproductive output is limited by energy allocation to egg production, so spawning more frequently may reduce fecundity if food resource acquisition does not also increase. Alternatively, it may be important to test the interpretation of these results to mean that breeding decisions are based directly on temperature, rather than on deviations from

some longer term average temperature (for example): perhaps females like it *hotter*, if not necessarily *hot*.

Spatial heterogeneity in productivity controls the response to dam removals in salmon

The relationship between population growth rates and environmental variation is central to the study of ecology. The link between population growth and environmental variation can be conceptualized in terms of habitat suitability and habitat quality, which are the ability of a habitat to support positive population growth, and the expected population growth rate of a habitat, respectively (Kellner et al. 1992). Though habitat occupancy does not necessarily equate to suitability or quality, observations of habitat occupancy across time can indicate variation in habitat suitability and habitat quality, where low-quality habitats are less likely to be regularly occupied than higher-quality habitats. In an analysis of Chinook salmon habitat occupancy in the Middle Fork Salmon River, I found that this near-pristine watershed holds abundant spawning habitat, the distribution of which is influenced by spatiotemporal variation in sediment deposition, debris flows, and wildfires. Further, I found that spawning habitat availability for the Middle Fork Salmon River (MFSR) Chinook salmon population should be relatively insensitive to increased temperatures from climate change over the next 60 years, due to the availability of high quality habitat at higher elevations (see also Isaak et al. 2016).

I developed a Chinook salmon life-cycle model with fine-scale, data-driven estimates of reproductive output and population growth heterogeneity among breeding habitats in the MFSR. My results suggest that a few localized areas support exceptionally high reproductive rates and thus play a disproportionate role in explaining the persistence of Chinook salmon in the Middle Fork Salmon River basin. When confronted with moderately conservative scenarios of dam removal benefits for Chinook salmon, my model suggested that the removal of all four Snake

River dams may result in 20-50% higher growth rates than experienced during recent decades, shifting the fraction of habitat in the MFSR basin that supports the persistence of salmon from 24% with no dam removals, to 67% with four Snake River dam removals. The results show a non-linear increase in the modal fraction of viable breeding habitat across variation in outside-basin survival that is scale-independent across three spatial scales of data aggregation, though the mean and median increase more linearly. These estimates omit the explicit influence of several important environmental variables on survival, especially carryover effects of freshwater conditions on the marine phase. In this sense, my estimates of the benefits of dam removal are more conservative than others in the literature (e.g., McCann et al. 2019). However, any estimates of the benefits of dam removal may be blunted by reduced survival arising from future degradation of riverine and marine habitats due to climate change (Crozier et al. 2020). My results demonstrate the link between temporal variation in survival in feeding and corridor habitats and the amount and distribution of suitable breeding habitat. Such results are important for migratory fish conservation generally because they document a long-distance spatial coupling of survival and reproduction processes of a migratory species, and demonstrate the utility of methods for measuring this phenomenon that may be used in other systems. Important extensions to this work should include estimation of density dependence in smolt production of Chinook salmon in the MFSR in order to project population growth into the future, and estimation of dispersal (or "straying") rates that may control recolonization processes.

REFERENCES

Aeberhard, W.H., F. J. Mills, and A. Nielsen. 2018. Review of state-space models for fisheries science. Annual Review of Statistics and Its Application, 5:215-235.

Able, K.P., and Able, M.A. 1998. The roles of innate information, learning rules and plasticity in migratory bird orientation. Journal of Navigation 51: 1–9.

Achord, S., Levin, P.S., and Zabel, R.W. 2003. Density-dependent mortality in Pacific salmon: The ghost of impacts past? Ecology Letters 6: 335–342. Wiley Online Library.

Allee, W.C. 1927. Animal aggregations. The Quarterly Review of Biology 2: 367–398. Williams; Wilkins.

Allen, P.J., Webb, M.A., Cureton, E., Bruch, R.M., Barth, C.C., Peake, S.J., and Anderson, W.G. 2009. Calcium regulation in wild populations of a freshwater cartilaginous fish, the lake sturgeon *Acipenser fulvescens*. Comparative Biochemistry and Physiology Part A: Molecular & Integrative Physiology 154: 437–450. Elsevier.

Arendt, J.D., Reznick, D.N., and López-Sepulcre, A. 2014. Replicated origin of female-biased adult sex ratio in introduced populations of the Trinidadian guppy (*Poecilia reticulata*). Evolution 68: 2343–2356. Wiley Online Library.

Auer, N.A. 1999. Population characteristics and movements of lake sturgeon in the sturgeon river and Lake Superior. Journal of Great Lakes Research 25: 282–293. Elsevier.

Bade, A.P., Binder, T.R., Faust, M.D., Vandergoot, C.S., Hartman, T.J., Kraus, R.T., Krueger, C.C., and Ludsin, S.A. 2019. Sex-based differences in spawning behavior account for male-biased harvest in Lake Erie walleye (*Sander vitreus*). Canadian Journal of Fisheries and Aquatic Sciences 76: 2003–2012. NRC Research Press.

Bartón, K. 2019. MuMIn: Multi-Model Inference. R package version 1.43.6. https://CRAN.R-project.org/package=MuMIn.

Bates, D., M. Maechler, B. Bolker, and S. Walker. 2015. Fitting linear mixed-effects models Using lme4. Journal of Statistical Software 67(1): 1-48. DOI: 10.18637/jss.v067.i01.

Baxter, C. V., and F. R. Hauer 2000. Geomorphology, hyporheic exchange, and selection of spawning habitat by bull trout (*Salvelinus confluentus*). Canadian Journal of Fisheries and Aquatic Sciences 57: 1470-1481.

Beechie, T., H. Moir, and G. Pess. 2008. Hierarchical physical controls on salmonid spawning location and timing. Pages 83-101 in D.A. Sear and P. DeVries, editors. Salmonid Spawning Habitat in Rivers: Physical Controls, Biological Responses, and Approaches to Remediation. American Fisheries Society Symposium 65, Bethesda, MD.

Benda, L., C. Veldhuisen, and J. Black. 2003. Debris flows as agents of morphological heterogeneity at low-order confluences, Olympic Mountains, Washington. Geological Society of America Bulletin 115(9): 1110-1121.

Bond, M.H., Miller, J.A., and Quinn, T.P. 2015. Beyond dichotomous life histories in partially migrating populations: Cessation of anadromy in a long-lived fish. Ecology 96: 1899–1910. Wiley Online Library.

Briggs, A.S., Hessenauer, J.-M., Thomas, M.V., Utrup, B.E., and Wills, T.C. 2020. Trends and effects of a recreational lake sturgeon fishery in the St. Clair system. North American Journal of Fisheries Management. Wiley Online Library.

Brooks, M. E., K. Kristensen, K. J., van Benthem, A. Magnusson, C. W. Berg, A. Nielsen, H. J. Skaug, M. Machler, and B. M. Bolker. 2017. glmmTMB balances speed and flexibility among packages for zero-inflated generalized linear mixed modeling. The R Journal 9(2): 378-400.

Bruch, R., Haxton, T., Koenigs, R., Welsh, A., and Kerr, S. 2016. Status of lake sturgeon (*Acipenser fulvescens* Rafinesque 1817) in North America. Journal of Applied Ichthyology 32: 162–190. Wiley Online Library.

Bruch, R.M. 2008. Modeling the population dynamics and sustainability of lake sturgeon in the Winnebago system, Wisconsin. PhD thesis.

Bruch, R.M., and Binkowski, F. 2002. Spawning behavior of lake sturgeon (*Acipenser fulvescens*). Journal of Applied Ichthyology 18: 570–579. Blackwell Science Ltd Oxford, UK.

Bruestle, E. 2017. Lake sturgeon (*Acipenser fulvescens*) trophic position and movement patterns in the lower niagara river, ny.

Budy, P., Thiede, G.P., Bouwes, N., Petrosky, C., and Schaller, H. 2002. Evidence linking delayed mortality of Snake River salmon to their earlier hydrosystem experience. North American Journal of Fisheries Management 22: 35–51. Taylor & Francis.

Buffington, J. M., and D. R. Montgomery. 1999. Effects of hydraulic roughness on surface textures of gravel-bed rivers. Water Resources Research 35(11):3507-3522.

Buffington, J. M., D. R. Montgomery, and H. M. Greenberg. 2004. Basin-scale availability of salmonid spawning gravel as influenced by channel type and hydraulic roughness in mountain catchments. Canadian Journal of Fisheries and Aquatic Sciences 61(11): 2085-2096.

Bull, J.J., and Shine, R. 1979. Iteroparous animals that skip opportunities for reproduction. The American Naturalist 114: 296–303. University of Chicago Press.

Carlson, D.M. 1995. Lake Sturgeon waters and fisheries in New York State. Journal of Great Lakes Research 21: 35–41. doi: 10.1016/S0380-1330(95)71018-8.

Carmichael, R.A., Tonina, D., Keeley, E.R., Benjankar, R.M., and See, K.E. 2020. Some like it slow: A bioenergetic evaluation of habitat quality for juvenile Chinook salmon in the Lemhi River, Idaho. Canadian Journal of Fisheries and Aquatic Sciences. NRC Research Press.

Castro, J.I. 1996. Biology of the Blacktip Shark, Carcharhinus Limbatus, off the Southeastern United States. Bulletin of Marine Science 59: 508–522. Available from https://www.ingentaconnect.com/content/umrsmas/bullmar/1996/00000059/00000003/art00005.

Caudill, C.C., Keefer, M.L., Clabough, T.S., Naughton, G.P., Burke, B.J., and Peery, C.A. 2013. Indirect effects of impoundment on migrating fish: Temperature gradients in fish ladders slow dam passage by adult Chinook salmon and steelhead. PloS one 8: e85586. Public Library of Science.

CBR (Columbia Basin Research). 2020. Columbia River DART (data access in real time), PIT tag smolt-to-adult return (SAR) estimates. University of Washington Seattle. Available from http://www.cbr.Washington.edu/dart/query/pit_sar_esu.

Ceballos, G., Ehrlich, P.R., Barnosky, A.D., García, A., Pringle, R.M., and Palmer, T.M. 2015. Accelerated modern human–induced species losses: Entering the sixth mass extinction. Science advances 1: e1400253. American Association for the Advancement of Science.

Chapman, D. W. 1988. Critical review of variables used to define effects of fines in redds of large salmonids. Transactions of the American Fisheries Society 117(1): 1-21.

Chasco, B.E., Kaplan, I.C., Thomas, A.C., Acevedo-Gutiérrez, A., Noren, D.P., Ford, M.J., Hanson, M.B., Scordino, J.J., Jeffries, S.J., Marshall, K.N., and others. 2017a. Competing tradeoffs between increasing marine mammal predation and fisheries harvest of Chinook salmon. Scientific Reports 7: 1–14. Nature Publishing Group.

Chasco, B., Kaplan, I.C., Thomas, A., Acevedo-Gutiérrez, A., Noren, D., Ford, M.J., Hanson, M.B., Scordino, J., Jeffries, S., Pearson, S., and others. 2017b. Estimates of Chinook salmon consumption in Washington state inland waters by four marine mammal predators from 1970 to 2015. Canadian Journal of Fisheries and Aquatic Sciences 74: 1173–1194. NRC Research Press.

Chiotti, J.A,, J.C Boase, D.W. Hondorp, and A. S. Briggs. 2016. Assigning Sex and Reproductive Stage to Adult Lake Sturgeon Using Ultrasonography and Common Morphological Measurements. North American Journal of Fisheries Management 36(1): 21–29.

Collingsworth, P.D., Bunnell, D.B., Murray, M.W., Kao, Y.-C., Feiner, Z.S., Claramunt, R.M., Lofgren, B.M., Höök, T.O., and Ludsin, S.A. 2017. Climate change as a long-term stressor for the fisheries of the Laurentian Great Lakes of North America. Reviews in Fish Biology and Fisheries 27: 363–391. Springer.

Conn, P.B., Johnson, D.S., Williams, P.J., Melin, S.R., and Hooten, M.B. 2018. A guide to Bayesian model checking for ecologists. Ecological Monographs 88: 526–542. Wiley Online Library.

Copeland, T., Venditti, D.A., and Barnett, B.R. 2014. The importance of juvenile migration tactics to adult recruitment in stream-type Chinook salmon populations. Transactions of the American Fisheries Society 143: 1460–1475. Taylor & Francis.

Cormack, R. 1964. Estimates of survival from the sighting of marked animals. Biometrika 51: 429–438. JSTOR.

Crozier, L.G., McClure, M.M., Beechie, T., Bograd, S.J., Boughton, D.A., Carr, M., Cooney, T.D., Dunham, J.B., Greene, C.M., Haltuch, M.A., and others. 2019. Climate vulnerability assessment for Pacific salmon and steelhead in the California current large marine ecosystem. PloS one 14: e0217711. Public Library of Science San Francisco, CA USA.

Crozier, L.G., Siegel, J.E., Wiesebron, L.E., Trujillo, E.M., Burke, B.J., Sandford, B.P., and Widener, D.L. 2020. Snake River sockeye and Chinook salmon in a changing climate: Implications for upstream migration survival during recent extreme and future climates. PloS one 15: e0238886. Public Library of Science San Francisco, CA USA.

Dammerman, K.J., Webb, M.A., and Scribner, K.T. 2019. Riverine characteristics and adult demography influence female lake sturgeon (*Acipenser fulvescens*) spawning behavior, reproductive success, and ovarian quality. Canadian Journal of Fisheries and Aquatic Sciences 76: 1147–1160. NRC Research Press.

Dauwalter, D.C., K.A. Fesenmyer. R. Bjork, D.R. Leasure, and S.J. Wenger. 2017. Satellite and airborne remote sensing applications for freshwater fisheries. Fisheries, 42(10):526-537.

Deacy, W.W., Armstrong, J.B., Leacock, W.B., Robbins, C.T., Gustine, D.D., Ward, E.J., Erlenbach, J.A., and Stanford, J.A. 2017. Phenological synchronization disrupts trophic interactions between Kodiak brown bears and salmon. Proceedings of the National Academy of Sciences 114: 10432–10437. National Acad Sciences.

Denwood, M.J. 2016. Runjags: An r package providing interface utilities, model templates, parallel computing methods and additional distributions for mcmc models in jags. Journal of Statistical Software 71: 1–25. Foundation for Open Access Statistics.

Dingle, H. 2014. Migration: The biology of life on the move. Oxford University Press, USA.

Dingle, H., and Drake, V.A. 2007. What is migration? Bioscience 57: 113–121. American Institute of Biological Sciences.

Dodson, J.J. 1988. The nature and role of learning in the orientation and migratory behavior of fishes. Environmental Biology of Fishes 23: 161–182. Springer.

Dunham, J. B., M. K. Young, R. E. Gresswell, and B. E. Rieman. 2003. Effects of fire on fish populations: landscape perspectives on persistence of native fishes and nonnative fish invasions. Forest Ecology and Management 178(1-2): 183-196.

Eidenshink, J., B. Schwind, K. Brewer, Z. L. Zhu, B. Quayle, and S. Howard. 2007. A project for monitoring trends in burn severity. Fire Ecology 3(1): 3-21.

Elith, J., and J. R. Leathwick. 2009. Species distribution models: ecological explanation and prediction across space and time. Annual review of ecology, evolution, and systematics, 40, pp.677-697.

Erickson, D. L., and M.A.H. Webb. 2007. Spawning Periodicity, Spawning Migration, and Size at Maturity of Green Sturgeon, Acipenser Medirostris, in the Rogue River, Oregon. Environmental Biology of Fishes 79(3-4): 255–68.

Falcy, M. R. 2015. Density-dependent habitat selection of spawning Chinook salmon: broad-scale evidence and implications. Journal of Animal Ecology 84(2): 545-553.

Faulkner, J.R., Bellerud, B.L., Widener, D.L., and Zabel, R.W. 2019. Associations among fish length, dam passage history, and survival to adulthood in two at-risk species of Pacific salmon. Transactions of the American Fisheries Society 148: 1069–1087. Wiley Online Library.

Fausch, K. D., C. E. Torgersen, C. V. Baxter, and H. W. Li. 2002. Landscapes to riverscapes: bridging the gap between research and conservation of stream fishes: a continuous view of the river is needed to understand how processes interacting among scales set the context for stream fishes and their habitat. BioScience 52(6): 483-498.

Feist, G., C.B. Schreck, M.S. Fitzpatrick, and J.M. Redding. 1990. Sex Steroid Profiles of Coho Salmon (*Oncorhynchus kisutch*) During Early Development and Sexual Differentiation." General and Comparative Endocrinology 80 (2): 299–313.

Fitzpatrick, M.S., G. Van Der Kraak, and C.B. Schreck. 1986. Profiles of Plasma Sex Steroids and Gonadotropin in Coho Salmon, *Oncorhynchus kisutch*, During Final Maturation. General and Comparative Endocrinology 62 (3): 437–51.

Fitzpatrick, M.S., J.M. Redding, F.D. Ratti, and C.B. Schreck. 1987. Plasma Testosterone Concentration Predicts the Ovulatory Response of Coho Salmon (*Oncorhynchus kisutch*) to Gonadotropin-Releasing Hormone Analog." Canadian Journal of Fisheries and Aquatic Sciences 44 (7): 1351–7.

Fleischman, S.J., Catalano, M.J., Clark, R.A., and Bernard, D.R. 2013. An age-structured state-space stock–recruit model for Pacific salmon (*Oncorhynchus spp.*). Canadian Journal of Fisheries and Aquatic Sciences 70: 401–414. NRC Research Press.

Flitcroft, R. L., J. A. Falke, G. H. Reeves, P. F. Hessburg, K. M. McNyset, and L. E. Benda. 2016. Wildfire may increase habitat quality for spring Chinook salmon in the Wenatchee River subbasin, WA, USA. Forest Ecology and Management 359: 126-140.

Forsythe, P.S., Crossman, J.A., Bello, N.M., Baker, E.A., and Scribner, K.T. 2012. Individual-based analyses reveal high repeatability in timing and location of reproduction in lake sturgeon (*Acipenser fulvescens*). Canadian Journal of Fisheries and Aquatic Sciences 69: 60–72. NRC Research Press.

Fox, J., and G. Monette. 1992. Generalized Collinearity Diagnostics. Journal of the American Statistical Association 87(417): 178–83.

Fretwell, S.D., H.L. Lucas. 1969. On territorial behavior and other factors influencing habitat distribution in birds. Acta Biotheor 19: 16–36. https://doi.org/10.1007/BF01601953Fujiwara, M., and Caswell, H. 2002. Estimating population projection matrices from multi-stage mark–recapture data. Ecology 83: 3257–3265. Wiley Online Library.

Gallagher, C.P., Howland, K.L., Sandstrom, S.J., and Halden, N.M. 2019. Migration tactics affect spawning frequency in an iteroparous salmonid (Salvelinus malma) from the Arctic. PLOS ONE 13: e0210202. doi: 10.1371/journal.pone.0210202.

Gebhards, S.V. 1960. Biological notes on precocious male Chinook salmon parr in the Salmon River drainage, Idaho. The Progressive Fish-Culturist 22: 121–123. Taylor & Francis.

Gelman, A., and Rubin, D.B. 1992. Inference from iterative simulation using multiple sequences. Statist. Sci. 7: 457–472. The Institute of Mathematical Statistics. doi: 10.1214/ss/1177011136.

Gelman, A., 2006. Prior distributions for variance parameters in hierarchical models (comment on article by Browne and Draper). Bayesian analysis, 1(3): 515-534.

Goode, J. R., C. H. Luce, and J. M. Buffington. 2012. Enhanced sediment delivery in a changing climate in semi-arid mountain basins: Implications for water resource management and aquatic habitat in the northern Rocky Mountains. Geomorphology 139: 1-15.

Goode, J. R., J. M. Buffington, D. Tonina, D. J. Isaak, R. F. Thurow, S. Wenger, D. Nagel, C. Luce, D. Tetzlaff, and C. Soulsby. 2013. Potential effects of climate change on streambed scour and risks to salmonid survival in snow-dominated mountain basins. Hydrological Processes 27(5): 750-765.

Gosselin, J.L., Crozier, L.G., and Burke, B.J. 2021. Shifting signals: Correlations among freshwater, marine and climatic indices often investigated in Pacific salmon studies. Ecological Indicators 121: 107167. Elsevier.

Gosselin, J.L., Zabel, R.W., Anderson, J.J., Faulkner, J.R., Baptista, A.M., and Sandford, B.P. 2018. Conservation planning for freshwater–marine carryover effects on Chinook salmon survival. Ecology and evolution 8: 319–332. Wiley Online Library.

Greig, S. M., D. A. Sear, and P. A. Carling. 2007. A review of factors influencing the availability of dissolved oxygen to incubating salmonid embryos. Hydrological Processes 21(3): 323-334.

Haeseker, S.L., J.A. McCann, J. Tuomikoski, and B. Chockley. 2012. Assessing freshwater and marine environmental influences on life-stage-specific survival rates of Snake River spring–summer Chinook salmon and steelhead. Transactions of the American Fisheries Society, 141(1):121-138.

Hamann, E.J., and Kennedy, B.P. 2012. Juvenile dispersal affects straying behaviors of adults in a migratory population. Ecology 93: 733–740. Wiley Online Library.

Hamlet, A. F., M. M. Elsner, G. S. Mauger, S. Y. Lee, I. Tohver, and R. A. Norheim. 2013. An overview of the Columbia Basin Climate Change Scenarios Project: Approach, methods, and summary of key results. Atmosphere-Ocean 51(4): 392-415.

Hampton, S.E., C.A. Strasser, J.J. Tewksbury, W.K. Gram, A.E. Budden, A.L. Batcheller, C.S. Duke, and J.H. Porter. 2013. Big data and the future of ecology. Frontiers in Ecology and the Environment, 11(3):156-162.

Hardesty-Moore, M., Deinet, S., Freeman, R., Titcomb, G.C., Dillon, E.M., Stears, K., Klope, M., Bui, A., Orr, D., Young, H.S., and Miller-ter Kuile, A. 2018. Migration in the Anthropocene: How collective navigation, environmental system and taxonomy shape the vulnerability of migratory species. Philosophical Transactions of the Royal Society B: Biological Sciences 373: 20170017. The Royal Society.

Harkness, W.J.K., Dymond, J.R., Ontario., and Fish and Wildlife Branch. 1961. The lake sturgeon; the history of its fishery and problems of conservation, Fish & Wildlife Branch, Ontario Dept. of Lands; Forests, [Toronto.

Hartig, F. 2019. DHARMa: Residual Diagnostics for Hierarchical (Multi-Level / Mixed) Regression Models. R package version 0.2.4. https://CRAN.R-project.org/package=DHARMa

Heggberget, T. G. 1988. Timing of spawning in Norwegian Atlantic salmon (Salmo salar). Canadian Journal of Fisheries and Aquatic Sciences 45(5): 845-849.

Hendry, A.P., Berg, O.K., and Quinn, T.P. 2001. Breeding location choice in salmon: Causes (habitat, competition, body size, energy stores) and consequences (life span, energy stores). Oikos 93: 407–418. Wiley Online Library.

Hilborn, R., Quinn, T.P., Schindler, D.E., and Rogers, D.E. 2003. Biocomplexity and fisheries sustainability. Proceedings of the National Academy of Sciences 100: 6564–6568. National Acad Sciences.

Hill, R. A., M. H. Weber,S. G. Leibowitz, A. R. Olsen, and D. J. Thornbrugh. 2016. The Stream-Catchment (StreamCat) Dataset: A database of watershed metrics for the conterminous United States. JAWRA Journal of the American Water Resources Association 52(1), pp.120-128.

Hobbs, N.T., and Hooten, M.B. 2015. Bayesian models: A statistical primer for ecologists. Princeton University Press.

Hughes, T.C., Lowie, C.E., and Haynes, J.M. 2005. Age, Growth, Relative Abundance, and Scuba Capture of a New or Recovering Spawning Population of Lake Sturgeon in the Lower Niagara River, New York. North American Journal of Fisheries Management 25: 1263–1272. doi: 10.1577/M05-039.1.

ICTRT (Interior Columbia Technical Recovery Team). 2003. Working draft. Independent populations of Chinook, steelhead, and sockeye for listed evolutionarily significant units within the Interior Columbia River domain. NMFS: Portland, Oregon. http://www.nwfsc.noaa.gov/trt/col_docs/independentpopchinsteelsock.pdf

Isaak, D. J., R. F. Thurow, B. E. Rieman, and J. B. Dunham. 2003. Temporal variation in synchrony among chinook salmon (*Oncorhynchus tshawytscha*) redd counts from a wilderness area in central Idaho. Canadian Journal of Fisheries and Aquatic Sciences 60(7): 840-848.

Isaak, D. J., and R. F. Thurow, 2006. Network-scale spatial and temporal variation in Chinook salmon (*Oncorhynchus tshawytscha*) redd distributions: patterns inferred from spatially

continuous replicate surveys. Canadian Journal of Fisheries and Aquatic Sciences, 63(2): 285-296.
Isaak, D. J., Thurow, R.F., Rieman, B.E., and Dunham, J.B. 2007. Chinook salmon use of spawning patches: Relative roles of habitat quality, size, and connectivity. Ecological Applications 17: 352–364. Wiley Online Library.
Isaak, D. J., M. K. Young, C. H. Luce, S. W. Hostetler, S. J. Wenger, E. E. Peterson, J. M. Ver Hoef, M. C. Groce, D. L. Horan, and D. E. Nagel. 2016. Slow climate velocities of mountain streams portend their role as refugia for cold-water biodiversity. Proceedings of the National Academy of Sciences 113(16): 4374-4379.
Isaak, D. J., S. J. Wenger, E. E. Peterson, J. M. Ver Hoef, D. E. Nagel, C. H. Luce, S. W. Hostetler, J. B. Dunham, B. B. Roper, S. P. Wollrab, and G. L. Chandler. 2017a. The NorWeST summer stream temperature model and scenarios for the western US: A crowd-sourced database and new geospatial tools foster a user community and predict broad climate warming of rivers and streams. Water Resources Research 53(11): 9181-9205.
Isaak, D. J., Wenger, S.J., and Young, M.K. 2017b. Big biology meets microclimatology: Defining thermal niches of ectotherms at landscape scales for conservation planning. Ecological Applications 27: 977–990. Wiley Online Library.
Isaak, D. J., C. H. Luce, D. L. Horan, G. L. Chandler, S. P. Wollrab, and D. E. Nagel. 2018. Global warming of salmon and trout rivers in the Northwestern US: road to ruin or path through purgatory? Transactions of the American Fisheries Society 147(3): 566-587.
Jacobs, G.R., Thurow, R.F., Buffington, J.M., Isaak, D., and Wenger, S.J. 2021. Climate, fire regime, geomorphology, and conspecifics influence the spatial distribution of Chinook salmon redds. Transactions of the American Fisheries Society. Wiley Online Library.
Jarić, I., Riepe, C., and Gessner, J. 2018. Sturgeon and paddlefish life history and management: Experts' knowledge and beliefs. Journal of Applied Ichthyology 34: 244–257. Wiley Online Library.
Jensen, D. W., E. A. Steel, A. H. Fullerton, and G. R. Pess. 2009. Impact of fine sediment on egg-to-fry survival of Pacific salmon: a meta-analysis of published studies. Reviews in Fisheries Science 17(3): 348-359.
Johnston, F.D., and Post, J.R. 2009. Density-dependent life-history compensation of an iteroparous salmonid. Ecological Applications 19: 449–467. Wiley Online Library.
Joint Columbia River Management Staff. 2019. Joint staff report: stock status and fisheries for spring Chinook, summer Chinook, sockeye, steelhead, and other species. Joint Columbia River Management Staff, Oregon Department of Fish & Wildlife, Washington Department of Fish & Wildlife. February 8, 2019. https://wdfw.wa.gov/publications/02043, accessed 4/8/2021
Jolly, G.M. 1965. Explicit estimates from capture-recapture data with both death and immigration-stochastic model. Biometrika 52: 225–247. JSTOR.
Jolly, W. M., M. A. Cochrane, P. H. Freeborn, Z. A. Holden, T. J. Brown, G. J. Williamson, and D. M. Bowman. 2015. Climate-induced variations in global wildfire danger from 1979 to 2013. Nature Communications 6(1): 1-11.
Jones, L.A., Schoen, E.R., Shaftel, R., Cunningham, C.J., Mauger, S., Rinella, D.J., and St. Saviour, A. 2020. Watershed-scale climate influences productivity of Chinook salmon populations across southcentral Alaska. Global change biology 26: 4919–4936. Wiley Online Library.

Jørgensen, C., Ernande, B., Fiksen, Ø., and Dieckmann, U. 2006. The logic of skipped spawning in fish. Canadian Journal of Fisheries and Aquatic Sciences 63: 200–211. doi: 10.1139/f05-210.

Jouventin, P., and Dobson, F.S. 2002. Why breed every other year? The case of albatrosses. Proceedings of the Royal Society of London. Series B: Biological Sciences 269: 1955–1961. The Royal Society.

Keefer, M.L., Taylor, G.A., Garletts, D.F., Helms, C.K., Gauthier, G.A., Pierce, T.M., and Caudill, C.C. 2012. Reservoir entrapment and dam passage mortality of juvenile Chinook salmon in the Middle Fork Willamette River. Ecology of Freshwater Fish 21: 222–234. Wiley Online Library.

Keefer, M. L., and C. C. Caudill. 2014. Homing and straying by anadromous salmonids: a review of mechanisms and rates. Reviews in Fish Biology and Fisheries 24(1): 333-368.

Kellner, C.J., J.D. Brawn, and J.R. Karr. 1992. What is habitat suitability and how should it be measured?. In Wildlife 2001: populations (pp. 476-488). Springer, Dordrecht.

Kéry, M., and Schaub, M. 2012. Bayesian population analysis using WinBUGS: A hierarchical perspective. Academic Press.

Kieffer, M.C., and Kynard, B. 1996. Spawning of the shortnose sturgeon in the Merrimack River, Massachusetts. Transactions of the American Fisheries Society 125: 179–186. Wiley Online Library.

Kieffer, M.C., and Kynard, B. 2012. Spawning and non-spawning migrations, spawning, and the effect of river regulation on spawning success of Connecticut River shortnose sturgeon. Life history and behaviour of Connecticut River shortnose and other sturgeons. B. Kynard, P. Bronzi and H. Rosenthal (Eds.). WSCS. Demand GmbH, Norderstedt, Spec. Publ 4: 73–113.

Kleindl, W.J., M. C. Rains, L. A. Marshall, and F. R. Hauer. 2015. Fire and flood expand the floodplain shifting habitat mosaic concept. Freshwater Science 34(4): 1366-1382.

Kondolf, G.M., and M. G. Wolman. 1993. The sizes of salmonid spawning gravels. Water Resources Research 29: 2275-2285.

Krueger, C.C., Holbrook, C.M., Binder, T.R., Vandergoot, C.S., Hayden, T.A., Hondorp, D.W., Nate, N., Paige, K., Riley, S.C., Fisk, A.T., and others. 2018. Acoustic telemetry observation systems: Challenges encountered and overcome in the Laurentian Great Lakes. Canadian Journal of Fisheries and Aquatic Sciences 75: 1755–1763. NRC Research Press.

Kruschke, J. 2014. Doing Bayesian data analysis: A tutorial with R, JAGS, and Stan. Academic Press.

Kruschke, J.K., and Liddell, T.M. 2018. The Bayesian new statistics: Hypothesis testing, estimation, meta-analysis, and power analysis from a Bayesian perspective. Psychonomic Bulletin & Review 25: 178–206. Springer.

Leasure, D.R. 2014. Applications of a new geodata crawler for landscape ecology: From mapping natural stream hydrology to monitoring endangered beetles. Doctoral dissertation. University of Arkansas, Fayetteville.

Lee, K. N. 1997. Sustaining salmon: three principles. Pages 665-675 In: Stouder D.J., Bisson P.A., Naiman R.J., editors. Pacific Salmon and Their Ecosystems. Springer, Boston, MA.

Lee, A.M., Bjørkvoll, E.M., Hansen, B.B., Albon, S.D., Stien, A., Sæther, B.-E., Engen, S., Veiberg, V., Loe, L.E., and Grøtan, V. 2015. An integrated population model for a long-

lived ungulate: More efficient data use with Bayesian methods. Oikos 124: 806–816. doi: 10.1111/oik.01924.
Lennox, R.J., Paukert, C.P., Aarestrup, K., Auger-Méthé, M., Baumgartner, L., Birnie-Gauvin, K., Bøe, K., Brink, K., Brownscombe, J.W., Chen, Y., Davidsen, J.G., Eliason, E.J., Filous, A., Gillanders, B.M., Helland, I.P., Horodysky, A.Z., Januchowski-Hartley, S.R., Lowerre-Barbieri, S.K., Lucas, M.C., Martins, E.G., Murchie, K.J., Pompeu, P.S., Power, M., Raghavan, R., Rahel, F.J., Secor, D., Thiem, J.D., Thorstad, E.B., Ueda, H., Whoriskey, F.G., and Cooke, S.J. 2019. One hundred pressing questions on the future of global fish migration science, conservation, and policy. Frontiers in Ecology and Evolution 7: 286. Frontiers.
Lisi, P. J., D. E. Schindler, K. T. Bentley, and G. R. Pess. 2013. Association between geomorphic attributes of watersheds, water temperature, and salmon spawn timing in Alaskan streams. Geomorphology 185 (2013): 78-86.
Lockwood, J.L., Cassey, P., and Blackburn, T. 2005. The role of propagule pressure in explaining species invasions. Trends in ecology & evolution 20: 223–228. Elsevier.
Lucas, M., and Baras, E. 2008. Migration of freshwater fishes. John Wiley & Sons.
Luce, C. H., J. T. Abatzoglou, and Z. A. Holden. 2013. The missing mountain water: Slower westerlies decrease orographic enhancement in the Pacific Northwest USA. Science 342(6164): 1360-1364.
Luna, L. G. 1968. Manual of histological staining methods of the Armed Forces Institute of Pathology New York: McGraw-Hill.
Lynch, A. J., B. J. Myers, C. Chu, L. A. Eby, J. A. Falke, R. P. Kovach, T. J. Krabbenhoft, T. J. Kwak, J. Lyons, C. P. Paukert, and J. E. Whitney. 2016. Climate change effects on North American inland fish populations and assemblages. Fisheries 41(7): 346-361.
MacCall, A.D., Francis, T.B., Punt, A.E., Siple, M.C., Armitage, D.R., Cleary, J.S., Dressel, S.C., Jones, R.R., Kitka, H., Lee, L.C., Levin, P.S., McIsaac, J., Okamoto, D.K., Poe, M., Reifenstuhl, S., Schmidt, J.O., Shelton, A.O., Silver, J.J., Thornton, T.F., Voss, R., and Woodruff, J. 2018. A heuristic model of socially learned migration behaviour exhibits distinctive spatial and reproductive dynamics. ICES Journal of Marine Science 76: 598–608. doi: 10.1093/icesjms/fsy091.
Madej, M.A., and V. Ozaki. 1996. Channel response to sediment wave propagation and movement, Redwood Creek, California, USA. Earth Surface Processes and Landforms 21(10): 911-927.
Mantua, N.J., and Hare, S.R. 2002. The Pacific decadal oscillation. Journal of oceanography 58: 35–44. Springer.
Mason, L.A., Riseng, C.M., Gronewold, A.D., Rutherford, E.S., Wang, J., Clites, A., Smith, S.D., and McIntyre, P.B. 2016. Fine-scale spatial variation in ice cover and surface temperature trends across the surface of the Laurentian Great Lakes. Climatic Change 138: 71–83. Springer.
McCann, J., Chockley, B., Cooper, E., Scheer, G., Haeseker, S., Lessard, B., Copeland, T., Ebel, J., Storch, A., and Rawding, D. 2020. Comparative survival study of PIT-tagged spring/summer/fall Chinook, summer steelhead, and sockeye. Citeseer.
McKean, J., and D. Tonina. 2013. Bed stability in unconfined gravel bed mountain streams: With implications for salmon spawning viability in future climates. Journal of Geophysical Research: Earth Surface 118(3): 1227–1240.

McMichael, G.A., Skalski, J.R., and Deters, K.A. 2011. Survival of juvenile Chinook salmon during barge transport. North American Journal of Fisheries Management 31: 1187–1196. Taylor & Francis.

McIntyre, P.B., Liermann, C.A.R., and Revenga, C. 2016. Linking freshwater fishery management to global food security and biodiversity conservation. Proceedings of the National Academy of Sciences 113: 12880–12885. National Acad Sciences.

Megahan, W. F., W. S. Platts, and B. Kulesza. 1980. Riverbed improves over time: South Fork Salmon. Pages 380-395 in Symposium on Watershed Management, Boise, ID, July 21–23, American Society of Civil Engineers, New York, NY.

Minshall, G. W., D. A. Andrews, J. T. Brock, C. T. Robinson, and D. E. Lawrence. 1990. Changes in wild trout habitat following forest fire. In Wild trout IV: proceedings of the symposium. US Government Printing Office, Washington, DC (pp. 111-119).

Minshall, G. W. 2003. Responses of stream benthic macroinvertebrates to fire. Forest Ecology and Management 178(1-2): 155-161.

Moir, H. J., C. N. Gibbins, C. Soulsby, and J. H. Webb. 2006. Discharge and hydraulic interactions in contrasting channel morphologies and their influence on site utilization by spawning Atlantic salmon (Salmo salar). Canadian Journal of Fisheries and Aquatic Sciences 63: 2567-2585.

Montgomery, D. R., J. M. Buffington, N. P. Peterson, D. Schuett-Hames, and T. P. Quinn. 1996. Stream-bed scour, egg burial depths, and the influence of salmonid spawning on bed surface mobility and embryo survival. Canadian Journal of Fisheries and Aquatic Sciences 53(5): 1061-1070.

Montgomery, D.R., E. M. Beamer, G. R. Pess, and T. P. Quinn. 1999. Channel type and salmonid spawning distribution and abundance. Canadian Journal of Fisheries and Aquatic Sciences 56(3): 377-387.

Nagel, D. E., J. M. Buffington, S. L. Parkes, S .Wenger, and J. R. Goode. 2014. A landscape scale valley confinement algorithm: delineating unconfined valley bottoms for geomorphic, aquatic, and riparian applications. General Technical Report RMRS-GTR-321. Fort Collins, CO: US Department of Agriculture, Forest Service, Rocky Mountain Research Station.

Nagel, D., E. Peterson, D. Isaak, J. Ver Hoef, and D. Horan. 2015. National Stream Internet protocol and user guide. US Forest Service, Rocky Mountain Research Station Air, Water, and Aquatic Environments Program, Boise, Idaho. https://www.fs.fed.us/rm/boise/AWAE/projects/NationalStreamInternet/NSI_network.html

Nakagawa, S., P. C. Johnson, and H. Schielzeth. 2017. The coefficient of determination R2 and intra-class correlation coefficient from generalized linear mixed-effects models revisited and expanded. Journal of the Royal Society Interface 14(134): 20170213. DOI: 10.1098/rsif.2017.0213

Nathan, R., Getz, W.M., Revilla, E., Holyoak, M., Kadmon, R., Saltz, D., and Smouse, P.E. 2008. A movement ecology paradigm for unifying organismal movement research. Proceedings of the National Academy of Sciences 105: 19052–19059. National Acad Sciences.

Neville, H., Isaak, D., Dunham, J., Thurow, R., and Rieman, B. 2006. Fine-scale natal homing and localized movement as shaped by sex and spawning habitat in Chinook salmon:

Insights from spatial autocorrelation analysis of individual genotypes. Molecular ecology 15: 4589–4602. Wiley Online Library.
Neville, H., Isaak, D., Thurow, R., Dunham, J. and Rieman, B. 2007. Microsatellite variation reveals weak genetic structure and retention of genetic variability in threatened Chinook salmon (*Oncorhynchus tshawytscha*) within a Snake River watershed. Conservation Genetics 8(1): 133-147.
NOAA (National Oceanic and Atmospheric Administration). 1992. Endangered and Threatened Species; Threatened Status for Snake River Spring/Summer Chinook Salmon, Threatened Status for Snake River Fall Chinook Salmon. Federal Register 50(227): 14653 – 14663.
Northrup, J.M., and Gerber, B.D. 2018. A comment on priors for Bayesian occupancy models. PloS one 13: e0192819. Public Library of Science San Francisco, CA USA.
NPCC (Northwest Power and Conservation Council). 2014. Columbia River basin fish and wildlife program. NPCC, Council Document 2014-12. Available from Available: http://www.nwcouncil.org/media/7148624/2014-12.pdf. (April 2020).
NPCC (Northwest Power and Conservation Council). 2019. 2018 Columbia River Basin Fish and Wildlife Program Costs Report. 18th Annual Report to the Northwest Governors. NPCC Document 2019-5, March 2019.
NRC (National Research Council). 1996. Upstream: salmon and society in the Pacific Northwest. National Academies Press, Washington, DC.
Ohlberger, J., Ward, E.J., Schindler, D.E., and Lewis, B. 2018. Demographic changes in Chinook salmon across the northeast Pacific Ocean. Fish and Fisheries 19: 533–546. Wiley Online Library.
Parks, S. A., C. Miller, C. R. Nelson, and Z. A. Holden. 2014. Previous fires moderate burn severity of subsequent wildland fires in two large western US wilderness areas. Ecosystems 17(1): 29– 42.
Pearsons, T.N., and O'Connor, R.R. 2020. Stray rates of natural-origin Chinook salmon and steelhead in the upper Columbia River watershed. Transactions of the American Fisheries Society 149: 147–158. Wiley Online Library.
Pess, G., Kiffney, P.M., Liermann, M., Bennett, T., Anderson, J., and Quinn, T. 2011. The influences of body size, habitat quality, and competition on the movement and survival of juvenile coho salmon during the early stages of stream recolonization. Transactions of the American Fisheries Society 140: 883–897. Taylor & Francis.
Peterson, D. P., S. J. Wenger, B. E. Rieman, and D. J. Isaak. 2013. Linking climate change and fish conservation efforts using spatially explicit decision support tools. Fisheries 38(3): 112-127.
Petitgas, P., Reid, D., Planque, B., Nogueira, E., O'Hea, B., and Cotano, U. 2006. The entrainment hypothesis: An explanation for the persistence and innovation in spawning migrations and life cycle spatial patterns. ICES Document CM.
Petrosky, C., Schaller, H., and Budy, P. 2001. Productivity and survival rate trends in the freshwater spawning and rearing stage of Snake River Chinook salmon (*Oncorhynchus tshawytscha*). Canadian Journal of Fisheries and Aquatic Sciences 58: 1196–1207. NRC Research Press.
Petrosky, C., and Schaller, H. 2010. Influence of river conditions during seaward migration and ocean conditions on survival rates of Snake River Chinook salmon and steelhead. Ecology of Freshwater Fish 19: 520–536. Wiley Online Library.

Petrosky, C.E., Schaller, H.A., Tinus, E.S., Copeland, T., and Storch, A.J. 2020. Achieving productivity to recover and restore Columbia River stream-type Chinook salmon relies on increasing smolt-to-adult survival. North American Journal of Fisheries Management. Wiley Online Library.

Pianka, E.R., and Parker, W.S. 1975. Age-specific reproductive tactics. The American Naturalist 109: 453–464. University of Chicago Press.

Pledger, S., Baker, E., and Scribner, K. 2013. Breeding return times and abundance in capture–recapture models. Biometrics 69: 991–1001. doi: 10.1111/biom.12094.

Plummer, M. 2017. JAGS: A program for analysis of Bayesian graphical models using Gibbs sampling. Version 4.3. 0. URL: http://mcmc-jags. sourceforge. net.

Post, J.R., and Parkinson, E.A. 2012. Temporal and spatial patterns of angler effort across lake districts and policy options to sustain recreational fisheries. Canadian Journal of Fisheries and Aquatic Sciences 69: 321–329. NRC Research Press.

Powell, L.A., Conroy, M.J., Hines, J.E., Nichols, J.D., and Krementz, D.G. 2000. Simultaneous use of mark-recapture and radiotelemetry to estimate survival, movement, and capture rates. The Journal of Wildlife Management: 302–313. JSTOR.

R Core Team. 2019. R: A language and environment for statistical computing. R Foundation for Statistical Computing, Vienna, Austria. Available from https://www.R-project.org/.

R Core Team. 2020. R: A language and environment for statistical computing. R Foundation for Statistical Computing, Vienna, Austria. Available from https://www.R-project.org/.

Richter, A. and S. A. Kolmes. 2005. Maximum temperature limits for Chinook, coho, and chum salmon, and steelhead trout in the Pacific Northwest. Reviews in Fisheries Science, 13(1): 23-49.

Ricker, W. 1976. Review of the rate of growth and mortality of Pacific salmon in salt water, and noncatch mortality caused by fishing. Journal of the Fisheries Board of Canada 33: 1483–1524. NRC Research Press.

Rideout, R.M., and Tomkiewicz, J. 2011. Skipped Spawning in Fishes: More Common than You Might Think. Marine and Coastal Fisheries 3: 176–189. doi: 10.1080/19425120.2011.556943.

Riebe, C. S., L. S. Sklar, B. T. Overstreet, and J. K. Wooster. 2014. Optimal reproduction in salmon spawning substrates linked to grain size and fish length. Water Resources Research 50(2): 898–918, DOI: 810.1002/2013WR014231.

Roberts, D. R. , V. Bahn, S. Ciuti, M. S. Boyce, J. Elith, G. Guillera-Arroita, S. Hauenstein, J. J. Lahoz-Monfort, B. Schröder, W. Thuiller, and D. I. Warton. 2017. Cross-validation strategies for data with temporal, spatial, hierarchical, or phylogenetic structure. Ecography 40(8): 913-929, doi:10.1111/ecog.02881.

Roff, D.A. 2002. Life history evolution.

Roper, B. B., W. C. Saunders, and J. V. Ojala. 2019. Did changes in western federal land management policies improve salmonid habitat in streams on public lands within the Interior Columbia River Basin? Environmental Monitoring and Assessment 191(9), p.574.

Rose, G.A. 1993. Cod spawning on a migration highway in the north-west Atlantic. Nature 366: 458–461. Nature Publishing Group.

Royle, J.A. 2008. Modeling individual effects in the Cormack–Jolly–Seber model: A state–space formulation. Biometrics 64: 364–370. Wiley Online Library.

Ruff, C. P., D. E. Schindler, J. B. Armstrong, K. T. Bentley, G. T. Brooks, G. W. Holtgrieve, M. T. McGlauflin, C. E. Torgersen, and J. E. Seeb. 2011. Temperature-associated population diversity in salmon confers benefits to mobile consumers. Ecology 92(11): 2073-2084.

Schaller, H.A., Petrosky, C.E., and Langness, O.P. 1999. Contrasting patterns of productivity and survival rates for stream-type Chinook salmon (*Oncorhynchus tshawytscha*) populations of the Snake and Columbia Rivers. Canadian Journal of Fisheries and Aquatic Sciences 56: 1031–1045. NRC Research Press.

Schaller, H.A., Petrosky, C.E., and Tinus, E.S. 2014. Evaluating river management during seaward migration to recover Columbia River stream-type Chinook salmon considering the variation in marine conditions. Canadian Journal of Fisheries and Aquatic Sciences 71: 259–271. NRC Research Press.

Schaub, M., Gimenez, O., Schmidt, B.R., and Pradel, R. 2004. Estimating survival and temporary emigration in the multistate capture-recapture framework. Ecology 85: 2107–2113. doi: 10.1890/03-3110.

Scheuerell, M.D., Ruff, C.P., Anderson, J.H., and Beamer, E.M. 2019. An integrated population model for estimating the relative effects of natural and anthropogenic factors on a threatened population of Pacific trout. bioRxiv. Cold Spring Harbor Laboratory. doi: 10.1101/734996.

Schindler, D.E., Hilborn, R., Chasco, B., Boatright, C.P., Quinn, T.P., Rogers, L.A., and Webster, M.S. 2010. Population diversity and the portfolio effect in an exploited species. Nature 465: 609–612. Nature Publishing Group.

Scott, W.B., and Crossman, E.J. 1973. Freshwater fishes of Canada. Fisheries Research Board of Canada, Ottawa.

Seaber, P. R., F. P. Kapinos, and G. L. Knapp. 1987. Hydrologic unit maps. U.S. Geological Survey Water-Supply Paper 2294, Denver, CO. 63 pp.

Seber, G.A. 1965. A note on the multiple-recapture census. Biometrika 52: 249–259. JSTOR.

Shaw, A.K., and Levin, S.A. 2013. The evolution of intermittent breeding. Journal of mathematical biology 66: 685–703. Springer.

Shaw, A.K. 2016. Drivers of animal migration and implications in changing environments. Evolutionary Ecology 30: 991–1007. doi: 10.1007/s10682-016-9860-5.

Shaw, S., Chipps, S.R., Windels, S.K., Webb, M., McLeod, D.T., and Willis, D. 2012. Lake sturgeon population attributes and reproductive structure in the Namakan Reservoir, Minnesota and Ontario. Journal of Applied Ichthyology 28: 168–175. Wiley Online Library.

Sol, D., and Maspons, J. 2015. Integrating behavior into life-history theory: A comment on Wong and Candolin. Behavioral Ecology 26: 677–678. Oxford University Press UK.

Stanford, J. A., M. S. Lorang, M.S. and Hauer, F.R. 2005. The shifting habitat mosaic of river ecosystems. Internationale Vereinigung für theoretische und angewandte Limnologie: Verhandlungen 29(1): 123-136.

Stearns, S.C. 1989. Trade-offs in life-history evolution. Functional ecology 3: 259–268. JSTOR.

Su, Z., and Peterman, R.M. 2012. Performance of a Bayesian state-space model of semelparous species for stock-recruitment data subject to measurement error. Ecological Modelling 224: 76–89. Elsevier.

Tartu, S., Goutte, A., Bustamante, P., Angelier, F., Moe, B., Clément-Chastel, C., Bech, C., Gabrielsen, G.W., Bustnes, J.O., and Chastel, O. 2013. To breed or not to breed:

Endocrine response to mercury contamination by an arctic seabird. Biology Letters 9: 20130317. The Royal Society.
Thurow, R. F. 2000. Dynamics of Chinook salmon populations within Idaho's Frank Church wilderness: implications for persistence. In: Wilderness science in a time of change conference 3: 143-151.
Thurow, R.F., Copeland, T., and Oldemeyer, B.N. 2020. Wild salmon and the shifting baseline syndrome: Application of archival and contemporary redd counts to estimate historical Chinook salmon (*Oncorhynchus tshawytscha*) production potential in the central Idaho wilderness. Canadian Journal of Fisheries and Aquatic Sciences 77: 651–665. NRC Research Press.
Tillotson, M.D., and Quinn, T.P. 2017. Climate and conspecific density trigger pre-spawning mortality in sockeye salmon (*Oncorhynchus nerka*). Fisheries Research 188: 138–148. Elsevier.
Turvey, S.T., and Crees, J.J. 2019. Extinction in the anthropocene. Current Biology 29: R982–R986. Elsevier.
USGS (US Geological Survey). 2016. National water information system data available on the world wide web (USGS water data for the nation). https://waterdata.usgs.gov/ny/nwis/dv?referred_module=sw&site_no=04216000.
USGS (US Geological Survey). 2006. National Elevation Dataset, URL: http://ned.usgs.gov/. Updated August, 2006.
USGS (US Geological Survey). 2010. National Hydrography Dataset, URL: http://nhd.usgs.gov/index.html. Updated September 2, 2010.
Vélez-Espino, L.A., and Koops, M.A. 2009. Recovery potential assessment for lake sturgeon in Canadian designatable units. North American Journal of Fisheries Management 29: 1065–1090. doi: 10.1577/M08-034.1.
Vitousek, P.M. 1994. Beyond global warming: Ecology and global change. Ecology 75: 1861–1876. Wiley Online Library.
Vonesh, J.R., and De la Cruz, O. 2002. Complex life cycles and density dependence: Assessing the contribution of egg mortality to amphibian declines. Oecologia 133: 325–333. Springer.
Webb, M.A., Feist, G.W., Foster, E.P., Schreck, C.B., and Fitzpatrick, M.S. 2002. Potential classification of sex and stage of gonadal maturity of wild white sturgeon using blood plasma indicators. Transactions of the American fisheries society 131: 132–142. Taylor & Francis.
Webb, M.A., and Doroshov, S. 2011. Importance of environmental endocrinology in fisheries management and aquaculture of sturgeons. General and Comparative Endocrinology 170: 313–321. Elsevier.
Webb, M., Van Eenennaam, J., Crossman, J., and Chapman, F. 2019. A practical guide for assigning sex and stage of maturity in sturgeons and paddlefish. Journal of Applied Ichthyology 35: 169–186. Wiley Online Library.
Wenger, S. J., C. H. Luce, A. F. Hamlet, D. J. Isaak, and H. M. Neville. 2010. Macroscale hydrologic modeling of ecologically relevant flow metrics. Water Resources Research 46: W09513. doi:10.1029/2009WR008839.
Wenger, S. J., D. J. Isaak, C. H. Luce, H. M. Neville, K. D. Fausch, J. B. Dunham, D. C. Dauwalter, M. K. Young, M. M. Elsner B. E. Rieman, and A. F. Hamlet. 2011. Flow regime, temperature, and biotic interactions drive differential declines of trout species

under climate change. Proceedings of the National Academy of Sciences 108(34): 14175-14180.
Wenger, S. J., N. A. Som, D. C. Dauwalter, D. J. Isaak, H. M. Neville, C. H. Luce, J. B. Dunham, M. K. Young, K. D. Fausch, and B. E. Rieman. 2013. Probabilistic accounting of uncertainty in forecasts of species distributions under climate change. Global Change Biology, 19(11): 3343-3354.
Westerling, A. L., H. G. Hidalgo, D. R. Cayan, and T. W. Swetnam. 2006. Warming and earlier spring increase western U.S. forest wildfire activity. Science 313: 940-943 10.1126/science.1128834.
White, C.H., Heidinger, A.K., Ackerman, S.A., and McIntyre, P.B. 2018. A long-term fine-resolution record of AVHRR surface temperatures for the Laurentian Great Lakes. Remote Sensing 10: 1210. Multidisciplinary Digital Publishing Institute.
Widener, D.L., Faulkner, J.R., Smith, S.G., Marsh, T.M., and Zabel, R.W. 2018. Survival estimates for the passage of spring-migrating juvenile salmonids through Snake and Columbia River dams and reservoirs, 2017. Report of research by the National Marine Fisheries Service for the Bonneville Power Administration, Contract 40735.
Wiese, F.K., Parrish, J.K., Thompson, C.W., and Maranto, C. 2008. Ecosystem-based management of predator–prey relationships: Piscivorous birds and salmonids. Ecological Applications 18: 681–700. Wiley Online Library.
Wilcove, D.S., and Wikelski, M. 2008. Going, going, gone: Is animal migration disappearing. PLOS Biology 6: e188. doi: 10.1371/journal.pbio.0060188.
Williams, G.C. 1966. Natural selection, the costs of reproduction, and a refinement of Lack's principle. The American Naturalist 100: 687–690. Science Press.
Wilson, P.H. 2003. Using population projection matrices to evaluate recovery strategies for Snake River spring and summer Chinook salmon. Conservation Biology 17: 782–794. Wiley Online Library.
Winship, A.J., O'Farrell, M.R., and Mohr, M.S. 2014. Fishery and hatchery effects on an endangered salmon population with low productivity. Transactions of the American Fisheries Society 143: 957–971. Taylor & Francis.
Withers, J.L., Einhouse, D., Clancy, M., Davis, L., Neuenhoff, R., and Sweka, J. 2019. Integrating acoustic telemetry into a mark–recapture model to improve catchability parameters and abundance estimates of lake sturgeon in eastern Lake Erie. North American Journal of Fisheries Management 39: 913–920. doi: 10.1002/nafm.10321.
Withers, J.L., Gorsky, D., Biesinger, Z., Einhouse, D., Clancy, M., Davis, L., Karboski, C., Legard, C., Bruestle, E., Markley, N.D., and others. In Press. Age and growth of Niagara River lake sturgeon. Journal of Fish and Wildlife Management.
Zabel, R.W., Scheuerell, M.D., McCLURE, M.M., and Williams, J.G. 2006. The interplay between climate variability and density dependence in the population viability of Chinook salmon. Conservation Biology 20: 190–200.
Zipkin, E.F., and Saunders, S.P. 2018. Synthesizing multiple data types for biological conservation using integrated population models. Biological Conservation 217: 240–250. doi: 10.1016/j.biocon.2017.10.017.

APPENDICES

APPENDIX A

Variables, interactions, and corresponding hypotheses considered in candidate models for Chinook salmon redd occurrence.

	Variables	***Definition***	***Hypotheses***
Main effects			
1	S	Stream slope (percent)	Redd occurrence should vary negatively with slope, reflecting a preference for lower-gradient areas and associated geomorphic conditions: less risk of streambed scour, more suitable substrate sizes (gravel and cobble, rather than boulder), more suitable flow depths and velocities, and preferred stream types (pool-riffle and plane-bed, rather than cascade and step-pool).
2	$Q + Q^2$	Mean summer stream flow (m^3s^{-1}), log scale, polynomial	Spatial variation in flow is a surrogate for channel size, and occurrence is expected to vary in a non-linear fashion (unimodal) from very small to very large streams. This relationship reflects an optimal channel size and a reduction in suitability as streams become too large (high flow velocities) or too small (insufficient flow depth for large-bodied fish and risk of predation).
3	$D_{50} + D_{50}^2$	Median substrate size (mm), log scale, polynomial	Occurrence should vary in a non-linear fashion (unimodal), reflecting an intermediate optimum substrate size. Field surveys demonstrate a heavy-tailed, bell-shaped relationship between substrate size and redd density, such that preferred, reach-average, median substrate sizes for Chinook salmon are in the range of

			about 16-51 mm in the Middle Fork Salmon River (MFSR) (data of J. M. Buffington, D. J. Isaak , and R. F. Thurow (paper read at the American Geophysical Union Fall Meeting, 2003)).
4	V	Valley confinement (binary; 0=confined, 1=unconfined)	Occurrence should vary positively with the extent of unconfined stream length and associated geomorphic conditions: (1) overbank flooding that reduces scour risk; (2) off-channel habitat: (3) complex hyporheic exchange; and (4) lower-gradient channels and associated conditions as described above for the slope variable (Baxter and Hauer 2000; Stanford et al. 2005).
5	$T + T^2$	Stream temperature (°C), polynomial	Occurrence is expected to vary in a non-linear fashion (unimodal) from low to high stream temperature, reflecting an optimum temperature range between conditions that are too warm and conditions that are too cold for Chinook salmon spawning.
6	ΔT	Deviation in stream temperature (°C) from T	Deviation from average stream temperatures may moderate the effect of temperature on redd occurrence (see *Interactions*)
7	F_0	Within-year fire extent (km^2), local watershed area (5 km upstream)	Local fire in the current year should negatively affect redd occurrence due to degradation of water quality associated with the input of ash and fine sediment and due to elevated stream temperatures from loss of riparian and/or hillslope vegetation (shading).
8	F_3	3-year fire extent (km^2), local watershed area (5 km upstream)	Recent upstream fires are expected to have a positive effect on redd occurrence by increasing the supply of spawning gravels and wood from post-fire debris flows.

9	F_5	5-year fire extent (km^2), local watershed area (5 km upstream)	Anecdotally, we have observed spawning on post-fire debris fans, demonstrating a positive responsive to fire (Thurow and Buffington unpublished).
10	N_{MFSR}	Abundance of Chinook salmon redds	Count of redds in the entire surveyed MFSR basin.
11	N_{POP}		Count of redds in each NOAA ICTRT population sub-watershed (ICTRT 2003).
12	N_{SEG}		Count of redds in each distinct network segment defined in Isaak and Thurow (2006).
Interactions			
13	$D_{50} + D_{50}^2 + V + D_{50} * V + D_{50}^2 * V$	Substrate size by valley confinement	Substrate size preference may change with valley morphology (smaller, more marginal substrate may be tolerated because of other beneficial characteristics of unconfined valleys (as described above), leading to relatively greater occurrence).
14	$Q + Q^2 + V + Q * V + Q^2 * V$	Summer flow by valley confinement	Stream size preference may change with valley morphology: larger streams that are not preferred (as described above) may be tolerated in unconfined valleys because overbank flows mitigate both the risk of streambed scour and high flow velocities that would otherwise occur (and be magnified) in confined valleys for streams of the same size.
15	$F_0 + V + F_0 * V$	Within-year fire by valley confinement	Occurrence should be relatively lower in burned, confined valleys. Confined valleys will act as chimneys, increasing fire severity and extent, with consequently poorer water quality (greater inputs of ash and sediment, and warmer stream temperatures due to more extensive vegetation loss) compared to unconfined valleys with broad, wet floodplains. Alternatively, severe fires in unconfined valleys may lead to relatively lower

			occurrence of redds due to elevated stream temperatures compared to confined valleys where hillslope shading of the channel will persist despite forest denudation.
16	$F_3 + V + F_3 * V$	3-year fire by valley confinement	Steeper confined valleys may be more prone to delivery of sediment and large wood in post-fire precipitation events or snow avalanches than unconfined valleys, leading to relatively higher occurrence of redds over time. However, positive effects of fire may be transient due to higher entrainment rates of gravel and wood compared to lower-gradient, unconfined valleys that will store upstream, fire-related inputs of gravel and wood, providing long-term core-habitat areas.
17	$F_5 + V + F_5 * V$	5-year fire by valley confinement	
18	$S + N_{MFSR} + S * N_{MFSR}$		
19	$S + N_{POP} + S * N_{POP}$	Slope by abundance	Competition for nest sites will drive adults farther from their natal reaches with increasing abundance and density, leading to increasingly high occurrence among reaches with marginal habitat (steep slopes, small substrate sizes, warm stream temperatures) as abundance and density increase, while high-quality reaches remain consistently occupied. We consider separate hypotheses for substrate size and reach slope, and also for different scales for which abundance is measured.
20	$S + N_{SEG} + S * N_{SEG}$		
21	$N_{MFSR} + D_{50} + D_{50}^2 + D_{50} * N_{MFSR} + D_{50}^2 * N_{MFSR}$		
22	$N_{POP} + D_{50} + D_{50}^2 + D_{50} * N_{POP} + D_{50}^2 * N_{POP}$	Substrate size by density	
23	$N_{SEG} + D_{50} + D_{50}^2 + D_{50} * N_{SEG} + D_{50}^2 * N_{SEG}$		
24	$T + T^2 + \Delta T + T * \Delta T + T^2 * \Delta T$	Temperature, space by time	Deviation in annual stream temperature relative to the average may alter habitat suitability and redd occurrence. For example, unusually low temperatures in a given year may render high-temperature reaches more suitable for Chinook salmon spawning, and may be more likely to attract redds.

APPENDIX B

Algorithm to define Chinook salmon redd occurrence candidate model set. The following R code defines specific hypotheses outlined in Appendix A and combines them into a list of model formulas for use in generalized linear mixed-effects model analysis using R and the R package `lme4`. The factorial combination of habitat, temperature, immediate fire effects, and delayed fire effects results in 1,080 unique candidate models comprising the candidate model set.

```
# List plausible hypotheses for habitat effects
h.habitat <- c(
  "c.S+c.lnQ+c.lnQ2",
  "c.lnD50+c.lnD502+V",
  "(c.lnD50+c.lnD502)*V",
  "(c.lnD50+c.lnD502)*V+c.lnQ+c.lnQ2",
  "c.lnD50+c.lnD502+(c.lnQ+c.lnQ2)*V",
    "(c.lnD50+c.lnD502)*V+(c.lnQ+c.lnQ2)*V",

    "c.S*c.Nmfsr+c.lnQ+c.lnQ2",
    "(c.lnD50+c.lnD502)*c.Nmfsr+V",
    "(c.lnD50+c.lnD502)*V+(c.lnD50+c.lnD502)*c.Nmfsr",
    "(c.lnD50+c.lnD502)*V+(c.lnD50+c.lnD502)*c.Nmfsr+c.lnQ+c.lnQ2",
    "(c.lnD50+c.lnD502)*c.Nmfsr+(c.lnQ+c.lnQ2)*V",
    "(c.lnD50+c.lnD502)*V+(c.lnD50+c.lnD502)*c.Nmfsr+(c.lnQ+c.lnQ2)*V",

    "c.S*c.Nseg+c.lnQ+c.lnQ2",
    "(c.lnD50+c.lnD502)*c.Nseg+V",
    "(c.lnD50+c.lnD502)*V+(c.lnD50+c.lnD502)*c.Nseg",
    "(c.lnD50+c.lnD502)*V+(c.lnD50+c.lnD502)*c.Nseg+c.lnQ+c.lnQ2",
    "(c.lnD50+c.lnD502)*c.Nseg+(c.lnQ+c.lnQ2)*V",
    "(c.lnD50+c.lnD502)*V+(c.lnD50+c.lnD502)*c.Nseg+(c.lnQ+c.lnQ2)*V",

    "c.S*c.Npop+c.lnQ+c.lnQ2",
    "(c.lnD50+c.lnD502)*c.Npop+V",
    "(c.lnD50+c.lnD502)*V+(c.lnD50+c.lnD502)*c.Npop",
    "(c.lnD50+c.lnD502)*V+(c.lnD50+c.lnD502)*c.Npop+c.lnQ+c.lnQ2",
    "(c.lnD50+c.lnD502)*c.Npop+(c.lnQ+c.lnQ2)*V",
    "(c.lnD50+c.lnD502)*V+(c.lnD50+c.lnD502)*c.Npop+(c.lnQ+c.lnQ2)*V"
)
# List plausible hypotheses for temperature effects
h.temp <- c(
    "1",
```

```
    "c.T+c.T2",
    "(c.T+c.T2)*c.dT"
)
# List plausible hypotheses for immediate fire effects
h.firenow <- c(
    "1",
    "c.F0",
    "c.F0*V"
)
# List plausible hypotheses for delayed fire effects
h.firelater <- c(
    "1",
    "c.F3",
    "c.F3*V",
    "c.F5",
    "c.F5*V"
)
# nested random intercepts for inclusion in all model equations
h.ranef <- c("(1|HUC12/OBSPRED_ID)")

# Model equation list from factorial combinations of 4 hypothesis groups (+ r
andom effects)
hgrid <- expand.grid(h.habitat, h.temp, h.firenow, h.firelater, h.ranef)
makeformula <- function(x){
    gsub("\\+1", "", paste("occ~",paste(as.character(unlist(hgrid[x,])), coll
apse="+"), sep=""))
}
hlist <- sapply(1:nrow(hgrid), makeformula)

cat("There are ", length(hlist), " model hypotheses in the full candidate set
.")

## There are 1080 model hypotheses in the full candidate set.
```

APPENDIX C

Coefficients for 12 best, mixed-effects, logistic regression models of Chinook salmon redd occurrence in the Middle Fork Salmon River. Coefficients are mean-centered and standard deviation-scaled continuous explanatory variables. The 'weight' column reports the Akaike weights used for model-averaged predictions reported in the paper.

Model (Table 2)	1	**2**	**3**	**4**	**5**	**6**	**7**	**8**	**9**	**10**	**11**	**12**
Intercept	-0.91	-0.91	-0.91	-0.9	-0.85	-0.89	-0.9	-0.85	-0.89	-0.9	-0.85	-0.89
D_{50}	-1.1	-1.1	-1.1	-1.11	-1.22	-1.11	-1.1	-1.22	-1.1	-1.1	-1.22	-1.1
D_{50}^2	-0.21	-0.21	-0.21	-0.22	-0.22	-0.21	-0.22	-0.22	-0.21	-0.22	-0.22	-0.21
V	0.35	0.35	0.35	0.32	0.39	0.29	0.32	0.39	0.29	0.32	0.39	0.29
N_{MFSR}	0.98	0.97	0.98	0.98	0.98	0.98	0.97	0.97	0.97	0.97	0.97	0.97
Q	-0.24	-0.23	-0.23	-0.26	-0.29	-0.21	-0.25	-0.28	-0.21	-0.25	-0.28	-0.21
Q^2	-1.21	-1.21	-1.21	-1.22	-1.25	-1.26	-1.22	-1.24	-1.26	-1.22	-1.24	-1.26
T	0.23	0.23	0.23	0.25	0.31	0.25	0.25	0.31	0.24	0.25	0.3	0.24
T^2	-0.25	-0.25	-0.25	-0.25	-0.25	-0.24	-0.25	-0.25	-0.24	-0.25	-0.25	-0.24
ΔT	0.13	0.14	0.14	0.13	0.13	0.13	0.13	0.13	0.13	0.13	0.13	0.13
F_5	0.13	0.12	0.12	0.08	0.08	0.08	0.08	0.08	0.07	0.08	0.08	0.08
$D_{50} \times V$	-0.82	-0.81	-0.81	-0.85		-0.85	-0.85		-0.84	-0.85		-0.84
$D_{50}^2 \times V$	-0.25	-0.25	-0.25	-0.26		-0.26	-0.26		-0.26	-0.26		-0.26
$D_{50} \times N_{MFSR}$	-0.19	-0.19	-0.19	-0.19	-0.19	-0.19	-0.19	-0.19	-0.19	-0.19	-0.19	-0.19
$D_{50}^2 \times N_{MFSR}$	-0.03	-0.03	-0.03	-0.03	-0.03	-0.03	-0.03	-0.03	-0.03	-0.03	-0.03	-0.03
$T \times \Delta T$	-0.02	-0.02	-0.02	-0.02	-0.02	-0.02	-0.02	-0.02	-0.02	-0.02	-0.02	-0.02
$T^2 \times \Delta T$	-0.02	-0.02	-0.02	-0.01	-0.01	-0.01	-0.02	-0.02	-0.02	-0.02	-0.02	-0.02
F_0		-0.05	-0.04				-0.05	-0.05	-0.05	-0.04	-0.04	-0.04
$V \times F_0$			-0.03							-0.01	-0.01	-0.01

$V \times F_5$				0.22	0.21	0.22	0.21	0.21	0.21	0.21	0.21	0.21
$V \times Q$					-0.12	-0.1		-0.12	-0.1		-0.12	-0.1
$V \times Q^2$					0.03	0.04		0.03	0.04		0.03	0.04
Random Effects												
σ^2_{REACH}	1.99	1.99	1.99	2.01	2.03	2.01	2.01	2.03	2.01	2.01	2.03	2.01
$\sigma^2_{HUC\text{-}12}$	1.67	1.67	1.67	1.69	1.78	1.69	1.69	1.78	1.69	1.69	1.78	1.69
AIC weight	0.373	0.283	0.139	0.056	0.042	0.033	0.025	0.021	0.012	2.01	0.007	0.005

APPENDIX D

Lake Sturgeon Sex Assignment

Here, we compile field observations that identified the sex of lake sturgeon from the Niagara River and measurements of circulating sex steroids from blood samples taken at the time of capture, and to develop a classification algorithm to use blood sex steroids to determine the sex of unknown-sex lake sturgeon in the Niagara River (sensu Webb et al. 2002, 2019; Allen et al. 2009; Webb and Doroshov 2011).

Methods

Between 2012 and 2017, lake sturgeon were captured during spring in the lower Niagara River and in Lake Ontario near the lower Niagara River mouth (LNR) in US Fish and Wildlife Service (USFWS) set-line surveys. We recorded length (TL), and in three years we also took a blood sample from which sex steroids were quantified: see next paragraph for detailed methods. While handling fish, we also made observations that led to the definitive classification of male and female fish (hereafter "known-sex" fish) and their reproductive status (immature, maturing, or mature gametes): see below.

During 2012-2014, six-ml blood samples were taken from the caudal vasculature of 191 fish using heparinized vacutainers for plasma sex steroid analysis. All blood samples used to inform sex assignment methods were collected in the spring when water temperatures were between 5 and 21˚C as measured at the New York Power Authority intake in the upper Niagara River. We focused on this range of water temperatures (5-21 ˚C), because it is easier to differentiate pre-spawning and spawning fish using sex steroid concentrations than during other

parts of the year. Heparinized blood samples were centrifuged at 3,400 rpm for 5 minutes in the field, and blood plasma was separated and stored at -20˚ C until analysis. The steroids testosterone (T) and 17β-estradiol (E2) were extracted from plasma following the method of Fitzpatrick et al. (1987), and plasma concentrations of T and E2 were measured by radioimmunoassay as described in Fitzpatrick et al. (1986) as modified by Feist et al. (1990). All samples were analyzed in duplicate. A charcoal solution (6.25 g charcoal and 4.0 g dextran/L PBSG) was used for all assays to reduce non-specific binding. The intra- and inter-assay coefficients of variation for all assays were less than 5 and 10%, respectively. Steroid levels were validated by verifying that serial dilutions were parallel to standard curves. E2 and T concentrations below detection limits were assigned the value of the minimum detection limit for (0.16 ng/L for E2, and 0.1 ng/L for T).

Known-sex classification

We identified the sex of fish through (1) external observation of gametes from mature fish, (2) internal visual inspection of organs in the body cavity during surgery (hereafter referred to as "internal observation"), (3) gonad biopsy collection followed by histology, and (4) observation via ultrasonography following Chiotti et al. (2016) (see Webb et al. (2019) for a review of these methods in detail). When possible, gonad maturation stage was classified sensu Erickson and Webb (2007), to later account for the difficulty of predicting sex of immature-stage fish based on hormone profiles. We classified the sex of individuals using external observation when mature gametes, milt (males) or eggs (females), were released or expressed during handling. Gonad histology and internal visual inspection of gonad tissue required non-lethal but invasive celiotomy to access the body cavity of live sturgeon. Celiotomies were performed in concert with radio and acoustic telemetry implantation, when possible, to minimize the number

of surgeries conducted. Each fish that underwent celiotomy was anesthesetized using a buffered MS-222 solution of 200 mg/L for 5 minutes, and then switched to a maintenance dose of 87 mg/L until the procedure was completed. Incisions were closed with PDS II absorbable monofilament sutures. We embedded gonads in paraffin, sectioned them at 5 μm, and applied Periodic Acid Schiff stain (PAS; Luna 1968). Slides were examined under a compound microscope (10-100x, Leica DM2000), and the germ cells were scored for sex and stage of maturation according to the protocol of Erickson and Webb (2007).

Discriminant analysis

We classified sex based on plasma sex steroid concentration where plasma sex steroid samples overlapped with known-sex classifications comprised of external observation, internal observation, and histology-based sex assignments. We used a classification and regression tree (CART) model to classify known-sex individuals based on T and E2 concentration. We fit the CART model using *rpart* and *caret* packages in R 4.0.2 (R Core Team 2020), and evaluated prediction accuracy using leave-one-out cross validation. We classified the sex of unknown-sex fish using their blood plasma sex steroid concentrations.

Results

Our final dataset was composed of 249 observations of 243 individual lake sturgeon, with "known-sex" observations (n = 85) and plasma sex steroid observations (n = 195) that overlapped incompletely, resulting in 130 unknown-sex fish with steroid samples, 20 known-sex fish without steroid samples, and 65 known-sex fish paired with steroid samples (Figure D1). Of the 85 "known-sex" observations, we identified the sex of 60 fish using histology (58% female), 18 fish using external observation (0% female), 42 fish using celiotomy (50% female), and 13 fish using ultrasonography (62% female) (Table D1). Because repeated samples sometimes came

from fish observed during multiple sampling occasions, and because the relationship between sex steroid concentrations and reproductive stages is assumed to be a population-level phenomenon, we treated repeat observations of the same individual across different capture occasions as independent.

Our regression tree analysis correctly classified the reproductive class (male versus female versus immature) of our fish with 86.2% accuracy during leave one out cross-validation analysis. More specifically, these methods seemed to more accurately classify males than females (Table D3; Figure D2; Figure D3).

We combined our classifications of unknown-sex fish by sex steroid concentration with our known-sex fish, and linked these data to our physical capture dataset (where these samples originated) by their unique individual ID numbers (UID). For the purposes of estimating sex effects in our capture mark recapture model, we treated all assigned sex and known-sex classifications as "known". All fish without classifications and those classified as "immature" were treated as unknown and classified as NA.

Some individuals that were evaluated for sex classification were not included in our capture-mark-recapture study because they fell outside of the study window (e.g., fish first captured in 2017 were excluded), and multiple observations of recaptured individuals were consolidated to a single observation of sex per individual. Also, one paired gonad histology and blood sample was not attributable to an individual fish due to a label transcription error (UID = NA), so this sample contributed to training our sex classification algorithm, but did not result in a fish classification itself. Thus, fewer fish (160) were included in the capture-mark-recapture analysis than were sex-classified (201). Our methods resulted in the inclusion of 59 known sex

females, 57 known sex males, 16 steroid-classified females, and 28 steroid-classified males in our multi-state capture-mark-recapture analysis.

Appendix D Tables

Table D1: The number of known-sex fish for each method used to assign sex of lake sturgeon in this study, organized by sex and population.

Sex	Histology	External Observation	Celiotomy	Interpolation	Ultrasonography	Total
F	21	35	3	8	0	59
M	21	25	0	5	18	64
All	42	60	3	13	18	123

Table D2: A table detailing sex steroids (T and E2), Total Length, sex, and sex assignment method measured for recaptured fish in the dataset during each of their capture occasions. UID is an ID number unique to each individual fish across all captures.

UID	*Release Date*	T	E2	*Total Length (mm)*	*Sex assignment method*	*Observed Sex*	*Predicted Sex*
18	2013-05-01	198.93	0.47	1443	External	M	M
18	2012-04-19	24.34	0.16	1420	Histology	M	I
247	2012-04-17	1.10	0.16	1450	Histology	F	I
247	2012-04-04	0.43	0.16	1434	Interpolated	F	I
247	2013-04-18	0.10	0.16	1465	Interpolated	F	I
382	2013-05-08	1.71	0.16	1450	Interpolated	F	I
382	2013-04-24	0.10	0.16	1450	Histology	F	I
383	2013-04-25	20.57	1.77	1675	Histology	F	F
383	2016-06-01	NA	NA	1723	Celiotomy	F	I
396	2013-04-30	220.01	0.16	1441	Histology	M	M
396	2017-05-09	NA	NA	1473	External	M	I

Table D3: Confusion matrix from regression tree classification analysis. Columns indicate the true classification, rows indicate the predicted classification. Numbers across the diagonal are the number of correctly classified individuals by class.

	Male	Immature	Female
Male	22	2	2
Immature	13	64	6
Female	13	0	73

Appendix D Figures

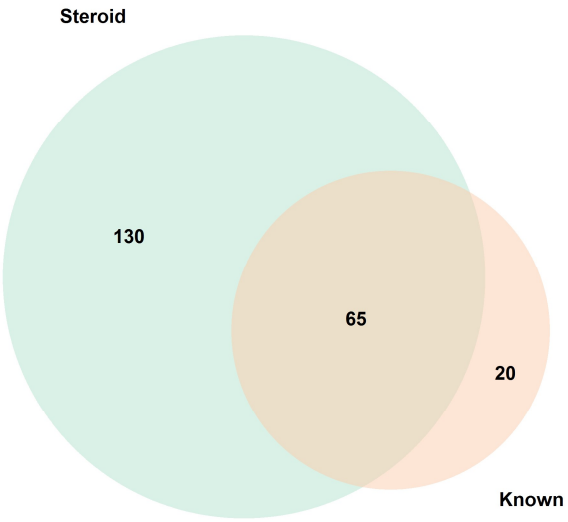

Figure D1: A Venn diagram showing the number of known-sex fish, the number of fish with blood steroid samples, and their overlap.

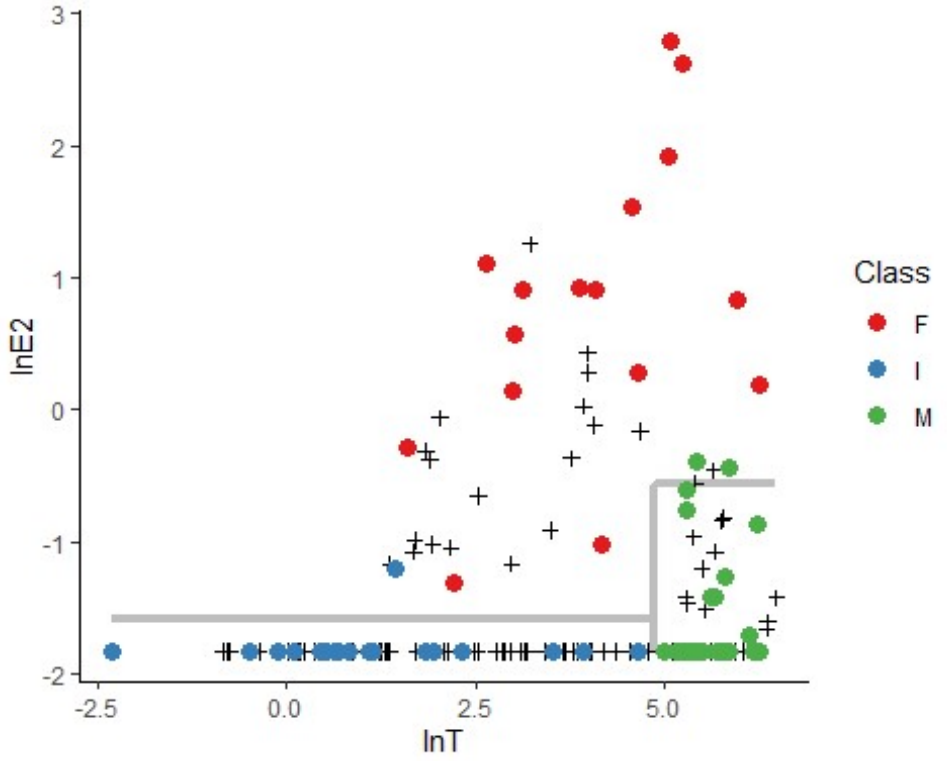

Figure D2: The natural logarithm of plasma sex steroid concentrations T (x-axis) and E2 (y-axis) for males (green points), females (red points), and immatures (blue points). The grey line is the decision boundary between classes of Niagara River lake sturgeon, as specified by our CART model results.

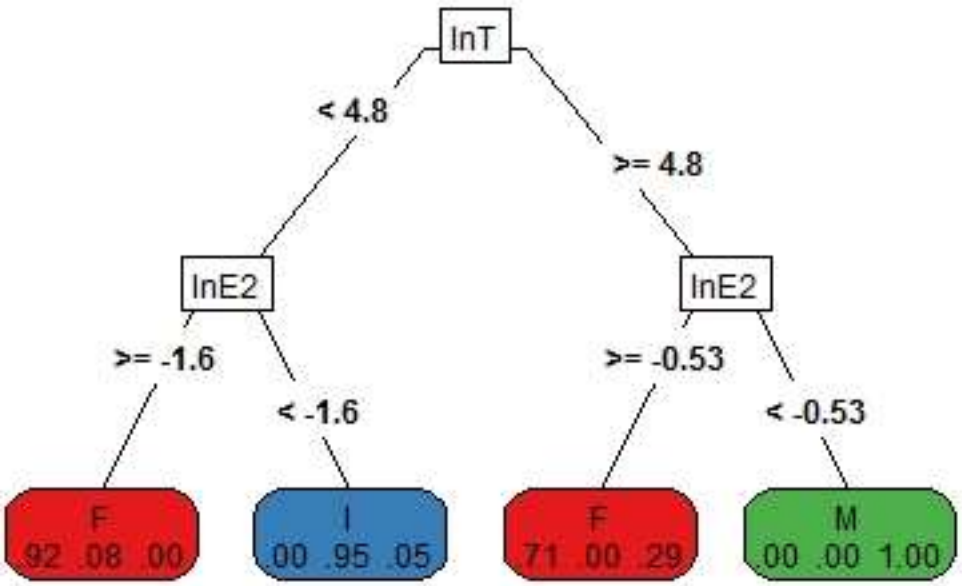

Figure D3: The classification tree for sex and class in response to sex steroids T and E2 from our CART analysis. The classification algorithm proceeds from the top down. White boxes indicate variables used for classification, numbers along lines linking boxes indicate the classification criteria for the variable at its origin, and rounded boxes indicate the target classes: Female (orange), Immature (blue), and Male (Green). The three numbers in the class boxes at the bottom are the proportional representation of 'true' classes in that node, in the order: Female, Immature, Male.

APPENDIX E

Description of indexes and model objects for Chapter 3.

Object	Description
i	Individual fish
t	Sampling occasion (year)
k	Observation dataset. There are three observation datasets: {1, 2, 3}, which represent physical capture, radio telemetry, and acoustic telemetry.
u	breeding state. When parameters are indexed by breeding state, they are indexed by u, which takes on a value of either 1 (breeding breeding state) or 2 (non-breeding state).
$nind$	Number of individual fish
$n.occasions$	Number of sampling occasions (years)
f	the occasions at first capture
$f2$	the occasion first observable in the radio telemetry dataset
$ff2$	the occasion last observable in the radio telemetry dataset
$f3$	the occasion first observable in the acoustic telemetry dataset
$ff3$	the occasion last observable in the acoustic telemetry dataset
$nind2$	the number of individuals observed in the radio telemetry dataset
$inds2$	the indexes (i) of individuals observed in the radio telemetry dataset
$nind3$	the number of individuals observed in the acoustic telemetry dataset
$inds3$	the indexes (i) of individuals observed in acoustic radio telemetry dataset
$nind.g.na$	The indexes (i) of individuals without sex information (G = NA)
z	The array of latent states, indexed by i and t and with elements, $z_{(i,t)}$. Fish can be in one of three states: the 'breeding' state, the 'non-breeding' state, or dead.
Y	Sampling effort for $y1$, in units of nights fished
$y1, y2, y3$	The multi-state capture history data matrix of all individual fish, indexed by k, i, and t. Fish can be observed in one of three states: the 'breeding' state, the 'non-breeding' state, and dead.
E	The multi-state capture history data matrix of all individual fish, from the k-th dataset, indexed by i, and t. Fish can be observed in one of three states: the 'breeding' state, the 'non-breeding' state, and dead.
X	Our time-varying temperature variable, DOY5: the day of year water temperatures first rise to 5^∘ C.
G	Sex (individually-varying covariate): female = 0, male = 1

ϕ	Annual survival probability, invariant in our analysis
θ	The sex ratio of individuals without a sex classification
ψ_1	State transition probability from state 1 ('breeding') to state 2 ('non-breeding')
ψ_2	State transition probability from state 2 ('non-breeding') to state 1 ('breeding')
$p1$	Detection probability for the physical capture dataset, indexed by time and individual
$p2$	Detection probability for the radio telemetry dataset, indexed by time and number of years at large (max of 2)
$p3$	Detection probability of the acoustic telemetry dataset, invariant in our analysis
ε_2	State mis-classification rate for the radio telemetry dataset
ε_3	State mis-classification rate for the acoustic telemetry dataset
β	Logistic regression parameters describing variation in transition probabilities
α	Logistic regression parameters describing variation in detection probabilities
p_1^*	Time varying observation probability of naive lake sturgeon (without trap response)
Ψ_1	Average state transition probability from breeding to non-breeding. For males: Ψ_1^M, for females: Ψ_1^F
Ψ_2	Average state transition probability from breeding to non-breeding. For males: Ψ_2^M, for females: Ψ_2^F
T	Breeding interval, the average number of years between breeding bouts. For males: T_M, for females: T_F
PSR	Observed population sex ratio, the number of males per female of all fish observed during the study

APPENDIX F

JAGS code for the multi-state capture-mark-recapture model for lake sturgeon

```
model {
# ------------------------------------------------
# Priors and constraints
# ------------------------------------------------
# assign sex
theta  ~ dbeta(3, 3)
for (i in 1:nind.g.na){ #female: G=0; male: G=1
  G[inds.g.na[i]] ~ dbern(theta)
}
# State transition and observation model coefficient priors
# use priors that are reasonably flat on the probability scale, when transfor
med
prec.coef <- 1/sqrt(2)
  gamma0 ~ dnorm(0, prec.coef) #Priors for logit(phi) intercept
  gamma1 ~ dnorm(0, prec.coef) #Priors for logit(phi) sex effect
for (u in 1:2){
  beta0[u] ~ dnorm(0, prec.coef) #Priors for logit(psi) intercept
  beta1[u] ~ dnorm(0, prec.coef) #Priors for logit(psi) sex effect
  beta2[u] ~ dnorm(0, prec.coef) #Priors for logit(psi) temperature covariate
effect
  beta3[u] ~ dnorm(0, prec.coef) #Priors for logit(psi) sex-temperature inter
action effect
  alpha0[u] ~ dnorm(0, prec.coef) #Priors for logit(p1) intercept
  alpha1[u] ~ dnorm(0, prec.coef) #Priors for logit(p1) effort covariate effe
ct
  alpha2[u] ~ dnorm(0, prec.coef) #Priors for logit(p1) trap response effect
  alpha3[u] ~ dnorm(0, prec.coef) #Priors for logit(psi) sex-effort interacti
on effect
}
# Telemetry observation probability
for (u in 1:2){
   for (c in 1:2){ #different p for 2 years radio tags were extant
      p2[u,c] ~ dunif(0, 1)
    }
   p3[u] ~ dunif(0, 1)
}
# State assignment error
eps1 <- 1 # because study design and location states, this is always 1
eps2 ~ dunif(0, 1)  # z=1 state assignment error
eps3 ~ dunif(0, 1)  # z=1 state assignment error
# ------------------------------------------------
```

```
# Logistic regressions predicting transition and observation parameters
# ------------------------------------------------
# for all individuals
for (i in 1:nind){
   logit(phi[i]) <- gamma0 + gamma1 * G[i]
}
# for all occasions from which state transitions may be observed in the next
year
for (u in 1:2){
   for (i in 1:nind){
      for (t in 1:(n.occasions-1)){
         logit(psi[u,i,t]) <- beta0[u] + beta1[u] * G[i] + beta2[u] * X[t] +
beta3[u] * G[i] * X[t]
      }
   }
}
# for every state, individual, and occasion after the first capture f[i]
for (u in 1:2){
   for (i in 1:nind){
      for (t in (f[i]+1):n.occasions){
     logit(p1[u,i,t]) <- alpha0[u] + alpha1[u] * E[t] + alpha2[u] * G[i] + al
pha3[u] * E[t] * G[i]
      }
   }
}
# ------------------------------------------------
# Define state-transition and observation matrices
# ------------------------------------------------
for (i in 1:nind){
   # Define probabilities of state z(i,t+1) given z(i,t)
   # indexing: matrix[to, from, individual, time]
   for (t in f[i]:(n.occasions-1)){
      A[1,1,i,t] <- phi[i] * (1-psi[1,i,t]) #psi21
      A[2,1,i,t] <- phi[i] * psi[1,i,t]     #psi21
      A[3,1,i,t] <- 1-phi[i]
      A[1,2,i,t] <- phi[i] * psi[2,i,t]     #psi12
      A[2,2,i,t] <- phi[i] * (1-psi[2,i,t]) #psi12
      A[3,2,i,t] <- 1-phi[i]
      A[1,3,i,t] <- 0
      A[2,3,i,t] <- 0
      A[3,3,i,t] <- 1
   } # t
} # i
# ------------------------------------------------
# Define probabilities of y(k,i,t) given z(i,t)
# ------------------------------------------------
# Observation process k = 1
for (i in 1:nind){
   for (t in (f[i]+1):n.occasions){
      P1[1,1,i,t] <- 0 #p1[1,i,t] * (1-eps1)
```

```
      P1[2,1,i,t] <- p1[1,i,t] * eps1
      P1[3,1,i,t] <- 1-p1[1,i,t]
      P1[1,2,i,t] <- 0
      P1[2,2,i,t] <- p1[2,i,t]
      P1[3,2,i,t] <- 1-p1[2,i,t]
      P1[1,3,i,t] <- 0
      P1[2,3,i,t] <- 0
      P1[3,3,i,t] <- 1
   } # t
} # i
# Observation process k = 2
for (i in 1:nind2){
   for (t in f2[inds2[i]]:ff2[inds2[i]]){
      P2[1,1,i,t] <- p2[1, (1+t-f2[inds2[i]]) ]  * (1-eps2)
      P2[2,1,i,t] <- p2[1, (1+t-f2[inds2[i]]) ]  * eps2
      P2[3,1,i,t] <- 1- p2[1, (1+t-f2[inds2[i]]) ]
      P2[1,2,i,t] <- 0
      P2[2,2,i,t] <- p2[2, (1+t-f2[inds2[i]]) ]
      P2[3,2,i,t] <- 1- p2[2, (1+t- f2[inds2[i]]) ]
      P2[1,3,i,t] <- 0
      P2[2,3,i,t] <- 0
      P2[3,3,i,t] <- 1
   } # t
} # i
# Observation process k = 3
for (i in 1:nind3){
   for (t in f3[inds3[i]]:ff3[inds3[i]]){
      P3[1,1,i,t] <- p3[1] * (1-eps3)
      P3[2,1,i,t] <- p3[1] * eps3
      P3[3,1,i,t] <- 1-p3[1]
      P3[1,2,i,t] <- 0
      P3[2,2,i,t] <- p3[2]
      P3[3,2,i,t] <- 1-p3[2]
      P3[1,3,i,t] <- 0
      P3[2,3,i,t] <- 0
      P3[3,3,i,t] <- 1
   } # t
} # i
# -------------------------------------------------
# Likelihood
# -------------------------------------------------
for (i in 1:nind){
   for (t in 1:f[i]){
         # Define latent state at first capture
         z[i,t] <- ifelse(f[i] == t, min_y_it[i,f[i]], 0)
      } # t
   for (t in (f[i]+1):n.occasions){
      # State process: draw z(t) given z(t-1)
      z[i,t] ~ dcat(A[,z[i,t-1], i, t-1])
      # Physical Capture Observation process: draw y(t) given z(t)
```

```
      y1[i,t] ~ dcat(P1[,z[i,t], i, t])
      #
   } # t
} # i
for (i in 1:nind2){
   for (t in f2[inds2[i]]:ff2[inds2[i]]){
      # Radio Telemetry Observation process: draw y(t) given z(t)
      y2[inds2[i],t] ~ dcat(P2[,z[inds2[i],t], i, t])
   } # t
} # i
for (i in 1:nind3){
   for (t in f3[inds3[i]]:ff3[inds3[i]]){
      # Acoustic Telemetry Observation process: draw y(t) given z(t)
      y3[inds3[i],t] ~ dcat(P3[,z[inds3[i],t], i, t])
   } # t
} # i
# ------------------------------------------------
# Derived quantities
# ------------------------------------------------
# Do females have higher survival?
# Survival varies by sex
for (g in 1:2){
   logit(phi.g[g]) <- gamma0 + gamma1 * (g-1)
}
phi.diff <- phi.g[1]-phi.g[2] #positive values for higher female survival

# monitor observed sex ratio (male:female)
PSR <- sum(G[ ])/(nind-sum(G[ ]))

# monitor time-varying p for females and males
for (u in 1:2){
   for (t in 1:n.occasions){
      logit(p1.male[u,t]) <- alpha0[u] + alpha1[u] * E[t] + alpha2[u] + alpha
3[u] * E[t]
      logit(p1.female[u,t]) <- alpha0[u] + alpha1[u] * E[t]
      p.diff[u,t] <- p1.female[u,t]-p1.male[u,t] #positive values for higher
female survival
   }
}

# sex-specific transition probabilities by year
for (u in 1:2){
   for (t in 1:(n.occasions-1)){
      logit(psi.male[u,t]) <- beta0[u] + beta1[u] + beta2[u] * X[t] + beta3[u
] * X[t]
      logit(psi.female[u,t]) <- beta0[u] + beta2[u] * X[t]
   }
}
# mean sex-specific transition probabilities
for (u in 1:2){
```

```
   logit(PSI.male[u]) <- beta0[u] + beta1[u]
   logit(PSI.female[u]) <- beta0[u]
}
# probability of returning in 1 through 10 years
P.female.ret[1] <- 1-PSI.female[1]
P.male.ret[1] <- 1-PSI.male[1]
for (t in 2:100){
   P.female.ret[t] <- PSI.female[1] * pow(1-PSI.female[2], t-2) * PSI.female[
2]
   P.male.ret[t] <- PSI.male[1] * pow(1-PSI.male[2], t-2)  * PSI.male[2]
}
# ...weighted by time
for (t in 1:100){
   Pt.male.ret[t] <- P.male.ret[t] * t
   Pt.female.ret[t] <- P.female.ret[t] * t
}
# average breeding interval by sex (approximate)
T.male <- 1+sum(Pt.male.ret[])
T.female <- 1+sum(Pt.female.ret[])
# is transition probabilty a Markov process?
for (t in 1:(n.occasions-1)){
   # if $Psi_12 - (1-Psi_21) == 0$, then no evidence of Markov
   R.male[t] <- psi.male[1,t] - (1-psi.male[2,t])
   R.female[t] <- psi.female[1,t] - (1-psi.female[2,t])
}
# ------------------------------------------------
}
```

APPENDIX G

Goodness of fit plots for Chapter 4. The Freeman-Tukey discrepancy statistic was calculated for our redd count dataset (Tobs) and compared to one calculated from simulated data (Tsim) for all iterations of the model at each scale of inference (panel a). The proportion of iterations for which Tsim > Tobs is our posterior predictive check (P) (panel b).

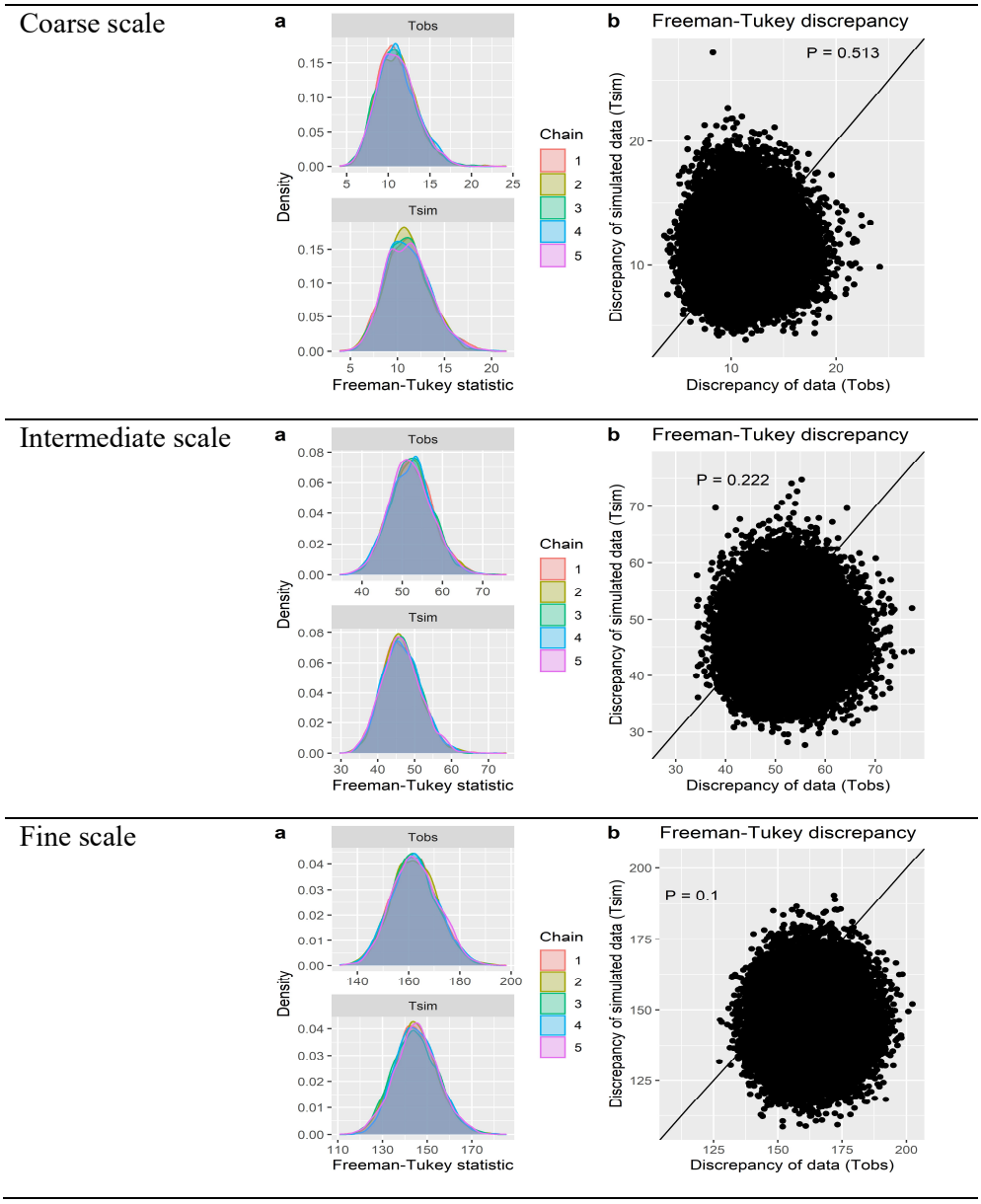

APPENDIX H

JAGS code for the coarse scale lifecycle model for Chinook salmon.

```
model {

  # Smolt production rate, varying in space
  # per-capita fecundity * egg survival rate * parr survival rate
  log.b ~ dgamma(64,14)
  tau.log.b ~ dt(0, pow(2.5,-2), 1)T(0,)
  sigma.log.b <- sqrt(1/tau.log.b)
  for (i in 1:n){
    alpha.log.b[i] ~ dnorm(0, tau.log.b)
    b[i] <- exp(log.b + alpha.log.b[i])
  }

  # Smolt transport
  mean.p.T ~ dnorm(0, 1/sqrt(2))
  slope.p.T ~ dnorm(0, 1/sqrt(2))T(,0) #only consider negative slope
  tau.p.T ~ dt(0, pow(2.5,-2), 1)T(0,)
  sigma.p.T <- sqrt(1/tau.p.T)
  r.T ~ dt(0, pow(2.5,-2), 1)T(0,)
  for (t in 1:Y){
    alpha.p.T[t] ~dnorm(0, tau.p.T)
    logit(p.T[t]) <- mean.p.T + slope.p.T*T.sched[t] + alpha.p.T[t]
    y.T[t] ~ dbeta(r.T*p.T[t], r.T*(1-p.T[t]))
  }
  phi.T <- 0.98

  # Smolt hydrosystem survival
  mu.h ~ dnorm(0, 1/sqrt(2))
  tau.h ~ dt(0, pow(2.5,-2), 1)T(0,)
  sigma.h <- sqrt(1/tau.h)
  r.h ~ dt(0, pow(2.5,-2), 1)T(0,)
  for(t in 1:Y){
    alpha.h[t] ~ dnorm(0, tau.h)
    logit(phi.h[t]) <- mu.h + alpha.h[t]
    y.h[t] ~ dbeta(r.h*phi.h[t], r.h*(1-phi.h[t]))
  }

  # Ocean survival
  beta0.o ~ dnorm(0, 1/sqrt(2)) # intercept
  beta1.o ~ dnorm(0, 1/sqrt(2)) # September PDO in smolt year
  beta2.o ~ dnorm(0, 1/sqrt(2)) # April upwelling index in smolt year
  beta3.o ~ dnorm(0, 1/sqrt(2)) # October upwelling index in smolt year
```

```
  beta4.o ~ dnorm(0, 1/sqrt(2)) # 4-yr mean May-Jul PDO, ending smolt year+2
  tau.o ~ dt(0, pow(2.5,-2), 1)T(0,)
  sigma.o <- sqrt(1/tau.o)
  for (t in 1:Y){
    logit(phi.o[t]) <- beta0.o + beta1.o*X1[t] + beta2.o*X2[t] + beta3.o*p.T[
t] + beta4.o*X4[t] + alpha.o[t]
    alpha.o[t] ~ dnorm(0, tau.o)
  }

  # Probability of returning at age 4
  mu.theta4 ~ dnorm(0, 1/sqrt(2)) #weakly informative prior centered at 50%
  tau.theta4 ~ dt(0, pow(25,-2), 1)T(0,)
  sigma.theta4 <- pow(tau.theta4, -2)
  logit(theta4[1]) <- mu.theta4 # initial value
  for(t in 2:Y){
    delta.theta4[t-1] ~ dnorm(0, tau.theta4)
    logit(theta4[t]) <- logit(theta4[t-1]) + delta.theta4[t-1]
  }

  # Probability of returning at age 5
  mu.theta5 ~ dnorm(2, 1/sqrt(2)) #weakly informative prior centered at 88%
  logit(theta5) <- mu.theta5 # initial value

  # Adult hydrosystem survival
  phi.ret ~ dbeta(10, 2) #informative

  ############################################################################
  #####  Process model
  ############################################################################

  # Hindcast
  for (i in 1:n){ #for each basin
    for (t in 1:(a.max+1)){ #1:7
      # informative prior
      log.S[i,t] ~ dnorm(2.664888,  1e-0)
      S[i,t] <- exp(log.S[i,t])
    }
  }

  # Survival from age-1 smolt to adult return (SAR)
   for (t in 1:Y){
    phi.sar[t] <- ((1-p.T[t])*phi.h[t] + p.T[t]*phi.T) * phi.o[t]
  }

  for (i in 1:n){

    N0[i,2] <- S[i,1] * b[i]

    N0[i,3] <- S[i,2] * b[i]
    N1[i,3] <- N0[i,2]
```

```
  N0[i,4] <- S[i,3] * b[i]
  N1[i,4] <- N0[i,3]
  N2[i,4] <- N1[i,3] * phi.sar[3]

  N0[i,5] <- S[i,4] * b[i]
  N1[i,5] <- N0[i,4]
  N2[i,5] <- N1[i,4] * phi.sar[4]
  N3[i,5] <- N2[i,4]

  N0[i,6] <- S[i,5] * b[i]
  N1[i,6] <- N0[i,5]
  N2[i,6] <- N1[i,5] * phi.sar[5]
  N3[i,6] <- N2[i,5]
  N4[i,6] <- N3[i,5] * (1-theta4[5])
  Bon4[i,6] <- N3[i,5] * theta4[5]
  Redd4[i,6] <- Bon4[i,6] * phi.ret

  N0[i,7] <- S[i,6] * b[i]
  N1[i,7] <- N0[i,6]
  N2[i,7] <- N1[i,6] * phi.sar[6]
  N3[i,7] <- N2[i,6]
  N4[i,7] <- N3[i,6] * (1-theta4[6])
  N5[i,7] <- N4[i,6] * (1-theta5)
  Bon4[i,7] <- N3[i,6] * theta4[6]
  Bon5[i,7] <- N4[i,6] * theta5
  Redd4[i,7] <- Bon4[i,7] * phi.ret
  Redd5[i,7] <- Bon5[i,7] * phi.ret
}

# Population dynamics
# note, the transitions [.]->Bon->Redd->S occur within the same year
for (i in 1:n){
  for (t in (a.max+1):(Y-1)){
    # results of state transition probabilities
    N0[i,t+1] <- S[i,t] * b[i]
    N1[i,t+1] <- N0[i,t]
    N2[i,t+1] <- N1[i,t] * phi.sar[t]
    N3[i,t+1] <- N2[i,t]
    N4[i,t+1] <- N3[i,t] * (1-theta4[t])
    N5[i,t+1] <- N4[i,t] * (1-theta5)
    Bon4[i,t+1] <- N3[i,t] * theta4[t]
    Bon5[i,t+1] <- N4[i,t] * theta5
    Bon6[i,t+1] <- N5[i,t]
    Redd4[i,t+1] <- Bon4[i,t+1] * phi.ret
    Redd5[i,t+1] <- Bon5[i,t+1] * phi.ret
    Redd6[i,t+1] <- Bon6[i,t+1] * phi.ret
    S[i,t+1] <- Redd4[i,t+1] + Redd5[i,t+1] + Redd6[i,t+1]
  }
}
```

```
#########################################################################
#####  Define expectations for observation datasets
#########################################################################

# Expected proportion-at-age by year
for (i in 1:n){
  for (t in (a.max+2):(Y)){
    hat.p.age[i,t,1] <- Redd4[i,t] / S[i,t] # age-4
    hat.p.age[i,t,2] <- Redd5[i,t] / S[i,t] # age-5
    hat.p.age[i,t,3] <- Redd6[i,t] / S[i,t] # age-6
  }
}

#########################################################################
#####  likelihoods
#########################################################################

# Smolt-to-Adult Survival
for (t in init.sar:(Y-2)){
  y.sar[t-init.sar+1,2] ~ dbin(phi.sar[t+2], y.sar[t-init.sar+1,1])
}

# Adult Hydrosystem Survival
for (t in 1:ret.n){
  y.ret[ret.inds[t],2] ~ dbin(phi.ret, y.ret[ret.inds[t],1])
}

# Age distribution of returning females
for (i in r.i){
  for (t in r.t[i,(1:r.nt[i])]){
    y.age[i,t, ] ~ dmulti(hat.p.age[i,t, ], r[i,t])
  }
}

# Redd counts
# multiplicative extra-Poisson variance
tau.pois ~ dt(0, pow(2.5,-2), 1)T(0,)
sigma.pois <- 1/sqrt(tau.pois)
for (i in 1:n){
  for (t in (a.max+2):Y){

    # State-space with over-dispersed poisson observation process
    y[i,t] ~ dpois( mu[i,t] )
    mu[i,t] <- S[i,t] * exp.eps[i,t] # log(mu) = log(S) + eps
    exp.eps[i,t] <- exp(eps[i,t])
    eps[i,t] ~ dnorm(0, tau.pois) # eps ~ N(0, sigma.pois)
    Tobs0[i,t] <- (sqrt(y[i,t]) - sqrt(mu[i,t]))^2

    # Simulated data for state-space version
```

```
      ySim[i,t] ~ dpois(S[i,t] * exp.simeps[i,t] )
      exp.simeps[i,t] <- exp(simeps[i,t])
      simeps[i,t] ~ dnorm(0, tau.pois)
      Tsim0[i,t] <- (sqrt(ySim[i,t]) - sqrt(S[i,t] * exp.simeps[i,t]))^2

    }
    Tobsi[i] <- sum(Tobs0[i,(a.max+2):Y])
    Tsimi[i] <- sum(Tsim0[i,(a.max+2):Y])
  }
  # GOF assessment
  Tobs <- sum(Tobsi[])
  Tsim <- sum(Tsimi[])

  ########################################################################
  #####  Derived parameters
  ########################################################################

  # Lambda, discrete time population growth rate
  for (i in 1:n){
    for (t in (a.max+1):(Y-a.max-1)){
      R[i,t] <- Redd6[i,t+7] + Redd5[i,t+6] + Redd4[i,t+5]
      R.S[i,t] <- R[i,t]/S[i,t] #empirical lambda
    }
  }

} #model
```

APPENDIX I

JAGS code for the intermediate scale lifecycle model for Chinook salmon.

```
model {

  # Smolt production rate, varying in space
  # per-capita fecundity * egg survival rate * parr survival rate
  log.b ~ dgamma(64,14)
  tau.log.b ~ dt(0, pow(2.5,-2), 1)T(0,)
  sigma.log.b <- sqrt(1/tau.log.b)
  for (i in 1:n){
    alpha.log.b[i] ~ dnorm(0, tau.log.b)
    b[i] <- exp(log.b + alpha.log.b[i])
  }

  # Smolt transport
  mean.p.T ~ dnorm(0, 1/sqrt(2))
  slope.p.T ~ dnorm(0, 1/sqrt(2))T(,0) #only consider negative slope
  tau.p.T ~ dt(0, pow(2.5,-2), 1)T(0,)
  sigma.p.T <- sqrt(1/tau.p.T)
  r.T ~ dt(0, pow(2.5,-2), 1)T(0,)
  for (t in 1:Y){
    alpha.p.T[t] ~dnorm(0, tau.p.T)
    logit(p.T[t]) <- mean.p.T + slope.p.T*T.sched[t] + alpha.p.T[t]
    y.T[t] ~ dbeta(r.T*p.T[t], r.T*(1-p.T[t]))
  }
  phi.T <- 0.98

  # Smolt hydrosystem survival
  mu.h ~ dnorm(0, 1/sqrt(2))
  tau.h ~ dt(0, pow(2.5,-2), 1)T(0,)
  sigma.h <- sqrt(1/tau.h)
  r.h ~ dt(0, pow(2.5,-2), 1)T(0,)
  for(t in 1:Y){
    alpha.h[t] ~ dnorm(0, tau.h)
    logit(phi.h[t]) <- mu.h + alpha.h[t]
    y.h[t] ~ dbeta(r.h*phi.h[t], r.h*(1-phi.h[t]))
  }

  # Ocean survival
  beta0.o ~ dnorm(0, 1/sqrt(2)) # intercept
  beta1.o ~ dnorm(0, 1/sqrt(2)) # September PDO in smolt year
  beta2.o ~ dnorm(0, 1/sqrt(2)) # April upwelling index in smolt year
  beta3.o ~ dnorm(0, 1/sqrt(2)) # October upwelling index in smolt year
```

```
  beta4.o ~ dnorm(0, 1/sqrt(2)) # 4-yr mean May-Jul PDO, ending smolt year+2
  tau.o ~ dt(0, pow(2.5,-2), 1)T(0,)
  sigma.o <- sqrt(1/tau.o)
  for (t in 1:Y){
    logit(phi.o[t]) <- beta0.o + beta1.o*X1[t] + beta2.o*X2[t] + beta3.o*p.T[
t] + beta4.o*X4[t] + alpha.o[t]
    alpha.o[t] ~ dnorm(0, tau.o)
  }

  # Probability of returning at age 4
  mu.theta4 ~ dnorm(0, 1/sqrt(2)) #weakly informative prior centered at 50%
  tau.theta4 ~ dt(0, pow(25,-2), 1)T(0,)
  sigma.theta4 <- pow(tau.theta4, -2)
  logit(theta4[1]) <- mu.theta4 # initial value
  for(t in 2:Y){
    delta.theta4[t-1] ~ dnorm(0, tau.theta4)
    logit(theta4[t]) <- logit(theta4[t-1]) + delta.theta4[t-1]
  }

  # Probability of returning at age 5
  mu.theta5 ~ dnorm(2, 1/sqrt(2)) #weakly informative prior centered at 88%
  logit(theta5) <- mu.theta5 # initial value

  # Adult hydrosystem survival
  phi.ret ~ dbeta(10, 2)

  ############################################################################
  #####  Process model
  ############################################################################

  # Hindcast
  for (i in 1:n){ #for each basin
    for (t in 1:(a.max+1)){ #1:7
      # informative prior
      log.S[i,t] ~ dnorm(2.6,  1e-0)
      S[i,t] <- exp(log.S[i,t])
    }
  }

  # Survival from age-1 smolt to adult return (SAR)
  for (t in 1:Y){
    phi.sar[t] <- ((1-p.T[t])*phi.h[t] + p.T[t]*phi.T) * phi.o[t]
  }

  for (i in 1:n){

    N0[i,2] <- S[i,1] * b[i]

    N0[i,3] <- S[i,2] * b[i]
    N1[i,3] <- N0[i,2]
```

```
  N0[i,4] <- S[i,3] * b[i]
  N1[i,4] <- N0[i,3]
  N2[i,4] <- N1[i,3] * phi.sar[3]

  N0[i,5] <- S[i,4] * b[i]
  N1[i,5] <- N0[i,4]
  N2[i,5] <- N1[i,4] * phi.sar[4]
  N3[i,5] <- N2[i,4]

  N0[i,6] <- S[i,5] * b[i]
  N1[i,6] <- N0[i,5]
  N2[i,6] <- N1[i,5] * phi.sar[5]
  N3[i,6] <- N2[i,5]
  N4[i,6] <- N3[i,5] * (1-theta4[5])
  Bon4[i,6] <- N3[i,5] * theta4[5]
  Redd4[i,6] <- Bon4[i,6] * phi.ret

  N0[i,7] <- S[i,6] * b[i]
  N1[i,7] <- N0[i,6]
  N2[i,7] <- N1[i,6] * phi.sar[6]
  N3[i,7] <- N2[i,6]
  N4[i,7] <- N3[i,6] * (1-theta4[6])
  N5[i,7] <- N4[i,6] * (1-theta5)
  Bon4[i,7] <- N3[i,6] * theta4[6]
  Bon5[i,7] <- N4[i,6] * theta5
  Redd4[i,7] <- Bon4[i,7] * phi.ret
  Redd5[i,7] <- Bon5[i,7] * phi.ret
}

# Population dynamics
# note, the transitions [.]->Bon->Redd->S occur within the same year
for (i in 1:n){
  for (t in (a.max+1):(Y-1)){
    # results of state transition probabilities
    N0[i,t+1] <- S[i,t] * b[i]
    N1[i,t+1] <- N0[i,t]
    N2[i,t+1] <- N1[i,t] * phi.sar[t]
    N3[i,t+1] <- N2[i,t]
    N4[i,t+1] <- N3[i,t] * (1-theta4[t])
    N5[i,t+1] <- N4[i,t] * (1-theta5)
    Bon4[i,t+1] <- N3[i,t] * theta4[t]
    Bon5[i,t+1] <- N4[i,t] * theta5
    Bon6[i,t+1] <- N5[i,t]
    Redd4[i,t+1] <- Bon4[i,t+1] * phi.ret
    Redd5[i,t+1] <- Bon5[i,t+1] * phi.ret
    Redd6[i,t+1] <- Bon6[i,t+1] * phi.ret
    S[i,t+1] <- Redd4[i,t+1] + Redd5[i,t+1] + Redd6[i,t+1]
  }
}
```

```
#########################################################################
#####  Define expectations for observation datasets
#########################################################################

# Expected proportion-at-age  by year
for (i in 1:n){
  for (t in (a.max+2):(Y)){
    hat.p.age[i,t,1] <- Redd4[i,t] / S[i,t] # age-4
    hat.p.age[i,t,2] <- Redd5[i,t] / S[i,t] # age-5
    hat.p.age[i,t,3] <- Redd6[i,t] / S[i,t] # age-6
  }
}

#########################################################################
#####  likelihoods
#########################################################################

# Smolt-to-Adult Survival
for (t in init.sar:(Y-2)){
  y.sar[t-init.sar+1,2] ~ dbin(phi.sar[t+2], y.sar[t-init.sar+1,1])
}

# Adult Hydrosystem Survival
for (t in 1:ret.n){
  y.ret[ret.inds[t],2] ~ dbin(phi.ret, y.ret[ret.inds[t],1])
}

# Age distribution of returning females
for (i in r.i){
  for (t in r.t[i,(1:r.nt[i])]){
    y.age[i,t, ] ~ dmulti(hat.p.age[i,t, ], r[i,t])
  }
}

# Redd counts
# multiplicative extra-Poisson variance
tau.pois ~ dt(0, pow(2.5,-2), 1)T(0,)
sigma.pois <- 1/sqrt(tau.pois)
for (i in 1:n){
  for (t in (a.max+2):Y){

    # State-space with over-dispersed poisson observation process
    y[i,t] ~ dpois( mu[i,t] )
    mu[i,t] <- S[i,t] * exp.eps[i,t] # log(mu) = log(S) + eps
    exp.eps[i,t] <- exp(eps[i,t])
    eps[i,t] ~ dnorm(0, tau.pois) # eps ~ N(0, sigma.pois)
    Tobs0[i,t] <- (sqrt(y[i,t]) - sqrt(mu[i,t]))^2

    # Simulated data for state-space version
```

```
      ySim[i,t] ~ dpois(S[i,t] * exp.simeps[i,t] )
      exp.simeps[i,t] <- exp(simeps[i,t])
      simeps[i,t] ~ dnorm(0, tau.pois)
      Tsim0[i,t] <- (sqrt(ySim[i,t]) - sqrt(S[i,t] * exp.simeps[i,t]))^2

    }
    Tobsi[i] <- sum(Tobs0[i,(a.max+2):Y])
    Tsimi[i] <- sum(Tsim0[i,(a.max+2):Y])
  }
  # GOF assessment
  Tobs <- sum(Tobsi[])
  Tsim <- sum(Tsimi[])

  ########################################################################
  #####  Derived parameters
  ########################################################################

  # Lambda, discrete time population growth rate
  for (i in 1:n){
    for (t in (a.max+1):(Y-a.max-1)){
      R[i,t] <- Redd6[i,t+7] + Redd5[i,t+6] + Redd4[i,t+5]
      R.S[i,t] <- R[i,t]/S[i,t] #empirical lambda
    }
  }

} #model
```

APPENDIX J

JAGS code for the fine scale lifecycle model for Chinook salmon.

```
model {

  # Smolt production rate, varying in space
  # per-capita fecundity * egg survival rate * parr survival rate
  log.b ~ dgamma(64,14) #dnorm(4.5, 0.5)
  tau.log.b ~ dt(0, pow(2.5,-2), 1)T(0,)
  sigma.log.b <- sqrt(1/tau.log.b)
  for (i in 1:s){
    alpha.log.b[i] ~ dnorm(0, tau.log.b)
    b[i] <- exp(log.b + alpha.log.b[i])
  }

  # Smolt transport
  mean.p.T ~ dnorm(0, 1/sqrt(2))
  slope.p.T ~ dnorm(0, 1/sqrt(2))T(,0) #only consider negative slope
  tau.p.T ~ dt(0, pow(2.5,-2), 1)T(0,)
  sigma.p.T <- sqrt(1/tau.p.T)
  r.T ~ dt(0, pow(2.5,-2), 1)T(0,)
  for (t in 1:Y){
    alpha.p.T[t] ~dnorm(0, tau.p.T)
    logit(p.T[t]) <- mean.p.T + slope.p.T*T.sched[t] + alpha.p.T[t]
    y.T[t] ~ dbeta(r.T*p.T[t], r.T*(1-p.T[t]))
  }
  phi.T <- 0.98

  # Smolt hydrosystem survival
  mu.h ~ dnorm(0, 1/sqrt(2))
  tau.h ~ dt(0, pow(2.5,-2), 1)T(0,)
  sigma.h <- sqrt(1/tau.h)
  r.h ~ dt(0, pow(2.5,-2), 1)T(0,)
  for(t in 1:Y){
    alpha.h[t] ~ dnorm(0, tau.h)
    logit(phi.h[t]) <- mu.h + alpha.h[t]
    y.h[t] ~ dbeta(r.h*phi.h[t], r.h*(1-phi.h[t]))
  }

  # Ocean survival
  beta0.o ~ dnorm(0, 1/sqrt(2)) # intercept
  beta1.o ~ dnorm(0, 1/sqrt(2)) # September PDO in smolt year
  beta2.o ~ dnorm(0, 1/sqrt(2)) # April upwelling index in smolt year
  beta3.o ~ dnorm(0, 1/sqrt(2)) # October upwelling index in smolt year
```

```
  beta4.o ~ dnorm(0, 1/sqrt(2)) # 4-yr mean May-Jul PDO, ending smolt year+2
  tau.o ~ dt(0, pow(2.5,-2), 1)T(0,)
  sigma.o <- sqrt(1/tau.o)
  for (t in 1:Y){
    logit(phi.o[t]) <- beta0.o + beta1.o*X1[t] + beta2.o*X2[t] +
beta3.o*p.T[t] + beta4.o*X4[t] + alpha.o[t]
    alpha.o[t] ~ dnorm(0, tau.o)
  }

  # Probability of returning at age 4
  mu.theta4 ~ dnorm(0, 1/sqrt(2)) #weakly informative prior centered at 50%
  tau.theta4 ~ dt(0, pow(25,-2), 1)T(0,)
  sigma.theta4 <- pow(tau.theta4, -2)
  logit(theta4[1]) <- mu.theta4 # initial value
  for(t in 2:Y){
    delta.theta4[t-1] ~ dnorm(0, tau.theta4)
    logit(theta4[t]) <- logit(theta4[t-1]) + delta.theta4[t-1]
  }

  # Probability of returning at age 5
  mu.theta5 ~ dnorm(2, 1/sqrt(2)) #weakly informative prior centered at 88%
  logit(theta5) <- mu.theta5 # initial value

  # Adult hydrosystem survival
  phi.ret ~ dbeta(10, 2)

  ############################################################################
  #####  Process model
  ############################################################################

  # Hindcast
  for (i in 1:s){ #for each basin
    for (t in 1:(a.max+1)){ #1:7
      # informative prior;
      log.S[i,t] ~ dnorm(2.2,  1e-0)
      S[i,t] <- exp(log.S[i,t])
    }
  }

  # Survival from age-1 smolt to adult return (SAR)
  for (t in 1:Y){
    phi.sar[t] <- ((1-p.T[t])*phi.h[t] + p.T[t]*phi.T) * phi.o[t]
  }

  for (i in 1:s){

    N0[i,2] <- S[i,1] * b[i]

    N0[i,3] <- S[i,2] * b[i]
```

```
    N1[i,3] <- N0[i,2]

    N0[i,4] <- S[i,3] * b[i]
    N1[i,4] <- N0[i,3]
    N2[i,4] <- N1[i,3] * phi.sar[3]

    N0[i,5] <- S[i,4] * b[i]
    N1[i,5] <- N0[i,4]
    N2[i,5] <- N1[i,4] * phi.sar[4]
    N3[i,5] <- N2[i,4]

    N0[i,6] <- S[i,5] * b[i]
    N1[i,6] <- N0[i,5]
    N2[i,6] <- N1[i,5] * phi.sar[5]
    N3[i,6] <- N2[i,5]
    N4[i,6] <- N3[i,5] * (1-theta4[5])
    Bon4[i,6] <- N3[i,5] * theta4[5]
    Redd4[i,6] <- Bon4[i,6] * phi.ret

    N0[i,7] <- S[i,6] * b[i]
    N1[i,7] <- N0[i,6]
    N2[i,7] <- N1[i,6] * phi.sar[6]
    N3[i,7] <- N2[i,6]
    N4[i,7] <- N3[i,6] * (1-theta4[6])
    N5[i,7] <- N4[i,6] * (1-theta5)
    Bon4[i,7] <- N3[i,6] * theta4[6]
    Bon5[i,7] <- N4[i,6] * theta5
    Redd4[i,7] <- Bon4[i,7] * phi.ret
    Redd5[i,7] <- Bon5[i,7] * phi.ret
  }

  # Population dynamics
  # note, the transitions [.]->Bon->Redd->S occur within the same year
  for (i in 1:s){
    for (t in (a.max+1):(Y-1)){
      # results of state transition probabilities
      N0[i,t+1] <- S[i,t] * b[i]
      N1[i,t+1] <- N0[i,t]
      N2[i,t+1] <- N1[i,t] * phi.sar[t]
      N3[i,t+1] <- N2[i,t]
      N4[i,t+1] <- N3[i,t] * (1-theta4[t])
      N5[i,t+1] <- N4[i,t] * (1-theta5)
      Bon4[i,t+1] <- N3[i,t] * theta4[t]
      Bon5[i,t+1] <- N4[i,t] * theta5
      Bon6[i,t+1] <- N5[i,t]
      Redd4[i,t+1] <- Bon4[i,t+1] * phi.ret
      Redd5[i,t+1] <- Bon5[i,t+1] * phi.ret
      Redd6[i,t+1] <- Bon6[i,t+1] * phi.ret
      S[i,t+1] <- Redd4[i,t+1] + Redd5[i,t+1] + Redd6[i,t+1]
```

```
    }
  }

  ########################################################################
  #####  Define expectations for observation datasets
  ########################################################################

  # Expected proportion-at-age by year
  # cant easily index i-th segment, so expanded
  for (t in (a.max+2):(Y)){
    hat.p.age[1,t,1] <- sum(Redd4[inds1,t]) / sum(S[inds1,t]) # age-4
    hat.p.age[1,t,2] <- sum(Redd5[inds1,t]) / sum(S[inds1,t]) # age-5
    hat.p.age[1,t,3] <- sum(Redd6[inds1,t]) / sum(S[inds1,t]) # age-6

    hat.p.age[2,t,1] <- sum(Redd4[inds2,t]) / sum(S[inds2,t]) # age-4
    hat.p.age[2,t,2] <- sum(Redd5[inds2,t]) / sum(S[inds2,t]) # age-5
    hat.p.age[2,t,3] <- sum(Redd6[inds2,t]) / sum(S[inds2,t]) # age-6

    hat.p.age[3,t,1] <- sum(Redd4[inds3,t]) / sum(S[inds3,t]) # age-4
    hat.p.age[3,t,2] <- sum(Redd5[inds3,t]) / sum(S[inds3,t]) # age-5
    hat.p.age[3,t,3] <- sum(Redd6[inds3,t]) / sum(S[inds3,t]) # age-6

    hat.p.age[4,t,1] <- sum(Redd4[inds4,t]) / sum(S[inds4,t]) # age-4
    hat.p.age[4,t,2] <- sum(Redd5[inds4,t]) / sum(S[inds4,t]) # age-5
    hat.p.age[4,t,3] <- sum(Redd6[inds4,t]) / sum(S[inds4,t]) # age-6

    hat.p.age[5,t,1] <- sum(Redd4[inds5,t]) / sum(S[inds5,t]) # age-4
    hat.p.age[5,t,2] <- sum(Redd5[inds5,t]) / sum(S[inds5,t]) # age-5
    hat.p.age[5,t,3] <- sum(Redd6[inds5,t]) / sum(S[inds5,t]) # age-6

    hat.p.age[6,t,1] <- sum(Redd4[inds6,t]) / sum(S[inds6,t]) # age-4
    hat.p.age[6,t,2] <- sum(Redd5[inds6,t]) / sum(S[inds6,t]) # age-5
    hat.p.age[6,t,3] <- sum(Redd6[inds6,t]) / sum(S[inds6,t]) # age-6

    hat.p.age[7,t,1] <- sum(Redd4[inds7,t]) / sum(S[inds7,t]) # age-4
    hat.p.age[7,t,2] <- sum(Redd5[inds7,t]) / sum(S[inds7,t]) # age-5
    hat.p.age[7,t,3] <- sum(Redd6[inds7,t]) / sum(S[inds7,t]) # age-6

    hat.p.age[8,t,1] <- sum(Redd4[inds8,t]) / sum(S[inds8,t]) # age-4
    hat.p.age[8,t,2] <- sum(Redd5[inds8,t]) / sum(S[inds8,t]) # age-5
    hat.p.age[8,t,3] <- sum(Redd6[inds8,t]) / sum(S[inds8,t]) # age-6
  }

  ########################################################################
  #####  likelihoods
  ########################################################################

  # Smolt-to-Adult Survival
  for (t in init.sar:(Y-2)){
```

```
    y.sar[t-init.sar+1,2] ~ dbin(phi.sar[t+2], y.sar[t-init.sar+1,1])
  }

  # Adult Hydrosystem Survival
  for (t in 1:ret.n){
    y.ret[ret.inds[t],2] ~ dbin(phi.ret, y.ret[ret.inds[t],1])
  }

  # Age distribution of returning females
  for (i in r.i){
    for (t in r.t[i,(1:r.nt[i])]){
      y.age[i,t, ] ~ dmulti(hat.p.age[i,t, ], r[i,t])
    }
  }

  # Redd counts
  # multiplicative extra-Poisson variance
  tau.pois ~ dt(0, pow(2.5,-2), 1)T(0,)
  sigma.pois <- 1/sqrt(tau.pois)
  for (i in 1:s){
    for (t in (a.max+2):Y){

      # State-space with over-dispersed poisson observation process
      y[i,t] ~ dpois( mu[i,t] )
      mu[i,t] <- S[i,t] * exp.eps[i,t] # log(mu) = log(S) + eps
      exp.eps[i,t] <- exp(eps[i,t])
      eps[i,t] ~ dnorm(0, tau.pois) # eps ~ N(0, sigma.pois)
      Tobs0[i,t] <- (sqrt(y[i,t]) - sqrt(mu[i,t]))^2

      # Simulated data for state-space version
      ySim[i,t] ~ dpois(S[i,t] * exp.simeps[i,t] )
      exp.simeps[i,t] <- exp(simeps[i,t])
      simeps[i,t] ~ dnorm(0, tau.pois)
      Tsim0[i,t] <- (sqrt(ySim[i,t]) - sqrt(S[i,t] * exp.simeps[i,t]))^2

    }
    Tobsi[i] <- sum(Tobs0[i,(a.max+2):Y])
    Tsimi[i] <- sum(Tsim0[i,(a.max+2):Y])
  }
  # GOF assessment
  Tobs <- sum(Tobsi[])
  Tsim <- sum(Tsimi[])

  ############################################################################
  #####  Derived parameters
  ############################################################################

  # Lambda, discrete time population growth rate
  for (i in 1:s){
```

```
    for (t in (a.max+1):(Y-a.max-1)){
      R[i,t] <- Redd6[i,t+7] + Redd5[i,t+6] + Redd4[i,t+5]
      R.S[i,t] <- R[i,t]/S[i,t] #empirical lambda
    }
  }

} #model
```